



UNIVERSIDADE FEDERAL DE PERNAMBUCO
CENTRO DE TECNOLOGIA E GEOCIÊNCIAS
DEPARTAMENTO DE GEOLOGIA
PROGRAMA DE PÓS-GRADUAÇÃO EM GEOCIÊNCIAS

JOÃO VICENTE TAVARES CALANDRINI DE AZEVEDO

**ASPECTOS DIAGENÉTICOS, TECTONO-ESTRATIGRÁFICOS E POTENCIAL
EXPLORATÓRIO DE HIDROCARBONETOS DA FORMAÇÃO POTI, BACIA DO
PARNAÍBA, NORDESTE DO BRASIL**



Recife

2022

JOÃO VICENTE TAVARES CALANDRINI DE AZEVEDO

**ASPECTOS DIAGENÉTICOS, TECTONO-ESTRATIGRÁFICOS E POTENCIAL
EXPLORATÓRIO DE HIDROCARBONETOS DA FORMAÇÃO POTI, BACIA DO
PARNAÍBA, NORDESTE DO BRASIL**

Dissertação apresentada ao Programa de Pós-Graduação em Geociências da Universidade Federal de Pernambuco como preenchimento parcial dos requisitos para obtenção do grau de Mestre em Geociências.

Área de concentração: Geologia sedimentar e ambiental

Orientador: Prof. Dr. Mário Ferreira de Lima Filho

Coorientadora: Profª Drª Zenilda Vieira Batista

Recife

2022

Catalogação na fonte:

Bibliotecário Carlos Moura, CRB-4 / 1502

A994a	<p>Azevedo, João Vicente Tavares Calandrini de. Aspectos diagenéticos, tectono-estratigráficos e potencial exploratório de hidrocarbonetos da Formação Poti, Bacia do Parnaíba, Nordeste do Brasil. / João Vicente Tavares Calandrini de Azevedo. – 2022. 116 f.: il.</p> <p>Orientador: Dr. Mário Ferreira de Lima Filho. Coorientadora: Profª Drª Zenilda Vieira Batista. Dissertação (mestrado) – Universidade Federal de Pernambuco. CTG. Programa de Pós-Graduação em Geociências, 2022. Inclui referências.</p> <p>1. Geociências. 2. Formação Poti. 3. Bacia do Parnaíba. 4. Rochas reservatório. 5. Sistemas petrolíferos. 6. Diagênese de arenitos. 7. Caracterização petrográfica. I. Lima Filho, Mário Ferreira de (orientador). II. Batista, Zenilda Vieira (coorientadora). III. Título.</p>
-------	---

JOÃO VICENTE TAVARES CALANDRINI DE AZEVEDO

**ASPECTOS DIAGENÉTICOS, TECTONO-ESTRATIGRÁFICOS E POTENCIAL
EXPLORATÓRIO DE HIDROCARBONETOS DA FORMAÇÃO POTI, BACIA DO
PARNAÍBA, NORDESTE DO BRASIL**

Dissertação apresentada ao Programa de Pós-Graduação em Geociências do Centro de Tecnologia e Geociências da Universidade Federal de Pernambuco como preenchimento parcial dos requisitos para obtenção do grau de Mestre em Geociências.

Área de concentração: Geologia sedimentar e ambiental

Aprovado em: 29/07/2022.

BANCA EXAMINADORA

Prof. Dr. Mário Ferreira de Lima Filho (Orientador)
Universidade Federal de Pernambuco - UFPE

Prof. Dr. Claus Fallgatter (Examinador Interno)
Universidade Federal de Pernambuco - UFPE

Profª. Drª. Marcela Marques Vieira (Examinadora Externa)
Universidade Federal do Rio Grande do Norte - UFRN

AGRADECIMENTOS

À minha família pelo apoio incondicional em todos os momentos.

Aos professores Mário F. de Lima Filho e Zenilda Vieira Batista por todo apoio científico e carinho durante o período de mestrado. À professora Sônia pelo apoio, carinho e ajuda nos momentos importantes. Ao pesquisador visitante José Gedson Fernandes da Silva pelo apoio e ajuda na resolução das dificuldades.

Ao Conselho Nacional de Desenvolvimento Científico (CNPQ-143630/2019-9) e Programa de Recursos Humanos (PRH-47-Finep) da Agência Nacional de Petróleo, Gás Natural e Biocombustíveis (ANP) pela concessão de bolsas, através da Resolução nº 50/2015, que foram de extrema importância. À Fundação de Apoio ao Desenvolvimento da Universidade Federal de Pernambuco (FADE).

À Universidade Federal de Pernambuco (UFPE), por me acolher e cumprir, brilhantemente, a sua missão de formar os seus alunos e realizar o sonho desses.

Aos amigos Emmanuel Franco Neto, José Alves, Willian Alexandre, Wilson Andrade, Valdielly L. Silva e Thales pelo apoio técnico e ajuda no desenvolvimento do trabalho.

Ao Laboratório de Geologia Sedimentar (LAGESE) e Universidade Federal de Alagoas (UFAL-CETC) pela infraestrutura usada para o desenvolvimento e finalização do trabalho. Ao professor Virgílio Neumann por disponibilizar o equipamento de catodoluminescência e matérias de consulta.

À secretaria de pós-graduação pelo apoio e resolução de problemas, especialmente nesse período de pandemia.

Muito obrigado à todos que de alguma forma ajudaram na finalização dessa dissertação.

RESUMO

Na bacia Parnaíba, os estudos sobre sistemas petrolíferos estão aumentando em função dos investimentos feitos por empresas que compraram blocos em diferentes áreas da bacia. A ANP também investiu na coleta de dados geofísicos e geoquímicos, além de fomentar parcerias com as universidades para expandir o conhecimento geológico na bacia. Esta pesquisa apresenta uma análise sedimentológica e estratigráfica de detalhe da Formação Poti exposta à sudeste da cidade de Itaueira, Bacia do Parnaíba. O estudo tem como objetivo a caracterização faciológica, definição dos sistemas deposicionais, identificar os eventos diagenéticos e fazer considerações sobre a proveniência e qualidade das rochas como reservatório da Formação Poti. Neste trabalho, foram aplicadas as técnicas de catodoluminescência, difratometria de Raios-x, descrição de fácies, medição de paleocorrentes e petrografia, com impregnação por epóxi azul para determinar a porosidade. Foram identificadas cinco fácies sedimentares, as quais foram associadas à um ambiente de plataforma dominada por ondas de tempestade, dividido em duas associações de fácies: *Shoreface Superior* (AF1) e *Shoreface Inferior/Offshore* (AF2). As plataformas registraram variação climática periódica, que mudava a linha de base de ação das ondas, e variações eustáticas na plataforma, evidenciada pelo padrão deposicional. Os arenitos têm uma composição detritica correspondente à subarcósios modificados para quartzoarenitos devido as modificações diagenéticas, texturalmente imaturos e composicionalmente maduros. A integração de dados indica que o Domínio Rio Grande do Norte (Terreno Granjeiro) na Província Borborema, é a principal fonte de sedimentos de idade Arqueana e Neoproterozóica, assim como os granitos brasileiros do tipo I, representando blocos continentais, segundo o diagrama de ambiente tectônico fonte. Os processos diagenéticos identificados foram: infiltração mecânica de argila, compactação mecânica e química, cimentação de sílica e hematita, alteração de grãos instáveis, dissolução, e substituição. Há ocorrências pouco significativas de cimento óxido de titânio e carbonático, identificadas por catodoluminescência. A porosidade média dessas rochas é 11%, sendo representada por porosidade intergranular, intragranular, móldica. Os principais processos diagenéticos que modificaram a porosidade primária, foram a infiltração mecânica de argila e cimentação de hematita. A compactação mecânica e química e mecânica tiveram pouca relevância, já que não foram identificados grãos fraturados, micas deformadas e formação de pseudomatriz em grande proporção, o que conferiu à rocha um empacotamento fraco grão-suportado. Portanto, mesmo a diagênese tendo modificado a porosidade original desses arenitos, a associação de fácies de *Shoreface Superior* e camadas superiores dos arenitos estudados apresentaram as melhores características de reservatório.

Palavras-chave: Formação Poti; Bacia do Parnaíba; rochas reservatório; sistemas petrolíferos; diagênese de arenitos; caracterização petrográfica.

ABSTRACT

In the Parnaíba basin, studies on petroleum systems are increasing due to investments made by companies that have purchased blocks in different areas of the basin. The ANP also invested in the acquisition of geophysical and geochemical data, in addition to encouraging partnerships with universities to expand geological knowledge in the basin. This research presents a detailed sedimentological and stratigraphic analysis of the Poti Formation exposed in the southeast of the Itaueira city, Parnaíba Basin. The study produce faciological characterization, definition of depositional systems, and identified the diagenetic events and produced considerations about the provenance and reservoir quality of the Poti Formation sandstones. In this work, the techniques of cathodoluminescence, X-ray diffractometry, facies description, paleocurrent measurement and, petrography were performed. The blue epoxy impregnation on 15 thin sections determined porosity quantification. Five sedimentary facies were identified and associated to a shallow storm wave- dominated platform environment, divided into two facies associations: Upper Shoreface (AF1) and Lower Shoreface/Offshore (AF2). This associations recorded periodic climatic variation, which changed the fair-weather wave base line, and eustatic variations in the platform, evidenced by the depositional pattern. The sandstones exhibits a detrital composition corresponding to subarkose sandstones, modified to quartzarenites due to diagenetic modifications, texturally immature, and compositionally mature. The data integration indicates that the Rio Grande do Norte Domain (Granjeiro Terrain), in the Borborema Province, is the main source of sediments of Archean and Neoproterozoic age, as well as the type I Brasiliano granites, representing continental blocks, according to the tectonic source environment diagram. Mechanical infiltration of clay, mechanical and chemical compaction, cementation of silica and hematite, alteration of unstable grains, dissolution, and substitution were the diagenetic processes identified. There are negligible occurrences of titanium oxide and carbonate cement, identified by cathodoluminescence. The average porosity of these rocks is 11%, represented by intergranular, intragranular and moldic porosity. The main diagenetic processes that modified the primary porosity were mechanical infiltration of clay and hematite cementation. Mechanical, chemical and mechanical compaction had little relevance, since fractured grains, deformed micas and pseudomatrix formation in large proportions were not identified, which gave the rock a weak grain-supported packing. Therefore, even though diagenesis modified the original porosity of these sandstones, the association of Upper Shoreface facies and upper layers of the studied sandstones showed the best reservoir characteristics.

Keywords: Poti Formation; Parnaíba Basin; reservoir rocks; petroleum systems; sandstone diagenesis; petrographic characterization.

LISTA DE FIGURAS

DISSERTAÇÃO

Figura 1 –	Embasamento da Bacia do Parnaíba e suas delimitações estruturais	20
Figura 2 –	Principais estruturas da Bacia do Parnaíba.	21
Figura 3 –	Carta litoestratigráfica da Bacia do Parnaíba	22
Figura 4 –	Proposta de classificação de arenitos de FOLK (1968) que termina as quantidades relativas dos fragmentos de rocha, feldspatos e grãos de quartzo.	28
Figura 5 –	A) Localização da Bacia do Parnaíba no contexto da Plataforma Sul-Americanana; B) Unidades limítrofes da bacia. C) Mapa de localização e logística da área de estudo e dos pontos visitados, onde foram feitos os perfis geológicos e coleta de amostras. As cores utilizadas estão baseadas no mapa geológico da CPRM (2004).	31

ARTIGO 1 – FACIES ANALYSIS AND PROVENANCE CONSIDERATIONS OF THE POTI FORMATION SANDSTONES, UPPER CARBONIFEROUS OF THE PARNAÍBA BASIN, IN THE ITAUEIRA REGION – PI

Figura 1 –	Location map of the Parnaíba Basin. A) South American platform with emphasis on the Parnaíba Basin. B) Geological map of the Parnaíba Basin, highlighting the Poti Formation and the study area near to the region of Itaueira – PI.	36
Figura 2 –	Location map of the stratigraphic logs	39
Figura 3 –	Stratigraphic logs of the studied area and collected sample positioning. The vertical log scale is 1:50 and 1:20, in the log 5, in order to show more details	41
Figura 4 –	Panoramic view of Poti Formation outcrops and erosive contact relationship with the upper unit.	42
Figura 5 –	A) Metric scale swaley cross bedding truncating low angle (100) overlapping layers B) Siliceous deformation bands concentrated in sandstone with hummocky cross-stratification C) Hummocky cross-stratification with metric layers covered by clay (Facies 5). D)	43

Clay layer above the hummocky cross-stratification. E and F) Sandstone with plane-undulating stratification (Facies 3) overlaid by siltstones with plane-undulating stratification/lamination (Facies 4). G) Massive gray mudstone layer on the top of hummocky cross-stratification (Facies 2)

Figura 6 – Detrital composition of the Poti Formation sandstones. A) Subangular to subrounded monocrystalline quartz grains with straight extinction (arrow); the grains exhibit mostly punctual and subordinately straight contacts; PX. B) Rounded polycrystalline quartz grain with undulating extinction (arrow); Potassium feldspar grain with crosshatching (arrow); PX. C) Plagioclase subrounded grain with albite twinning (arrow); PX. D) Muscovite lamellar grain with edges altering to clay; PX. E) Biotite grain altering to iron oxides (arrow); P//. F) Grain of gneiss exhibiting internal orientation and undulating extinction (arrow); PX. Caption: PX – Crossed nicols, P// - Parallel nicols.

Figura 7 – Poti Formation compositional diagram, according to de Folk (1968).

Figura 8 – Main diagenetic aspects of the Poti Formation. A) Discontinuous quartz overgrowth around quartz grains with clearly visible dust lines (arrow); PX. B) Quartz overgrowth with prismatic shapes at the edges of the quartz grain (arrow); PX. C) Partial dissolution process generating secondary porosity on feldspar grain surfaces (arrow); P//. D) Discontinuous hematite cementation (yellow arrow) and mechanical infiltration of clay into the intergranular spaces (blue arrow); P//. Caption: PX – Crossed nicols, P// - Parallel nicols

Figura 9 – Tectonic discrimination diagrams for the Poti Formation sandstones of the Parnaíba Basin. A) QmFLt triangular diagram. B) QtFLt triangular diagram. Both indicate craton interior field.

Figura 10 – Paleocurrents measured in the cross-stratified sandstones of the Poti Formation. The measurements show a predominance for NW and dispersion for W and SW, in all six stratigraphic logs. Number of measurements - 23.

- Figura 11 – Diffractograms exhibiting the most important mineral peaks 49 identified.
- Figura 12 – A) High relief and interference colors in a rounded zircon grain. B) 50 Rounded epidote grain with low relief and high interference color. C) Rounded rutile grains rarely alter to titanium oxide. D) Prismatic titanite grain with high relief. E) Sub-rounded amphibole grain with moderate relief. F) Prismatic and elongated zircon grain. G) Amphibole grain with moderate relief. H) Tourmaline grain with numerous inclusions showing high interference colors. I) Amphibole grain with corroded edges and rounded corners. The scale bar measures 60 micrometers
- Figura 13 – A) Location of the Parnaíba Basin on the South American Platform. 54 B) Geographical distribution of the Poti Formation in the Parnaíba Basin. C) Paleogeographic contextualization of the Parnaíba Basin in the Carboniferous. The arrow indicates the paleocurrent recorded in the field in accordance with the paleogeographic position; Parnaíba Basin in yellow; during this period, the Tethys Sea influenced in the rising epicontinental seas on the basin. D) Depositional model of the Poti Formation and location of the main subenvironments of the storm wave-dominated shallow platform system
- Figura 14 – Cathodoluminescence applied on quartz and feldspar grains from 56 the Poti Formation. A) Brown quartz grains (yellow arrow). B) Fragment of siltstone exhibiting dark brown color (yellow arrow). C) Prismatic feldspar grains exhibiting bright blue color (white arrow. D) Clay and cements without luminescence (blue arrow) and feldspars with a bright blue color (yellow arrow).

ARTIGO 2 – PETROGRAPHY, DIAGENESIS, PROVENANCE CONSIDERATIONS, AND
RESERVOIR CHARACTERISTICS OF THE POTI FORMATION, PARNAÍBA BASIN,
NORTHEASTERN BRAZIL

- Figura 1 – A) Localization of the Parnaíba Basin contextualized in the South- 74 American Platform. B) Simplified geological map of the Parnaíba

Basin and the basement tectonic subdivision. TOAA: Tocantins-Araguaia Lineament; FUSL: Ferrer-Urbano Santos Lineament; PSIL: Picos-Santa Inês Lineament; TBL: Transbrasiliano Lineament. Modified of CPRM (2004).

- Figura 2 – Localization map of the study area and stratigraphic logs of the Poti 74 Formation
- Figura 3 – Simplified chronostratigraphic chart of the Parnaíba Basin, Canindé 75 Group. Adapted from Vaz et al (2007).
- Figura 4 – Panoramic view of the Poti Formation sandstones in the Itaueira 77 region, Parnaíba Basin and vertical distribution of the sedimentary facies. The blue line represents an unconformity between the Poti Formation and the overlying Piauí Formation
- Figura 5 – A) Fine-grained sandstone exhibiting fining-upward 79 stratifications/laminations. The quartz grain is rounded to subrounded and bimodal (P//). B) Fine-grained sandstone with subrounded and well-sorted grains, which show homogeneous framework without orientation (P//). C) Fine-grained sandstone with subrounded and poorly sorted quartz grains, exhibiting straight extinction, predominantly (PX). D) Polycrystalline quartz grain with internal sutured contacts between grains (PX). E) Plagioclase grain with poorly preserved albite twinning (PX). F) Poorly preserved Potassium feldspar with crosshatched twinning, exhibiting border limit slightly replaced by clay minerals (PX).
- Figura 6 – A) Subrounded quartzite grain with sutured grains and preferential 80 orientation (PX). B) Rounded siltstone lithic fragment. C) Prismatic zircon grain, exhibiting high interference colors. D) Prismatic epidote grain with high, intermediate interference colors, and a smaller relief compared to zircon grains (PX). E) Rutile grain showing darker borders and dark red interference colors. F) Tourmaline grain with medium relief and dark borders, being common the presence of inclusions (PX). Zr- Zircon; Ru- Rutile; Ep- Epidote; Tur- Tourmaline.

- Figura 7 – Classification of the Poti Formation sandstones, according to Folk 81 (1968).
- Figura 8 – Stratigraphic logs of the Poti Formation exhibiting sedimentary 82 structures, main lithology and collected sample of each log. Horizontal scale is 1:50.
- Figura 9 – Diffractograms of the Poti Formation. Emphasis in the illite and 83 kaolinite peaks. Different colors identify the samples.
- Figura 10 – A) Clay in the form of discontinuous cuticles (arrow) 85 enveloping the quartz grain - (P//). B) Occurrence of pendular aggregates (arrow), which are typical in the vadose zone infiltration - (P//). C) Infiltrated clay with a meniscus habit (arrow), which is characteristic of vadose zones - (P//). D) Clay aggregate morphology occupying the primary porosity spaces (arrow) - (P//). E) Muscovite grain slightly bent and exhibiting altered edges (arrow) - (PX). F) Fractured quartz grain (arrow), indicating the mechanical compaction degree. Note the infiltrated clay within the open fractures (P//). G) Poti Formation sandstones exhibiting low proportions of concave-convex contacts between quartz grains (arrow) - (PX). H) Occurrence of punctual contacts (arrows) - (P//). PX-Crossed polarizers; P// - Parallel polarizers.
- Figura 11 – A) Hematite cement as aggregates filling primary porosity (yellow 86 arrow) - P//. B) Biotite grain being replaced by Fe oxides at the cleavage orientations (black arrow) - P//. C) Discontinuous quartz overgrowth on the grain surface (yellow arrow) - PX. D) Silica overgrowth on the surface of quartz grains with prismatic forms (arrow) - PX
- Figura 12 – Cathodoluminescence of the Poti Formation sandstones. A and B) 87 The yellow and orange arrow indicate low presence of calcite and dolomite minerals in the rock framework, respectively. C and D) Rutile grains altering to titanium oxide along its borders limit (arrows).
- Figura 13 – A) Authigenic clay replacing muscovite grain on the expanded 89 lamellae's edges (arrow) - PX. B) Total replacement of plagioclase

grain to kaolinite (arrow) - PX. C) Alteration process on biotite grain, forming oxide Fe cement (arrow) - PX. D) Secondary porosity formation due to partial dissolution of potassium feldspar grain (arrow) - P//. E) Substitution process acting on plagioclase grains that forms kaolinite (arrow) - PX. F) Total substitution process on muscovite grain, resulting in booklet-shaped kaolinite cement (arrows) - PX.

Figura 14 –

A) The primary intergranular porosity. Detail of permeability based 90 on petrographic analyses in fine-grained sandstones (black arrows; P//). B) Secondary porosity within feldspar grains (P//). C) Moldic porosity caused by increasing mechanical compaction that produces total grain substitution (yellow arrow; P//). D) Fracturing porosity induced by mechanical compaction and filled with infiltrated clay (yellow arrow; PX).

Figura 15 –

Association between vertical and lateral porosity variation, silica 95 cementation and hematite cementation, in the Poti Formation stratigraphic logs. Log 1 (samples 1 - 5); log 2 (samples 6 - 9); log 3 (samples 10 - 13), log 4 (samples 14 - 15).

Figura 16 –

Contact between the Poti and Piauí formations, emphasizing the 96 general characteristics of faults and fractures, already studied by previous hydrocarbon generation models in the Parnaíba Basin.

Figura 17 –

A) Lower cement and clay values characterize the large pores in the 97 sandstones next to the intrusion of the Sardinha Formation. B and C) Lower shoreface/Offshore sandstones, characterized by a greater amount of infiltrated clay (arrows), silica, and hematite cementation (blue arrows). D) Upper shoreface sandstones exhibiting good porosity and permeability (arrows).

Figura 18 –

Porosity types and modal quantities identified by petrographic 97 analyses. From sample 6 to 9, the increase on porosity is noticeable, due to the predominance of upper shoreface facies association. The rise in porosity occurs particularly towards the top of the stratigraphic logs, and next to the influence of the Sardinha

Formation, where the process of secondary porosity generation is more prominent, reaching a maximum value of 4.0 %.

LISTA DE TABELAS

ARTIGO 1 – FACIES ANALYSIS AND PROVENANCE CONSIDERATIONS OF THE POTI FORMATION SANDSTONES, UPPER CARBONIFEROUS OF THE PARNAÍBA BASIN, IN THE ITAUEIRA REGION – PI

Tabela 1 –	Sedimentary facies description table of the Poti Formation, in the Itaueira region – PI.	41
------------	---	----

ARTIGO 2 – PETROGRAPHY, DIAGENESIS, PROVENANCE CONSIDERATIONS, AND RESERVOIR CHARACTERISTICS OF THE POTI FORMATION, PARNAÍBA BASIN, NORTHEASTERN BRAZIL

Tabela 1 –	Composition and petrographic features of the Poti Formation	81
Tabela 2 –	Diagenetic events that occurred in the Poti Formation	91

SUMÁRIO

1	INTRODUÇÃO	18
2	OBJETIVO GERAL	19
2.1	OBJETIVOS ESPECÍFICOS	19
3	CONTEXTO GEOLÓGICO	20
3.1	ARCABOUÇO ESTRUTURAL	20
3.2	ARCABOUÇO ESTRATIGRÁFICO	21
3.3	PROCESSOS TECTÔNICOS E SEDIMENTARES	22
3.4	FORMAÇÃO POTI	23
3.5	HIDROCARBONETOS NA BACIA DO PARNAÍBA	24
4	MATERIAIS E MÉTODOS	26
4.1	REVISÃO BIBLIOGRÁFICA	26
4.2	ANÁLISE FACIOLÓGICA E PROVENIÊNCIA	26
4.3	MICROSCOPIA ÓPTICA	27
4.3.1	<i>ABORDAGEM QUANTITATIVA</i>	27
4.4	DIFRATOMETRIA DE RAIOS – X	28
4.5	CATODOLUMINESCÊNCIA	29
4.6	CARACTERIZAÇÃO DIAGENÉTICA	29
4.7	ÁREA DE ESTUDO	30
5	RESULTADOS	32
5.1	ARTIGO 1 – FACIES ANALYSIS AND PROVENANCE CONSIDERATIONS OF THE POTI FORMATION SANDSTONES, UPPER CARBONIFEROUS OF THE PARNAÍBA BASIN, IN THE ITAUEIRA REGION – PI	33
5.2	ARTIGO 2 – PETROGRAPHY, DIAGENESIS, PROVENANCE CONSIDERATIONS, AND RESERVOIR CHARACTERISTICS OF THE POTI FORMATION, PARNAÍBA BASIN, NORTHEASTERN BRAZIL	70
6	CONSIDERAÇÕES FINAIS	111
	REFERÊNCIAS	113

1 INTRODUÇÃO

As pesquisas em torno da Bacia do Parnaíba começaram identificando e posicionando estratigraficamente as rochas do Paleozóico, através de trabalhos regionais (MESNER & WOLDRIDGE, 1964; LIMA & LEITE, 1984; PAIVA & MIRANDA, 1937 *apud* GÓES, 1995). Com o objetivo de tentar encontrar unidades que poderiam conter hidrocarbonetos, os trabalhos na bacia intensificaram-se a partir da década de 50, com o Conselho Nacional do Petróleo.

Mesmo com os avanços realizados, a Bacia do Parnaíba ainda carece de estudos locais em relação às diversas unidades de rochas que a compõe, tanto nos aspectos estratigráficos e faciológicos, como potencial para hidrocarbonetos. Apesar de aumentarem na década de 50, as pesquisas possuíam caráter regional e focava nos aspectos econômicos LIMA & LEITE, 1978; VAZ et, 2007). Apesar das ótimas exposições em afloramento, a Formação Poti possui uma quantidade de pesquisas restrita e pequena associada a descrição de fácies, paleogeografia e aspectos paleoambientais (CAPUTO, 1984; GÓES, 1995).

Essa dissertação aborda uma análise estratigráfica detalhada da Formação Poti baseada em seções estratigráficas e dados nanomineralógicos da porção central da Bacia do Parnaíba, à sudoeste da cidade de Itaueiras. Isso permitiu a reconstrução paleoambiental da seção Neocarbonífera a partir da descrição e a associação de fácies. Esses dados e a coleta de paleocorrentes produziu um arcabouço geral desses depósitos.

Além disso, por meio deste estudo estratigráfico integrado à análises petrográficas, sedimentológica e petrológicas, espera-se contribuir para um melhor entendimento das condições climáticas, deposicionais e considerações sobre a proveniência desses arenitos, bem como sobre a influência dos processos e constituintes diagenéticos na qualidade dessas rochas como reservatório de hidrocarbonetos.

2 OBJETIVO GERAL

O objetivo deste trabalho é caracterizar os eventos diagenéticos, paleogeografia e evolução tectono-estratigráfica dos depósitos da Formação Poti, contextualizados no mais importante evento geológico do Devoniano da Bacia do Parnaíba, bem como a viabilidade exploratória das sequências, já sugerida em estudos anteriores. Dessa forma, os dados oriundos desta pesquisa contribuíram para a caracterização dos arenitos da Formação Poti como rocha reservatório.

2.1 OBJETIVOS ESPECÍFICOS

- 1 – Fazer análise faciológica e determinar a proveniência dos depósitos estudados.
- 2 – Fazer a caracterização petrográfica e diagenética dos arenitos da Formação Poti.
- 3 – Fazer interpretação paleoambiental do período Neocarbonífero.
- 4 – Identificar os processos e constituintes diagenéticos que influenciam a qualidade dessas rochas como reservatórios de hidrocarbonetos.

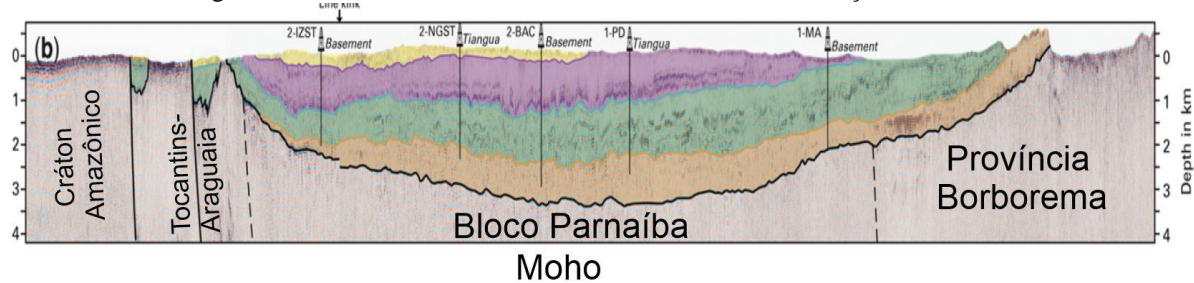
3 CONTEXTO GEOLÓGICO

3.1 AR CABOUÇO ESTRUTURAL

A Bacia do Parnaíba, classificada como intracratônica, ocorre na região Nordeste e Norte do Brasil, abrangendo os estados do Piauí, Maranhão, Ceará, Tocantins e Pará. A bacia possui forma ovalada e distribui-se por cerca de 600.000 km², tendo uma cobertura sedimentar de idade paleozóica, com espessura variando de 2,0 a 3,5 km (HASUI *et al.*, 2012; VAZ *et al.*, 2007; COELHO *et al.*, 2018).

As rochas do embasamento, definidas por sísmica de reflexão, são constituídas pela Província Borborema a leste, bloco central do Parnaíba, cinturão de dobramentos e Cráton Amazônico, ambos na borda oeste (DALY *et al.*, 2014). Esse embasamento desenvolveu-se durante estágio de estabilização da Plataforma Sul-Americana, cuja origem está associada a eventos térmicos finais e pós-orogênicos do Ciclo Brasiliense (Figura 01). O contexto estrutural geral desta unidade geotectônica inclui estruturas grabenformes, blocos falhados, dobras e outras estruturas resultantes da inclusão de corpos ígneos mesozoicos (OLIVEIRA E MOHRIAK, 2003; VAZ *et al.*, 2007).

Figura 1 - Embasamento da Bacia do Parnaíba e suas delimitações estruturais

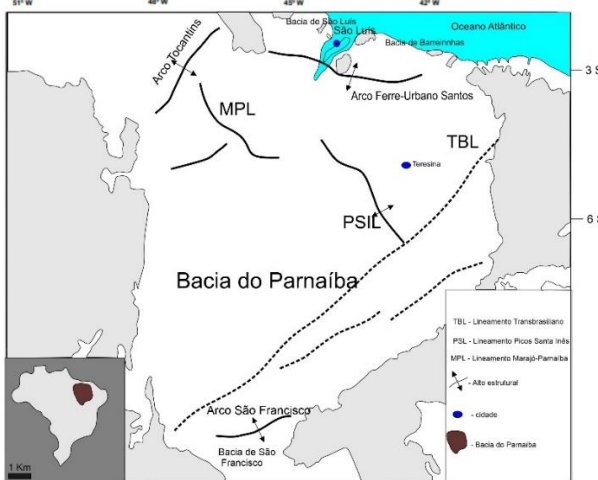


Fonte: DALY et al. (2018)

Estruturalmente, é limitada a noroeste pelo Arco Tocantins, que a separa das Bacias do Marajó e Amazonas; a sul pelo Arco São Francisco, que a separa da Bacia do São Francisco e a norte pelo Arco Ferre-Urbano-Santos, feição flexural positiva, relacionada com a abertura do Oceano Atlântico Sul durante o Mesozoico, que separa a Bacia do Parnaíba das de São Luiz e Barreirinhas, na margem equatorial (Figura 02). Além disso, é limitada por cinturões de dobramentos e lineamentos estruturais (GÓES, 1995; CAPUTO, 2005; VAZ *et al.*, 2007).

Os *riffs* formados entre o final do Proterozóico e início do Paleozóico controlaram o depocentro inicial da Bacia do Parnaíba. O Gráben de Jaibaras, Jagrarapi, Cococi e São Julião são correlacionáveis aos grábens identificados por dados sísmicos, os quais são preenchidos por sedimentos imaturos do Ordoviciano (OLIVEIRA & MOHRIAK, 2003; CUNHA, 1986).

Figura 2 - Principais estruturas da Bacia do Parnaíba.



Fonte: Adaptado de GÓES (1995)

3.2 AR CABOUÇO ESTRATIGRÁFICO

As rochas sedimentares, predominantemente siliciclásticas, e magmáticas definem a litoestratigrafia da Bacia do Parnaíba (Figura 03), agrupadas em cinco supersequências: Siluriana (Grupo Serra Grande), Mesodevoniana (Grupo Canindé), Carbonífera-Eotriássica (Grupo Balsas), Jurássica (Formação Pastos Bons) e Cretácea (Formações Codó, Corda, Grajaú e Itapecuru). As unidades paleozóicas são separadas por amplas discordâncias regionais, geradas por eventos erosivos de magnitude temporal significativa (GÓES E FEIJÓ, 1994, VAZ *et al*, 2007, HASUI *et al*, 2012).

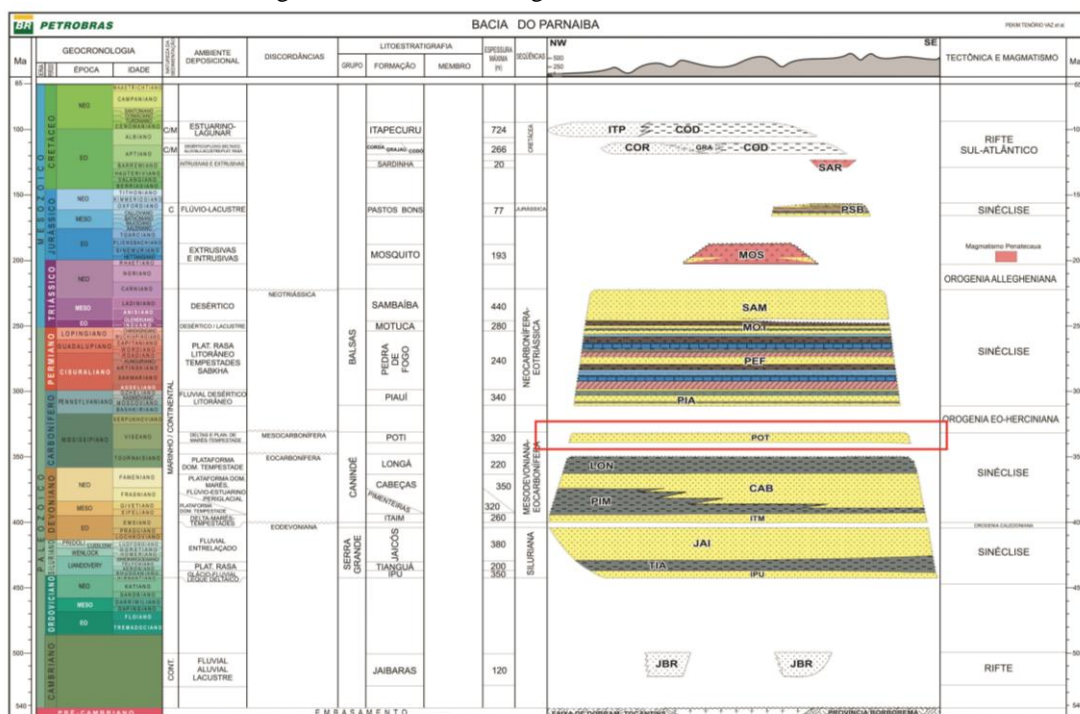
O Grupo Serra Grande (Supersequência siluriana) é composta da base para o topo pelas Formações Ipu, Tianguá e Jaicós, depositadas em ambientes glaciais e periglaciais, passando a ambientes neríticos e continentais (GÓES E FEIJÓ, 1994). Esse grupo representa a primeira incursão marinha na Bacia do Parnaíba, caracterizada por um ciclo transgressivo-regressivo completo. O contato com o Grupo Canindé, sobreposto, é discordante e se revela pela ausência de rochas eodevonianas no registro sedimentar (VAZ *et al*, 2007; CAPUTO E LIMA, 1984; HASUI *et al*, 2012).

O Grupo Canindé (Supersequência Carbonífera) é composto pelas Formações Itaim, Pimenteiras, Cabeças, Longá e Poti e representa a maior ingressão marinha na Bacia do Parnaíba. Essas rochas foram depositadas em ambientes deltaicos, plataformais e neríticos dominados por tempestades, além de ambientes com influência periglacial (GÓES E FEIJÓ, 1994; VAZ *et al*, 2007; CAPUTO, 1984). Segundo SILVA (2013) as rochas ricas em carbono orgânico das unidades Pimenteiras e Longá, e os arenitos das unidades Cabeças e Poti estão

relacionadas como rochas geradoras e reservatório, respectivamente, sugerindo potencial econômico petrolífero.

O Grupo Balsas (Supersequência Neocarbonífera-Eotriássica) é representado pelas Formações Piauí, Pedra de Fogo, Motuca e Sambaíba. Uma expressiva discordância regional é atribuída aos reflexos da orogenia Eo-herciniana, evidenciada pela ausência de rochas do Carbonífero Inferior e Superior. A sedimentação ocorreu em ambiente eólicos, lacustres e continentais relacionados a profundas mudanças climáticas na Bacia do Parnaíba, em virtude da formação do continente Pangea (SILVA *et al*, 2003; HASUI *et al*, 2012).

Figura 3 - Carta litoestratigráfica da Bacia do Parnaíba



Fonte: VAZ ET AL. (2007)

3.3 PROCESSOS TECTÔNICOS E SEDIMENTARES

O início do ciclo deposicional da Bacia do Parnaíba ocorreu após a estabilização de seu embasamento. Em seguida às deformações finais e pós orogênicas do Ciclo Brasiliano-Pan Africano e a formação de *riffs*, com rochas imaturas do Ordoviciano, iniciou-se a deposição de 5 supersequências. Essas rochas sedimentares foram depositadas do Siluriano ao Cretáceo e intrudidas por rochas vulcânicas jurássicas e cretáceas. E Adicionalmente registravam a ocorrência de outros eventos geológicos (ALMEIDA E CARNEIRO, 2004; VAZ *et al.*, 2007).

As três primeiras supersequências possuem rochas formadas em ambientes neríticos, cuja deposição foi causada por variações eustáticas do nível do mar. Como resultado de movimentos epirogênicos ocorridos na borda ativa do Gondwana, foram originados os contatos erosivos e

discordâncias regionais na Bacia do Parnaíba e em outras sinéclises brasileiras (ALMEIDA e CARNEIRO, 2004).

A entrada dos mares epicontinentais realizou-se pela margem ativa sudoeste do Gondwana e por inundações do mar Tethys, através de bacias que hoje se localizam no norte africano. O grupo Serra Grande iniciou o ciclo deposicional com a Formação Tianguá, através da ingressão marinha do mar Tethys. Devido aos efeitos da orogenia Caledoniana na margem sudoeste do Gondwana, houve uma regressão marinha. O grupo Canindé registra a maior ingressão marinha na Bacia do Parnaíba a partir do Tethys. O Grupo Balsas registrou a presença de depósitos marinhos no Permo-Carbonífero e a saída desses no Neopermiano. Nesse contexto há a formação do Pangea (ALMEIDA e CARNEIRO, 2004; VAZ *et al.*, 2007)

A sequência jurássica é representada pela Formação Pastos Bons, depositada em paleodepressões. Essas feições foram geradas com a subsidência proporcionada pelo peso de rochas basálticas da Formação Mosquito. Seu sistema deposicional era composto por lagos com influência de incursões fluviais e com condições anóxicas, sob climas áridos a semiáridos, que propiciaram a preservação de fósseis. Sua deposição cessou no fim do Cretáceo Inferior, quando teve início a abertura do Atlântico Equatorial (VAZ *et al.*, 2007; CARDOSO *et al.*, 2017)

A deposição da sequência cretácea ocorreu na porção norte e noroeste da Bacia do Parnaíba logo após a formação do oceano atlântico, o qual foi o responsável pela entrada marinha pela Bacia do Maranhão e deposição das Formações Codó e Grajaú. Esses depósitos são contemporâneos interdigitadas com a Formção desértica Corda (VAZ *et al.*, 2007). A Formação Itapecuru, de até 800 metros, recobre discordantemente as Formações Codó e Grajaú e ocupa de 50 a 60% da Bacia de seção cretácea da Bacia do Parnaíba (ROSSETTI & GÓES, 2003)

3.4 FORMAÇÃO POTI

A Formação Poti (Eocarbonífera) está em contato concordante e gradacional com a Formação Longá, e por vezes se torna difícil diferenciá-las devido à semelhança de litologias. Entretanto na região sul e sudoeste do Piauí, o contato é brusco. O contato superior com a Formação Piauí, unidade sotoposta, é nitidamente discordante marcado por superfície erosiva regional (LIMA & LEITE, 1978; SANTOS & CARVALHO, 2009). A granulometria das rochas da Formação Poti diminui a partir da porção sul em direção à norte (LIMA & LEITE, 1978; GÓES, 1995).

MESNER & WOOLDRIDGE (1964) subdividiram a Formação Poti em dois membros, ambos compostos por arenitos conglomeráticos intercalados com folhelhos micáceos, sendo que o membro superior possui intercalações com leitos finos de carvão. LIMA & LEITE (1978), utilizando essa subdivisão, determinaram que a unidade superior, mais representativa na região leste de Floriano (PI), é composta por arenitos finos à médios intercalados com siltitos e folhelhos. Enquanto que a unidade inferior, na região sul, é constituída por arenitos conglomeráticos e conglomerados polimíticos.

Segundo CAPUTO (1984) a Formação Poti é dividida em quatro unidades que alcançam 300 metros. A unidade basal é composta por arenitos finos e médios, com fragmentos de rochas, intercalados com siltitos. Sotopostos à essa unidade ocorrem siltitos, folhelhos micáceos e arenitos médios e grossos com fragmentos de rocha, pertencentes às unidades intermediárias. Na unidade superior há ocorrência de folhelhos e siltitos intercalados com diamictitos.

GÓES (1995), a partir da análise de poços feitos pela Petrobrás e do Projeto de Carvão, determinou que a Formação Poti é composta por Arenitos médios e finos, intercalados com siltitos e folhelhos. Não foram encontrados vestígios de influência glacial, porém a possibilidade não foi descartada.

A base da Formação Poti corresponde a sistemas deposicionais fluviais, sobrepostos à Formação Longá, com ocorrência de estratificação cruzada acanalada formando perfis granodecrescente ascendentes. Estes últimos estão sobrepostos por sistemas deposicionais de deltas e planícies de maré com influência de ondas de tempestade, que são representados por arenitos intercalados com siltitos e folhelhos com estratificação plano paralela e estratificação cruzada *Hummocky* (GÓES *et al*, 1994; SANTOS & CARVALHO, 2009). Ainda ocorrem processos de influência continental com caráter erosivo e de deposição rápida, formada por conglomerados sobrepostos por siltitos (LIMA & LEITE, 1978).

A partir de análise de afloramentos da borda leste e oeste foram determinados ambientes de planícies de maré e deltaico/estuarina com depósitos plataformais, litorâneos e fluviais. O clima era temperado, atestado pela ausência de carbonatos (GÓES, 1995). A sedimentação começa como marinha sendo substituída por depósitos continentais, que são a tendência geral da bacia do Parnaíba à continentalização (MESNER & WOOLDRIDGE, 1964).

3.5 HIDROCARBONETOS NA BACIA DO PARNAÍBA

As pesquisas pioneiras foram realizadas na década de 50 pelo Conselho Nacional de Petróleo (CNP), com estudos de geologia de superfície e perfuração de dois poços na região

centro-sul. A Petrobrás, entre as décadas de 50 e 60 passou a utilizar dados sismográficos para identificação de hidrocarbonetos nas bacias paleozóicas, entretanto a grande quantidade de soleiras e *sills* produziam resultados inconclusivos. Utilizou mapeamento geológico e estruturas de campo para perfuração de 27 poços pioneiros e estratigráficos, porém com resultados incompletos, logo as atividades na bacia foram interrompidas no ano de 1966. Entretanto foram reiniciadas em 1975, através de campanhas sísmicas, de aeromagnetometria e perfuração de quatro poços pioneiros, mesmo havendo dúvidas quanto a capacidade da existência de hidrocarbonetos (GÓES *et al.*, 1990; BACOCCOLI, 2003; MENDONÇA *et al.*, 2004).

Na década de 80 ocorreram as primeiras descobertas colocando, novamente em pauta o potencial petrolífero dessas bacias, agora averiguados pela geologia de subsuperfície, dados gravimétricos, magnetometria e/ou por malhas de amostragem estratigráfica, entretanto enfrentaram os mesmos empecilhos, em relação a interpretação dos dados, identificados na sísmica pela Petrobrás. No final da década de 80 iniciou-se uma fase exploratória com reinterpretação de dados e novos levantamentos (GÓES *et al.*, 1990; BACOCCOLI, 2003; MENDONÇA *et al.*, 2004).

Houve êxito em poços de Testa Branca 2 no estado do Maranhão, em que foi testemunhado um intervalo da Formação Cabeças (Mesodevoniana) impregnado de óleo biodegradado, além de outro intervalo de arenitos com queima de gás, referente a Formação Ipu (siluriano). O resultado mais significativo é referente ao poço de Capinzal – MA, perfurado em 1988. Outros resultados incluem a surgência de gás, na Formação Itaim e possibilidade de gás na Formação Cabeças (GÓES *et al.*, 1990; MENDONÇA *et al.*, 2004).

Um sistema petrolífero engloba rocha geradora, reservatório e processos que levam a geração, migração e acumulação destes por trapeamento. As informações em relação a Bacia do Parnaíba realizadas pelos diversos pesquisadores citados, além de produções acadêmicas científicas, mostraram sua capacidade para acumulação de hidrocarbonetos, com todas essas características (GÓES *et al.*, 1990; MAGOON & DOWN, 1994).

A partir da década de 70 houve esforço exploratório para hidrocarbonetos, pelo programa exploratório para carvão, com foco na Formação Poti, e esta carece de análise de fácies detalhada para esse objetivo. SOARES e BORGHI (2014) propuseram um modelo deposicional para o intervalo Longá-Poti, concluindo que existe um play exploratório para hidrocarbonetos. Atualmente, a Formação Poti é considerada a principal rocha reservatório do Carbonífero, com arenitos limpos e de boa porosidade (ANP, 2010; SOARES, 2007; SOARES & BORGHI, 2014).

4 MATERIAIS E MÉTODOS

4.1 REVISÃO BIBLIOGRÁFICA

Esta fase do trabalho compreende pesquisa a partir de livros e artigos científicos (Portal de Periódicos da Capes) e aprofundamento teórico sobre os aspectos geológicos e geoconômicos da Bacia do Parnaíba, em particular para a Formação Poti.

4.2 ANÁLISE FACIOLÓGICA E PROVENIÊNCIA

Para este estudo foram adotadas as propostas de READING (1986) e JAMES & WALKER (1992) que permitiram o detalhamento dos processos sedimentares envolvidos na gênese e associação de diferentes fácies. Essa etapa de campo restringiu-se à individualização de fácies que guardam características próprias de geometria, textura, estruturas sedimentares e padrões de paleocorrentes.

Walker (1992) complementou a análise das fácies cogenéticas e contemporâneas, ao associá-las com os seus respectivos ambientes de sedimentação. Para isso, ressaltou que a continuidade lateral e/ou vertical é fundamental para a interpretação correta da associação de fácies.

Para interpretações de fácies dos depósitos marinhos raso com influência de tempestades, serão utilizados os seguintes autores: WALKER & JAMES (1992), READING (1996) e JAMES & DALRYMPLE (2010).

O modelo de fácies utilizado consiste na descrição, individualização e associação de fácies, as quais são relacionadas a determinados sistemas deposicionais (WALKER, 1992). A nomenclatura de fácies consiste na numeração em ordem crescente, para facilitar a identificação das mesmas.

Atualmente, o termo proveniência possui um significado maior do que indicador de área fonte de sedimentos. Esse termo revela, além da área fonte de sedimentos, a litologia dessa área, ambiente tectônico e condições climáticas predominantes (BOGGS, 2009). Para determinar a proveniência de sedimentos é necessário combinar uma série de métodos e técnicas que incluem análise de minerais pesados, difratometria de Raios-x, catodoluminescência e coleta de paleocorrentes (DICKINSON, 1985).

Para fazer uma discussão sobre as rochas fonte de sedimentos foram realizadas análises petrográficas, medição de paleocorrentes, difratometria de Raios-x, catodoluminescência e análise dos minerais pesados, como indicadores de fonte sedimentar. Para inferir a proveniência

dos arenitos da Formação Poti, foi utilizado o diagrama QtFLt e QmFLt de Dicknson (1985) com o objetivo de determinar os ambientes tectônicos, que são: cráton estável, embasamento soerguido, arco magmático e reciclagem orogênica com sedimentos pobres em feldspatos e fragmentos vulcânicos (Dicknson, 1985)

4.3 MICROSCOPIA ÓPTICA

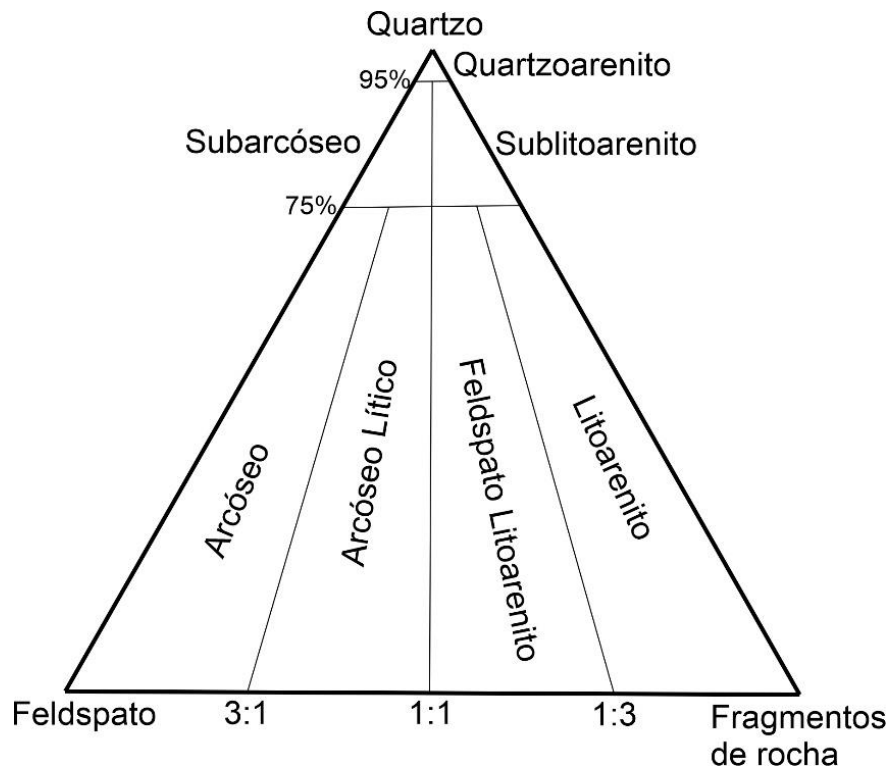
Os parâmetros como textura, composição mineralógica, tipos de porosidade, sequência diagenética e grau de empacotamento foram determinados através da microscopia óptica. As lâminas petrográficas foram impregnadas de *Epoxy Azul*, para uma caracterização correta da porosidade, a partir do método de CESERE *et. al.*, (1989). As lâminas foram produzidas no Laboratório de Laminação do Laboratório de Geologia Sedimentar (LAGESE) na Universidade Federal de Pernambuco (UFPE).

4.3.1 ABORDAGEM QUANTITATIVA

Para a caracterização mineralógica microscópica foram confeccionadas 16 lâminas delgadas sem lamínula, classificadas segundo a proposta de FOLK (1968) (Figura 04) que foi auxiliada por contagem de 300 a 500 pontos (GALEHOUSE, 1971). Características como textura, composição mineralógica e sequência diagenética, proporcionam interpretações de proveniência dos sedimentos. O suporte para esse fim foi conferido pelos laboratórios de laminação e petrografia do LAGESE/UFPE. O índice de empacotamento pode ser determinado como frouxo, normal ou fechado, segundo a classificação de Kahn (1956).

Para verificar os tipos de porosidade (primária e secundária) na descrição petrográfica foram utilizados TIAB & DONALDSON (2012) e Tucker (2001), para interpretações sobre as possíveis causas de geração de poros em rochas siliciclásticas.

Figura 4 - Proposta de classificação de arenitos de FOLK (1968) que termina as quantidades relativas dos fragmentos de rocha, feldspatos e grãos de quartzo.



Fonte: FOLK (1968)

4.4 DIFRATOMETRIA DE RAIOS – X

A difratometria de Raios – X revela detalhes da estrutura interna dos cristais e suas fases. Nas análises padrão as amostras são pulverizadas para obtenção de dados que são identificados através de software específico para esse fim (CULLITY & STOCK, 2014). Através desse método é possível inferir eventos diagenéticos e as fases minerais dos protólitos que deram origem a rocha estudada, reconstruindo, assim, a história geológica do litotipo e aumentando o conhecimento em relação ao seu contexto deposicional.

As análises foram realizadas no Laboratório de Caracterização de Materiais (LACMAT) do Centro de Tecnologias Estratégicas do Nordeste (CETENE), com a utilização de um difratômetro da marca BRUKER, modelo D8 Advance A25-X1. Os dados foram tratados pelo software X'pertHighScore, versão 2.1b da Panalytical. Na base de dados está incluído o PCPDFWIN (Powder Diffraction File-International Center for Diffraction Data), a qual identifica a ocorrência dos minerais mais prováveis na análises.

4.5 CATODOLUMINESCÊNCIA

Esse método fornece informações adicionais sobre proveniência dos grãos de quartzo do arcabouço, gerações de cimentação, fraturamentos e aspectos diagenéticos. Os minerais são bombardeados por feixes de elétrons que emitem fluorescência, fosforescência e comprimento de onda específico, o que ajuda a identificá-los (BERNET & BASSETT 2005). As análises foram realizadas em equipamento Cambridge Image, Technology LTD, modelo cl8200, acoplado à um microscópio óptico Nikon Eclipse E600 POL. As imagens foram tiradas a partir de uma câmera Nikon FDX-35 e as análises foram realizadas no Laboratório de Geologia Sedimentar (LAGESE) da Universidade Federal de Pernambuco (UFPE).

Os padrões de luminescência foram analisados com base nos trabalhos de Bernet & Bassett (2005), AUGUSTSSON (2012), BOGGS e KRINSLEY (2006) e OLIVEIRA (2017).

4.6 CARACTERIZAÇÃO DIAGENÉTICA

A diagênese compreende a atuação de processos nos sedimentos depositados sob uma conjunto de condições físicas e químicas (CHOQUETTE E PRAY, 1970). Logo após a deposição de sedimentos os processos diagenéticos atuam e à medida que o soterramento avança, os grãos passam por compactação e dissolução química e adicionalmente com interferência de fatores ambientais do sítio deposicional (Tucker, 2001). Os processos atuam desde a deposição inicial até o limite de transição para o metamorfismo, o qual ocorre a temperaturas menores que 200º C e pressões menores que 2000 kg/cm².

A diagênese é composta por três fases principais: Eodiagênese, mesodiagenese e telodiagênese. A Eodiagênese ocorre em cerca de 200 metros com temperaturas iguais ou menores que 70º C, compreendendo alterações que resultam da interação do sedimento com águas nos poros, cujas composições químicas são controladas por condições superficiais (KHATRI *et al.*, 2015). Nessa fase os ocorre a expulsão de água dos sedimentos e perda de porosidade, já que a compactação é iniciada (WORDEN *et al.*, 2018).

Na mesodiagenese as alterações nos sedimentos começam em profundidades superiores a 2000 m e com temperaturas superiores ou iguais a 70º C. Esse estágio é controlado pelo aumento da temperatura durante o soterramento e interação com águas de formação, os quais podem ser modificados pela interação com minerais (MORAD *et al.*, 2000; DE ROS, 1998). A mesodiagenese é dividida em rasa, com profundidades de 2 a 3,5 k, e profunda em que as

profundidades são maiores que 3,5 km com temperaturas maiores que 100⁰ C (QUASIM *et al.*, 2021; MORAD, 1991).

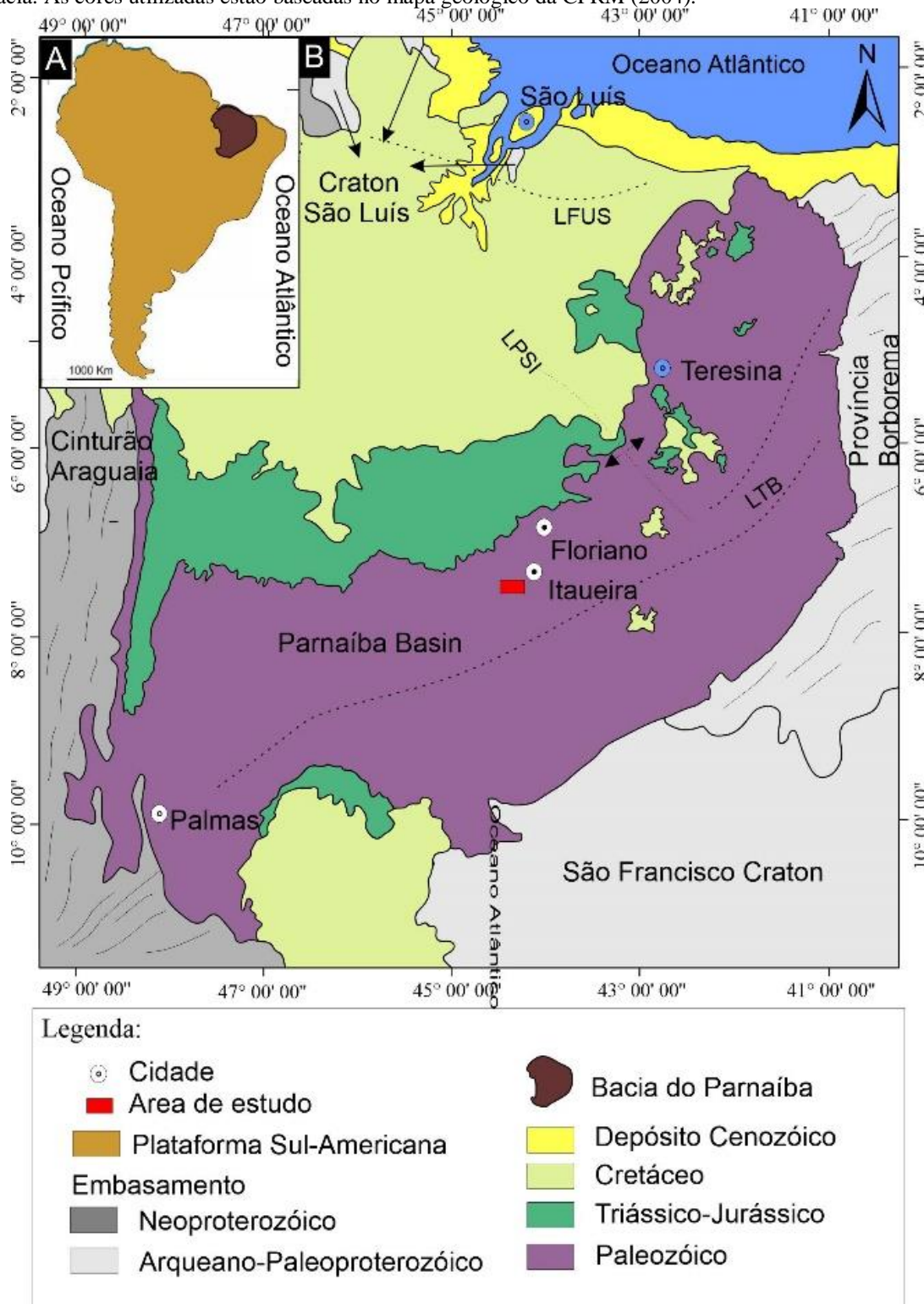
Na telodiagênese os processos atuam em arenitos afetados anteriormente pela mesodiagênese, próximos a superfície de erosão. As rochas são novamente submetidas a condições superficiais por conta do soerguimento e erosão. Além da infiltração profunda de águas meteóricas (MORAD *et al.*, 2000)

Portanto, a evolução diagenética foi avaliada a partir dos dados adquiridos em lâminas petrográficas e somada às análises de Raios X e catodoluminescência, as quais refinaram as interpretações, tendo em vista o detalhamento da história diagenética. Nessa etapa foi utilizado MORAD *et al.* (2010) para determinar os estágios diagenéticos e interpretar os processos ocorridos na unidade estudada.

4.7 ÁREA DE ESTUDO

O mapa geológico do Estado do Piauí (escala 1:1.000000) foi utilizado para determinar a logística de campo e visualização das unidades estratigráficas alvo desta pesquisa. Para a confecção do mapa de localização foi utilizada a Folha cartográfica SB.23 (Teresina). A área de estudo está situada cerca de 300 km ao sul de Teresina, porção sudeste da Bacia do Parnaíba. Os perfis produzidos estão à sudoeste da cidade de Itaueira. (Figura 05)

Figura 5 - A) Localização da Bacia do Parnaíba no contexto da Plataforma Sul-Americana; B) Unidades limítrofes da bacia. As cores utilizadas estão baseadas no mapa geológico da CPRM (2004).



Fonte: O autor (2022)

5 RESULTADOS

Os resultados dessa dissertação encontram-se sob a forma de artigos científicos. O primeiro artigo está intitulado: FACIES ANALYSIS AND PROVENANCE CONSIDERATIONS OF THE POTI FORMATION SANDSTONES, UPPER CARBONIFEROUS OF THE PARNAÍBA BASIN, IN THE ITAUEIRA REGION – PI. Esse artigo está submetido ao Journal of South American Earth Sciences.

O segundo artigo é intitulado: PETROGRAPHY, DIAGENESIS, AND CONSIDERATIONS ABOUT THE RESERVOIR QUALITY OF THE POTI FORMATION SANDSTONES, PARNAÍBA BASIN, NORTHEASTERN BRAZIL. Esse Artigo está submetido ao Journal of South American Earth Sciences.

5.1 ARTIGO 1 - FACIES ANALYSIS AND PROVENANCE CONSIDERATIONS ON THE POTI FORMATION SANDSTONES, UPPER CARBONIFEROUS OF THE PARNAÍBA BASIN, IN THE ITAUEIRA REGION – PI

João Vicente Tavares Calandrini de Azevedo¹, Mário Ferreira de Lima Filho¹, Zenilda Vieira Batista², Sonia Maria Oliveira Agostinho¹, Willian Alexandre Lima de Moura³

¹Programa de Pós-Graduação em Geociências/Centro de Tecnologia e Geociências (CTG), Universidade Federal de Pernambuco, Av. da Arquitetura s/n, Cidade Universitária, 50740-550, Recife, PE, Brasil.

²Centro de tecnologia, Universidade Federal de Alagoas Federal, Av. Lourival Melo Mota, s/n, Tabuleiro dos Martins 57072-900, Maceió, AL, Brasil.

³Centro de Pesquisas Manoel Teixeira da Costa, Instituto de Geociências, Universidade Federal de Minas Gerais (CPMTC-IGC-UFMG), Campus Pampulha, Av. Antônio Carlos, 6627, 31270-901, Belo Horizonte, MG, Brasil.

* Corresponding author:

joaovince2015@gmail.com (J.V. Azevedo)

ABSTRACT

Studies of sedimentary provenance have incorporated a broader number of approaches and procedures, because Sediment transport, burial, and diagenetic events alter grains characteristics. This study proposes to use petrography, cathodoluminescence, X-ray diffractometry, and facies analysis to determine the origin of the sediments that comprise the Poti Formation in the Itaueira region (Piauí), in the Parnaíba Basin. The depositional model for the study area was determined through faciological analysis, which consists of two facies associations (FA) deposited in a storm wave-dominated shallow platform environment: Upper Shoreface (FA1) and Lower Shoreface/Offshore (FA2). Paleocurrents indicate direction to the northwest and, to a lesser extent, to the southwest in the paleogeographic context. This direction indicates the connection of the epicontinental sea formed in the Parnaíba Basin with the Tethys paleomar in the Upper Carboniferous. The sandstones were classified as subarkose and quartzarenites by the petrographic study, and they were plotted on the Dickenson (1985) diagram of tectonic environments, suggesting inner craton environments (continental blocks). The cathodoluminescence, as well as the heavy mineral assemblage, indicated medium to high-grade peraluminous metamorphic sources, metasedimentary rocks and potassium feldspar-rich igneous sources. The data, therefore, indicated several sources of sediments for the carboniferous sandstones of the Parnaíba Basin. The data integration indicates that the Rio Grande do Norte Domain (Granjeiro Terrain) in the Borborema Province is the most probable source of sediments, which is composed of Archean and Neoproterozoic components. Furthermore, petrography and cathodoluminescence show that type I Brasiliano granites are an important source of sediments, as well.

Keywords: Poti Formation; Sediment Provenance; Petrography; Facies Associations; Upper Carboniferous.

1 introduction

The facies study, integrated with petrographic and diagenesis data, provides information that makes it possible to determine the environment, depositional conditions and sediment source areas, being important in the analysis of sedimentary basins (Bruckmann *et al.*, 2019; Costa e Remus, 2016). Petrographic analysis and facies association aid in identifying the composition of sediments and the conditions under which they were deposited (Tucker, 2001; Bruckmann *et al.*, 2019; Ocampo Díaz *et al.*, 2021). Facies differ depending on the sedimentary process, depositional environment, climate, and tectonic environment (Tucker, 2001; Corrêa Martins *et al.*, 2018); however, the intensity of the diagenetic processes that occurred during burial must be identified, as they alter the original composition of the rock, making it difficult to determine the tectonic environment (Worden *et al.*, 2018; Morad *et al.*, 2010).

Currently, the term provenance has a broader meaning than simply indicating the location of the sediment source. This term reveals the lithology, tectonic environment, and prevailing climatic conditions in addition to the sediment source area (Boggs, 2009). The Parnaíba Basin covers a sedimentary area that encompasses part of the states of Ceará, Piauí, Maranhão, Tocantins, and Pará. It is composed of rocks that were deposited in both coastal and continental marine environments, which characterize the Paleozoic of the South American Platform. The Paleozoic was a period of great importance for the paleoenvironmental evolution from the platform, due to the formation of epicontinental seas and desert environments, as climate, paleogeographic and eustatic sea level changes were recorded (Caputo, 1984; Memória *et al.*, 2021; Blakey, 2003 Armitage e Allen, 2010). Shallow marine deposits, deltaic and coastal plains formed during the Upper Carboniferous Period distinguishes the Poti Formation, the subject of this research (Góes and Feijó, 1994; Vaz *et al.*, 2007). The research site is located southeast of Itaueira city, in the state of Piauí (Figure 1).

Historically, studies related to the Poti Formation focus on regional geology and on determining its capacity as a reservoir rock; furthermore, the most recent research is related to sequence stratigraphy, diagenetic processes and paleontological content (Melo and Loboziak, 2000, Pasquo and Ianuzzi, 2014; Góes, 1995; Dutra, 2011; Paiva, 2018; Araújo, 2018; Ferraz *et al.*, 2016).

Despite the aforementioned research, data that allow an integrated petrographic and faciological analysis to investigate the origin of the sediments belonging to this unit are still scarce. Therefore, the main objective of this work is to carry out a facies analysis and considerations about the provenance of the sediments from petrographic data, determining the source areas (Gazzi-Dickinson method) and the most important diagenetic conditions. To reach

this goal, the research integrates these data with the results of cathodoluminescence and X-ray diffraction.

Nanomineralogical analyses such as X-ray diffractometry and cathodoluminescence can be incorporated into climatic and provenance studies, because they help to understand the mineral transformations that occurred during diagenesis and determine the probable sources of sediments through the luminescence of quartz grains (Boggs e Kinsley, 2006; Fan *et al.*, 2019; Lorentzen *et al.*, 2020).

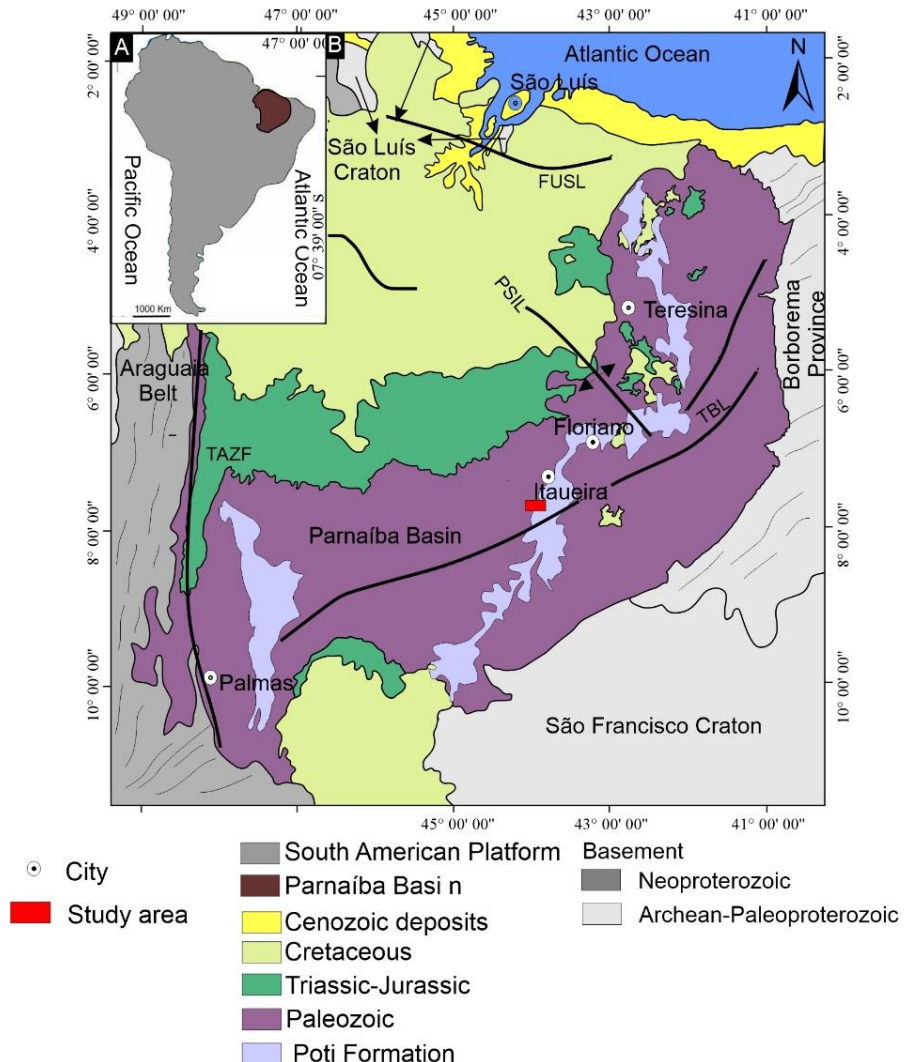


Figure 1 - Location map of the Parnaíba Basin. A) South American platform with emphasis on the Parnaíba Basin. B) Geological map of the Parnaíba Basin, highlighting the Poti Formation and the study area near to the region of Itaueira – PI.

2 Geological Context

The Parnaíba Basin occupies an area of approximately 600,000 km² and occurs in the North and Northeast regions of Brazil, and is filled by sedimentary strata ranging in age from the Paleozoic to the Mesozoic (Figure 2) reaching 3.5 km thick at its depocenter (Hasui *et al.*, 2012; Vaz *et al.*, 2007). The basement is composed of Precambrian crystalline rocks from the

Borborema Province to the east, the Parnaíba block to the center, and the Amazon Craton to the west. Its formation is related to the stabilization of the South American Platform, which records the final deformational events of the Brasiliano Cycle and the formation of rift-type basins such as the Jaibaras (Oliveira & Moriak, 2003; Coelho *et al.*, 2018; Daly *et al.*, 2018; Castro *et al.*, 2014).

The sedimentation period in the Parnaíba, Amazonas, and Paraná Basins started with the development of the Gondwana supercontinent and the stabilization of the South American Platform. The Silurian, Devonian, Carboniferous-Triassic, Jurassic, and Cretaceous supersequences comprise the Parnaíba Basin stratigraphy (Góes and Feijó, 1994). Following that, another classification suggested the presence of five supersequences: Silurian, MesoDevonian-Eocarboniferous, NeoCarboniferous, Eotriassic, Jurassic, and Cretaceous (Vaz *et al.*, 2007). These supersequences are composed of rocks formed in epicontinental seas and deposited through eustatic sea level variation, with the depocenter located in the center of the Parnaíba Basin (Soares *et al.*, 2018; Brito Neves *et al.*, 1984).

The Canindé Group (MesoDevonian-EoCarboniferous sequence) is composed of Itaim, Pimenteira, Cabeças, Longá and Poti formations, representing the most notable transgressive-regressive cycle in the Parnaíba Basin (Góes and Feijó, 1994). The Viseana Poti Formation is made up of conglomerates and fine to coarse-grained sandstones interspersed with siltstones and shales that reach 320 m in thickness, deposited on fluvial, deltaic, floodplain, and storm-dominated platforms (Lima and Leite, 1978; Caputo, 1984; Góes and Feijó, 1994; Góes, 1995).

The analysis of the outcrop on the eastern and western borders of the Parnaíba Basin revealed marine platform, coastal, and river settings with temperate climates, as shown by the lack of carbonates (Góes, 1995). The sedimentation begins as marine and evolves to continental deposits, reflecting the Parnaíba basin's overall tendency toward continentalization (Mesner & Wooldridge, 1964; Santos and Carvalho, 2009)

3 Material and Methods

This research was developed through the detailed analysis of six outcrops located in the central portion of the Parnaíba Basin, in the region of Itaueira (Figure 2). The data obtained allowed the establishment of sedimentary facies present and the production of six stratigraphic logs at a scale of 1:50 cm, which include sedimentary structures, layer geometry, lithology, and paleocurrent data from the Poti Formation. The Stereonet 11 program created the rose diagrams from paleocurrent data measured along each stratigraphic log; Corel Drawn 21 was applied to edit the rose diagrams and create the mosaic of images.

The employed facies model seeks to describe, individualize, and associate facies, which relates to certain depositional systems (Walker, 1992). To make it easier to identify them, the facies nomenclature uses ascending numbers.

The production of 15 thin sections from the six stratigraphic logs used for petrographic and diagenetic studies assisted in determining the identification of the Poti Formation sediment source area, from its mineralogical and textural aspects.

Sandstone samples were collected and 15 thin sheets were produced for petrographic and diagenetic studies, with the objective of assisting in the possible identification of the source areas of the sediments of this Formation, from the mineralogy and textural aspects, as well as in the determination of the facies present. Thin sections of the studied rocks were impregnated with blue epoxy resin in order to identify and characterize the porosity, according to Cesere *et al.* (1989) methodology. The utilization of a transmitted and reflected light microscope model O600P Opticam, with an attached digital camera, helped to describe and capture images of the thin sections. The granulometry, mineralogical composition, texture (selection, roundness and sphericity), matrix and porosity, in addition to the cement and contact between the grains, were carefully analyzed.

The Folk (1968) classification, which takes into consideration the total content of quartz, feldspars, and rock fragments, was applied. According to Gazzi-Dickson method, the constituent quantification considered the counting of 300 points per thin section along three perpendicular crossings to the rock's structure and framework. According to Zuffa (1980), grains higher than 0, 0625 mm are individual minerals, while grains smaller than 0, 0625 mm are lithic fragments. The provenance determination took into consideration the Gazzi-Dickinson diagrams (Dickinson, 1985).

To identify the clay content and other mineral phases, four sample of the studied sandstones, powdered fractions smaller than $2\mu\text{m}$ were analyzed by X-ray diffraction at the Northeast Technology Center (CETENE). The diffractometer utilized was a Bruker model D8 Advance A25-X1 that operated using the Bragg-Brentano method at ambient temperature and humidity (24.30/37 %). The angular interval was 5° - 80° ; step: 0.02° ; time per step: 1.0 s; primary slit: 0.1 mm; Secondary slit: 5.0 mm, rotation speed: 15 /min. The data treatment was made by software X'PertHighScore, version 2.1b, which includes the PCPDFWIN (Powder Diffraction File-International Centre for Diffraction Data), from PANanalytical, as well.

The cathodoluminescence operated with an acceleration voltage of 10 Kv and $100\mu\text{A}$ current, vacuum between 0.003 and 0.05Pa, exposure time firstly of 10–15s and, afterwards, 40s. Connected to an Axioskop microscop, the Nikon FDX-35 camera took the images in the

Sedimentary Geology Laboratory (LAGESE), located at the Petroleum and Energy Institute of Research (LITPEG). The luminescence pattern used to interpret and define the provenance source area was in accordance with Bernet & Bassett (2014), Augustsson (2012), Oliveira *et al.* (2017), and Boggs and Krinsley (2006) studies.

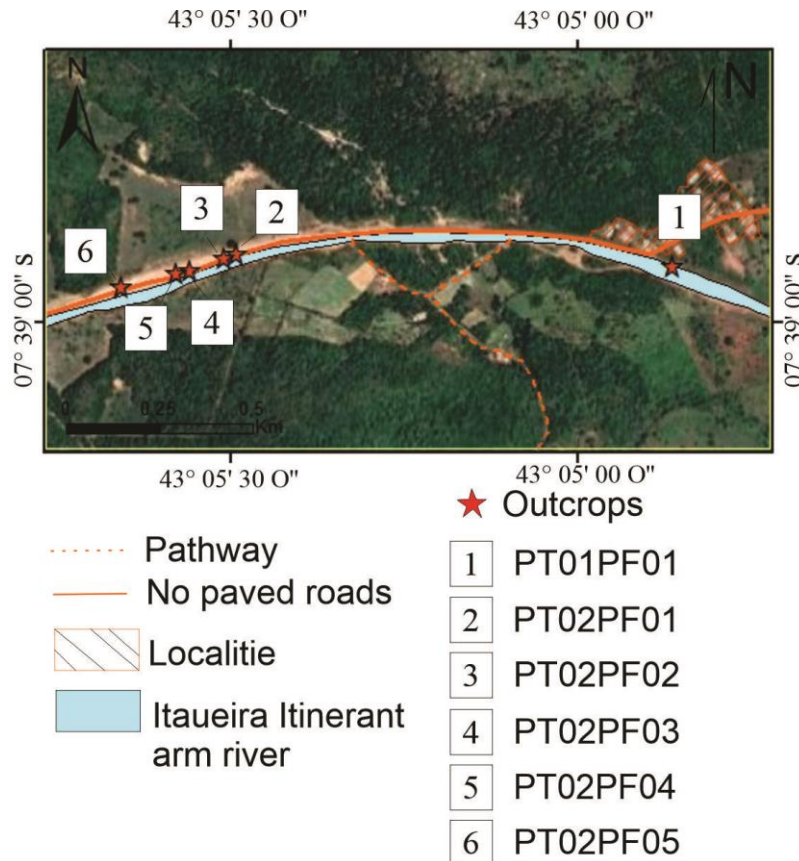


Figure 2 - Location map of the stratigraphic logs

4 Results

4.2 Facies Description of the Potti Formation

The granulometry, geometry, texture and sedimentary structures aided to determine five sedimentary facies (Figure 3; Table 1). The individual description, interpretations and grouping of these sedimentary facies appointed to a specific depositional environment. Figure 4 displays the general stratigraphic aspects of the studied outcrops.

4.2.1 Sandstone with swaley cross-stratification (Facies 1)

This facies is composed of fine-grained sandstones with subrounded and moderately to poorly-sorted grains. The layers ranges in thicknesses from 0.5 to 1.0 m (Figure 5A), exhibiting tabular geometry, upward concave-convex strata and shallow excavations, characterizing these beds. The slope angle among the excavated surfaces and the strata varies between 10⁰ and 15⁰;

the contact of this facies with facies 3 and 4 is erosive and its layers are laterally continuous for more than 600 m.

4.2.2 Sandstone with hummocky cross-stratification (*Facies 2*)

Facies 2 is composed of fine to very fine-grained sandstone with subrounded to rounded grains, moderate to poorly sorting. At the top of this facies, there are deformation bands filled with silica, in the form of venules. (Figure 5B); the layers exhibit hummocky cross stratification with convex upwards strata, reaching three meters in thickness (Figure 5C), and planar layers at the base of the succession. This facies is laterally continuous for more than 600 meters and covered by massive sheets of facies 5 clay in its upper layers (Figure 5D). Facies 2 is in gradational contact with facies 1 and 5.

4.2.3 Sandstone with plane-undulating stratification (*Facies 3*)

This facies is constituted of fine-grained sandstones with subrounded to rounded and moderately sorted grains. The layers exhibits tabular geometry with thicknesses ranging from 0.5 to 2.5 meters, characterized by planar to wavy strata (Figure 5E). There are small rounded (Diameter = 0.5 cm – 2.0 cm) and rectangular (Length = 0.2 cm – 2.0 cm) clay clasts. Facies 3 intercalates with facies 4 and exhibits gradational contact with facies 2.

4.2.4 Siltstone with plane-undulating stratification/lamination (*Facies 4*)

This facies is composed of very fine-grained siltstones with subrounded to rounded grains, moderately to well sorted. Layers feature tabular geometry and are continuous for over 600 meters, displaying planar to wavy bedding ranging from 5.0 to 50 cm. The top of this facies shows small discontinuous waveforms (Figure 5F); in addition, facies 4 intersperses with facies 1 and 2, showing erosive and gradual contact, respectively.

4.2.5 Massive mudstone (*Facies 5*)

This facies comprises gray mudstones with well-sorted grains, arranged in layers of tabular geometry (Figure 5G). The layers exhibit laterally continuous massive strata or laminations for more than 600 m, occurring mainly at the top of facies 2, whose upper contact is gradational.

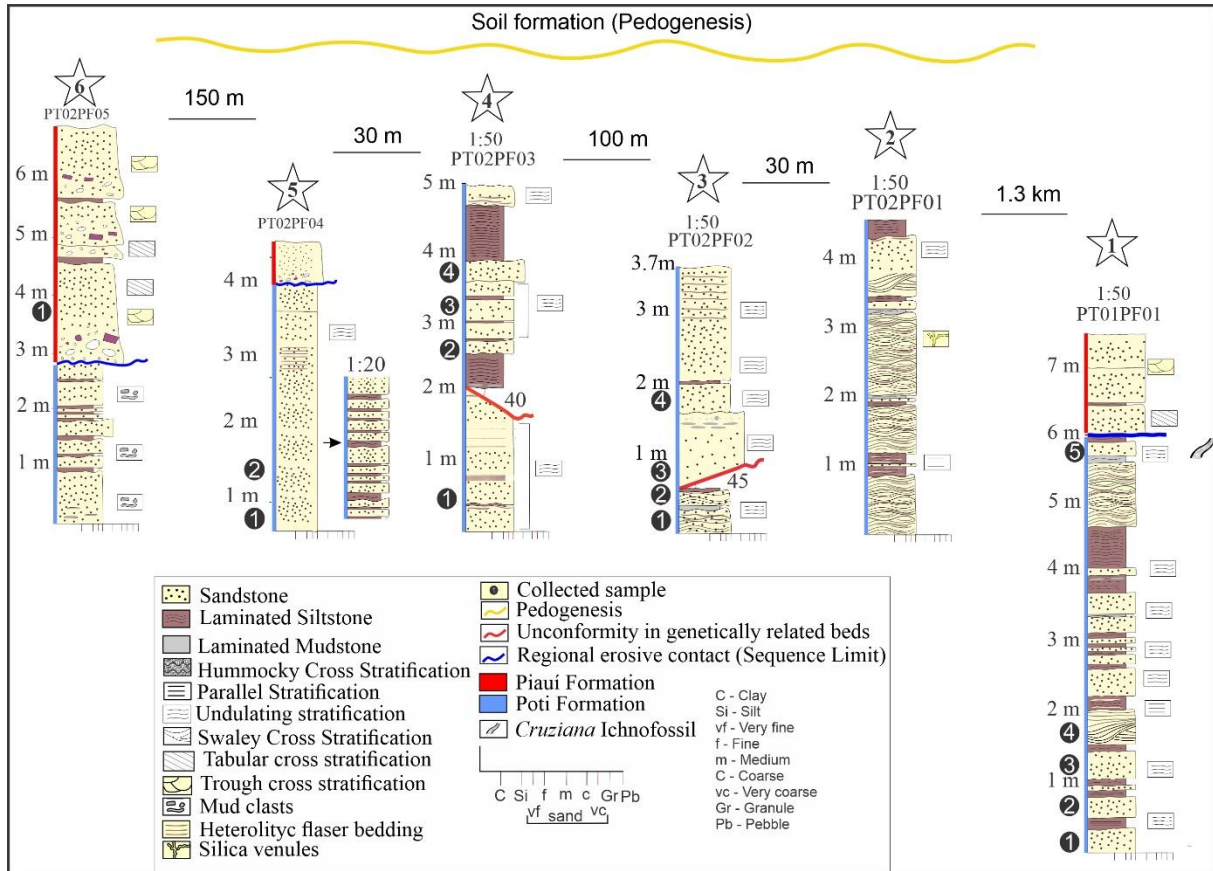


Figure 3 - Stratigraphic logs of the studied area and collected sample positioning. The vertical log scale is 1:50 and 1:20, in the log 5, in order to show more details.

Table 1 - Sedimentary facies description table of the Poti Formation, in the Itaueira region – PI.

Facies	Facies/structures	Granulometry	Interpretation
1	Sandstone with swaley cross-stratification	fine to coarse-grained	Tabular layers formed by combined flow. There is a predominance of the oscillatory compared to the unidirectional flow
2	Sandstone with hummocky cross-stratification	fine -grained	Tabular layers formed predominantly under oscillatory flow conditions, with little influence of unidirectional flows in the transition zone between lower shoreface and offshore
3	Sandstone with plane-undulating stratification	fine -grained	Tabular deposits generated in a shallow marine platform, with origin associated to combined flows
4	Siltstone with plane-undulating stratification/lamination	fine -grained with clay content in less proportion	When storm conditions stops, tabular deposits accumulate in the deeper parts of the platform, where low-energy flows and silt- and/or clay-grained sediments dominate the deposition mechanism.
5	Massive mudstone	Clay with small amounts of very fine-grained sand	Clay and silt deposition by suspension and decanting process, predominantly. This process occurs below the wave base line. Layers exhibits tabular geometry.



Figure 4 - Panoramic view of Poti Formation outcrops and erosive contact relationship with the upper unit.

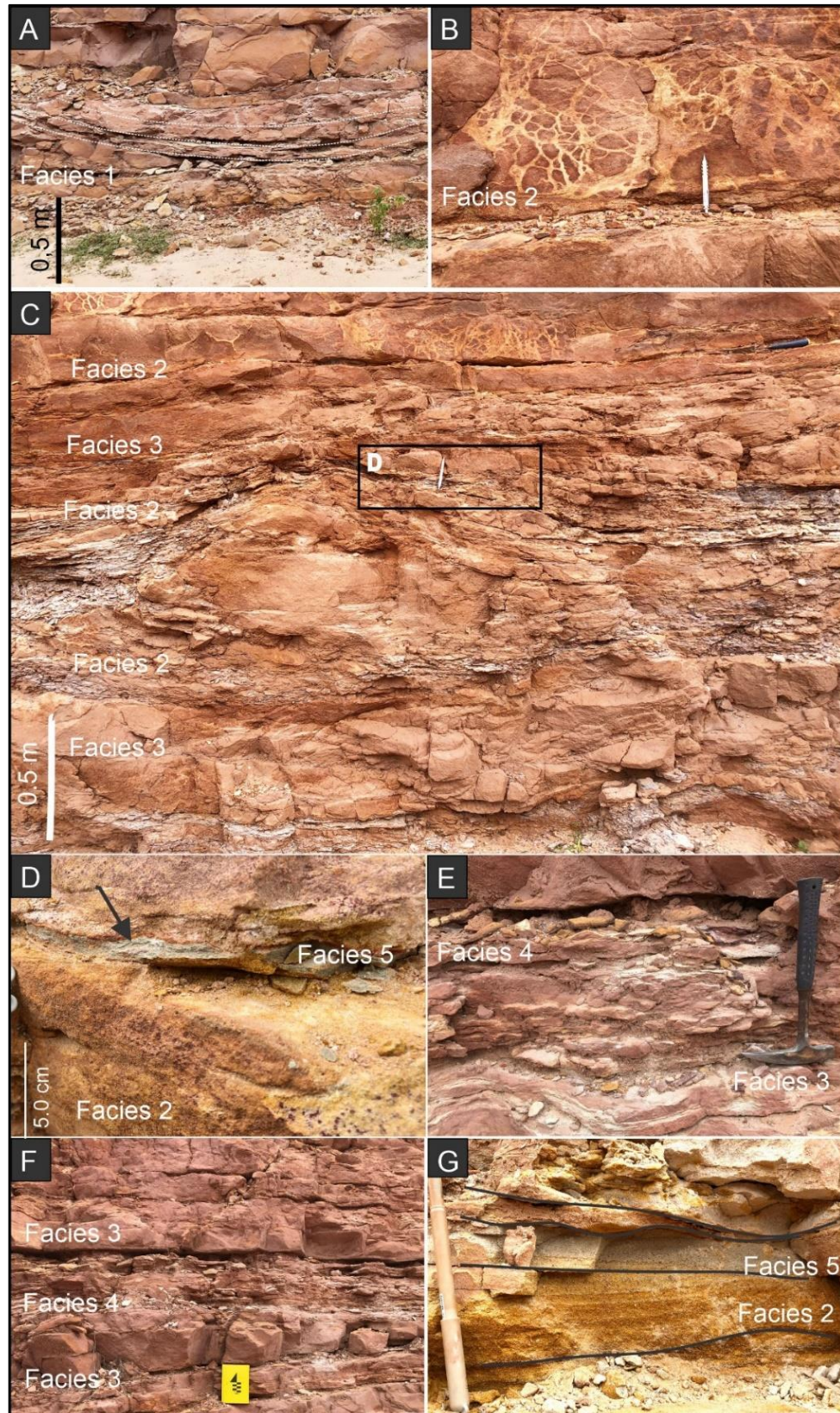


Figure 5 - A) Metric scale swaley cross bedding truncating low angle (10^0) overlapping layers B) Siliceous deformation bands concentrated in sandstone with hummocky cross-stratification C) Hummocky cross-stratification with metric layers covered by clay (Facies 5). D) Clay layer above the hummocky cross-stratification. E and F) Sandstone with plane-undulating stratification (Facies 3) overlaid by siltstones with plane-undulating stratification/lamination (Facies 4). G) Massive gray mudstone layer on the top of hummocky cross-stratification (Facies 2).

4.1 Petrographic and Mineralogical aspects

The sandstones that constitute the Poti Formation are fine to coarse-grained with poorly to moderately selected grains. The roundness degree ranges from sub-angular to sub-rounded, with the latter occurring more frequently; the quartz and feldspar grains sphericity is predominantly low. Punctual contacts among grains predominate, followed by straight and, rarely, concave-convex, generating loose packing in these supported-grain rocks.

Regarding textural maturity, most of these sandstones have low maturity, being characterized as immature (> 5% of depositional matrix), with subordinate occurrence of mature sandstones (< 5% of depositional matrix). Subarkose sandstones show a primary mineralogical composition rich in feldspars; in addition, the grains are angular to sub-angular and poorly sorted. On the other hand, quartzarenites are richer in monocrystalline quartz, insignificant amounts of feldspars and subangular and poorly sorted grains.

4.1.1 Detrital Composition

The petrographic studies identified that monocrystalline quartz (90-98 %), polycrystalline quartz (< 1 %), feldspars (1.0-3.5 %), lithic fragments and accessory minerals (<1%), with monocrystalline quartz, followed by feldspar are the predominant constituents, representing the mineralogical composition of the Poti Formation sandstones.

Quartz grains can be mono- and polycrystalline; however, the first presents straight and undulating extinction, to a lesser extent (Figure 6A), while polycrystalline grains exhibit undulating extinction (Figure 5B). Potassium feldspar (Figure 6B) and plagioclase (Figure 6C) represents feldspar grains, as indicated by petrography and XRD analysis.

The plagioclases show albite twinning, while the potassium feldspars (microcline) show crosshatching twinning, with both exhibiting alteration preferentially on the grains center; however, in plagioclase this alteration is more intense. The muscovite grains exhibit lamellar habits and occurs especially in the basal layers (Figure 6D; E).

These sandstones are composed of lithic fragments of quartzite, siltstone, gneiss and chert derived from sedimentary, metasedimentary and metamorphic rocks (Figure 6F), as well as heavy minerals and accessories such as muscovite, zircon, amphibole, tourmaline, rutile, titanite, hematite and opaque minerals. In the basal layers, muscovite occurs as an essential mineral, being important during the generation of clay in diagenesis.

According to Folk classification (1968), the sandstones of the Poti Formation are classified as quartzarenites and subarkose sandstones, based on quartz, feldspar, and lithic fragments content (Figure 7)

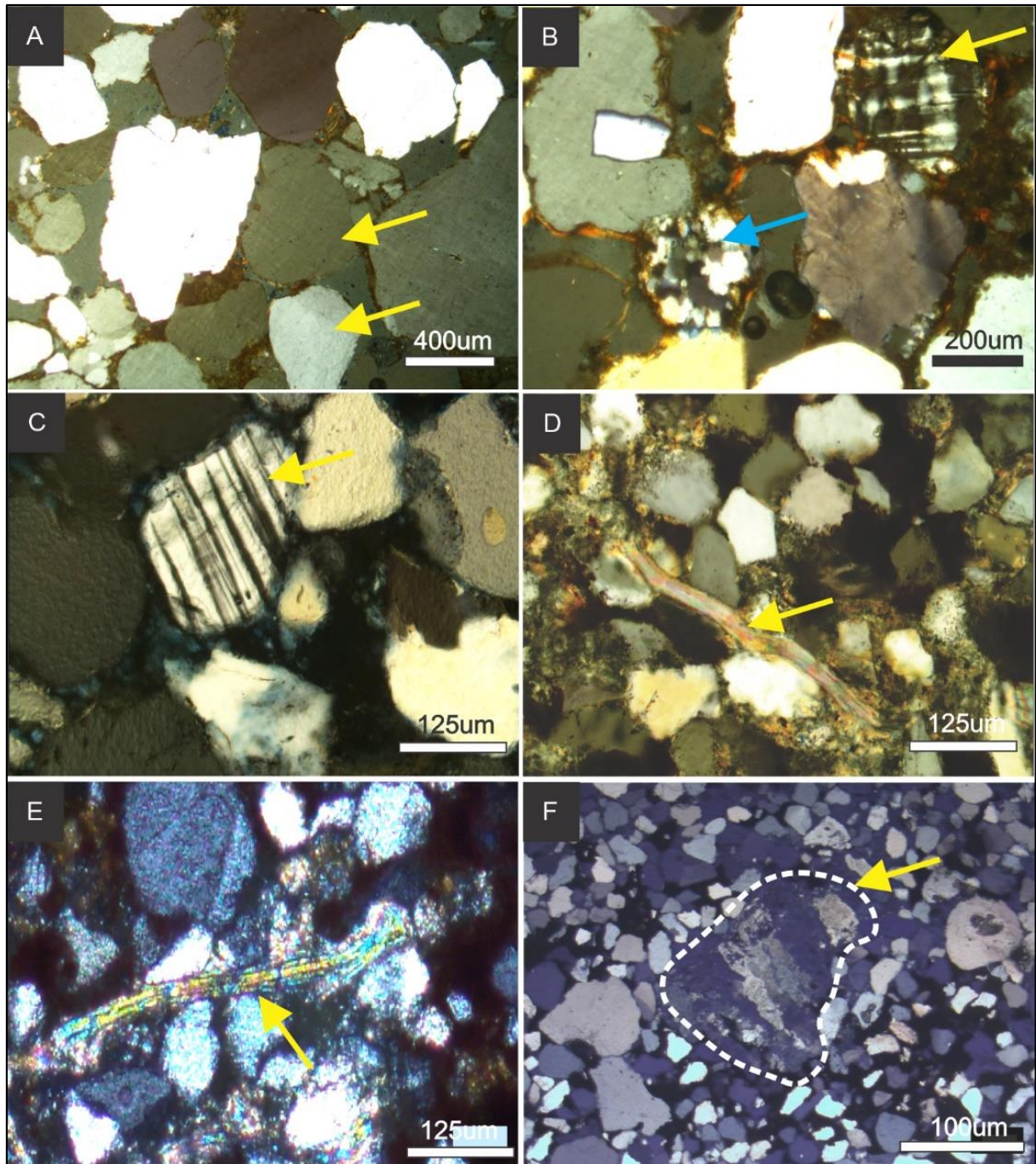


Figure 6 - Detrital composition of the Poti Formation sandstones. A) Subangular to subrounded monocristalline quartz grains with straight extinction (arrow); the grains exhibit mostly punctual and subordinately straight contacts; PX. B) Rounded polycrystalline quartz grain with undulating extinction (arrow); Potassium feldspar grain with crosshatching (arrow); PX. C) Plagioclase subrounded grain with albite twinning (arrow); PX. D) Muscovite lamellar grain with edges altering to clay; PX. E) Biotite grain altering to iron oxides (arrow); P//. F) Grain of gneiss exhibiting internal orientation and undulating extinction (arrow); PX. Caption: PX – Crossed nicols, P// – Parallel nicols.

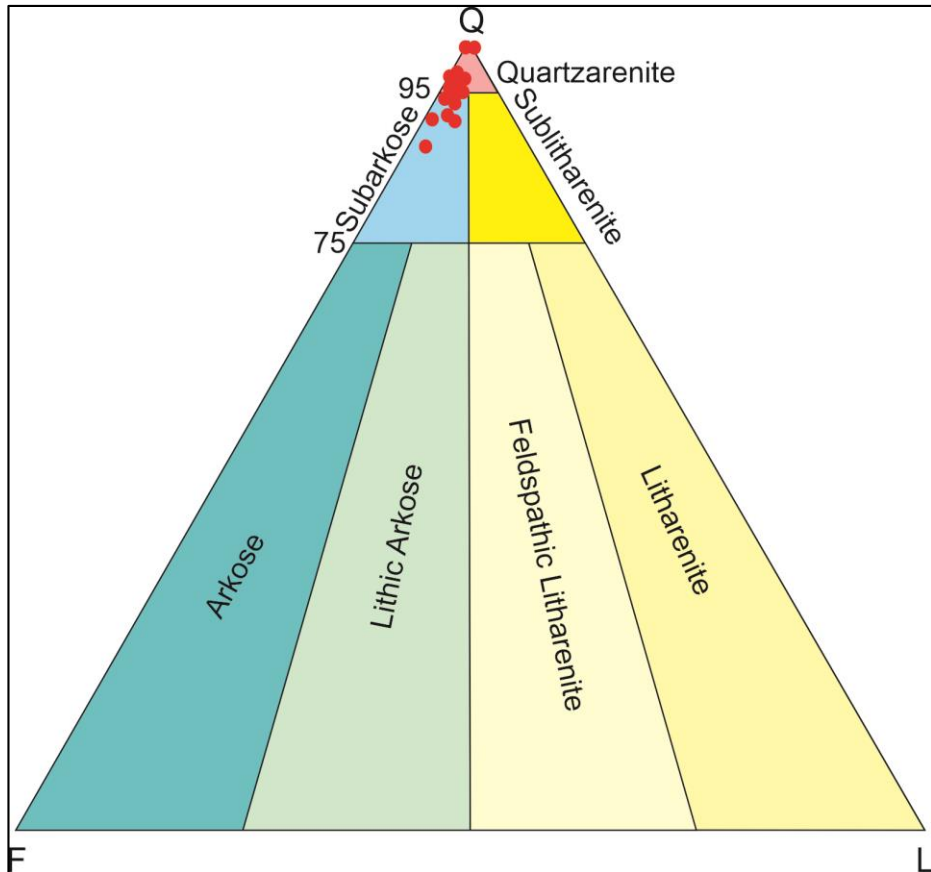


Figure 7 - Poti Formation compositional diagram, according to de Folk (1968).

4.1.2 Diagenetic Aspects

Different diagenetic processes with variable intensities were identified in the Poti Formation sandstones, which exhibits the three diagenetic stages: eodiagenesis, mesodiagenesis, and telodiagenesis.

The samples present a low extent of mechanical and chemical compaction, as well as a weak packing degree, evidenced by contact relationship between the grains and pore spaces, filled by mechanically infiltrated clay.

Slightly fractured quartz grains and incipient deformation of muscovite grains characterizes the mechanical compaction features. The greater presence of punctual and straight contacts indicates that this process had little intensity, just as chemical compaction, which locally produces dissolution by pressure in the studied samples. Therefore, the presence of concave-convex and sutured contacts is rare.

As diagenesis progresses, secondary growth of silica cement and silicate cement takes place; this cement occurs continuously and discontinuously around the grains, being visible as the extinction angle changes and by the presence of a dust line (Figure 8A) or through prismatic shapes on the surface of the grains (Figure 8B). The feldspar grains alter to kaolinite and illite

or undergo partial or total dissolution processes that can generate secondary porosity (Figure 8C).

Mechanical infiltration of clay; mechanical compaction; chemical compaction; silica cement as secondary quartz overgrowth; kaolinite/illite cement, grain dissolution; grain alteration; grain replacement by clay minerals; and hematite/titanium cement formation constitute the diagenetic processes and constituents identified.

The processes of mechanical infiltration of clay in eodiagenesis, which reduces the primary porosity of the rock, and the process of cementation by hematite in telodiagenesis were the most important diagenetic aspects (Figure 8D). Such processes are more intense in the basal layers samples of the studied area; in addition, the intergranular porosity and secondary porosity generated by the dissolution of feldspars are the most important types in the Poti Formation rocks, especially in the upper layers of the profiles studied.

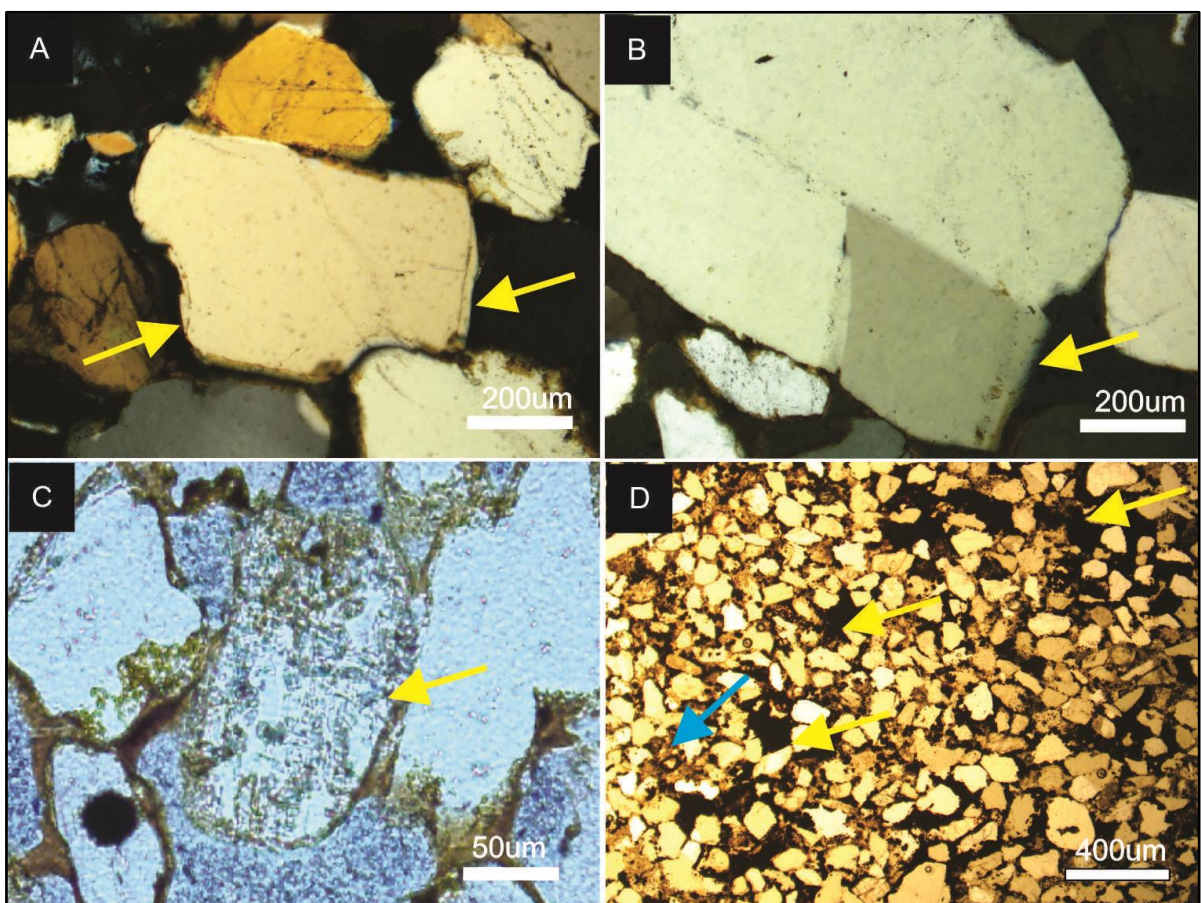


Figure 8 - Main diagenetic aspects of the Poti Formation. A) Discontinuous quartz overgrowth around quartz grains with clearly visible dust lines (arrow); PX. B) Quartz overgrowth with prismatic shapes at the edges of the quartz grain (arrow); PX. C) Partial dissolution process generating secondary porosity on feldspar grain surfaces (arrow); P//. D) Discontinuous hematite cementation (yellow arrow) and mechanical infiltration of clay into the intergranular spaces (blue arrow); P//. Caption: PX – Crossed nicols, P// - Parallel nicols.

4.3 Provenance

In order to discuss the sediment source rocks, petrography analysis, paleocurrent measurement, X-ray diffraction (XRD), cathodoluminescence (CL) and heavy minerals analysis were applied, as indicators of sedimentary source areas. Dickson's (1985) QtFLt and QmFLt diagrams were used to infer the provenance of the Poti Formation sandstones, in order to determine the tectonic environments, which are stable craton, uplifted basement, magmatic arc and recycled orogenic (Dickson, 1985), as well as possible sediment source areas.

Based on Gazzi-Dickson method, the point counting and modal analyses of 15 thin sections made it possible to determine the provenance of the Poti Formation sandstones, as indicated by the provenance diagram (Figure 9). According to QtFLt and QmFLT diagram, the Poti Formation sandstones are plotted in craton interior field.

Paleocurrent data from the Poti Formation were collected in cross-stratifications of six outcrops along 1.5 km of this unit. The measures have a dominant trend towards NW and subordinately towards O and SW (Figure 10). The general pattern of paleocurrents in this unit is NW, which suggests areas located to the SE and E, represented by crystalline rocks of different metamorphic grades, as will be seen in the discussion topic.

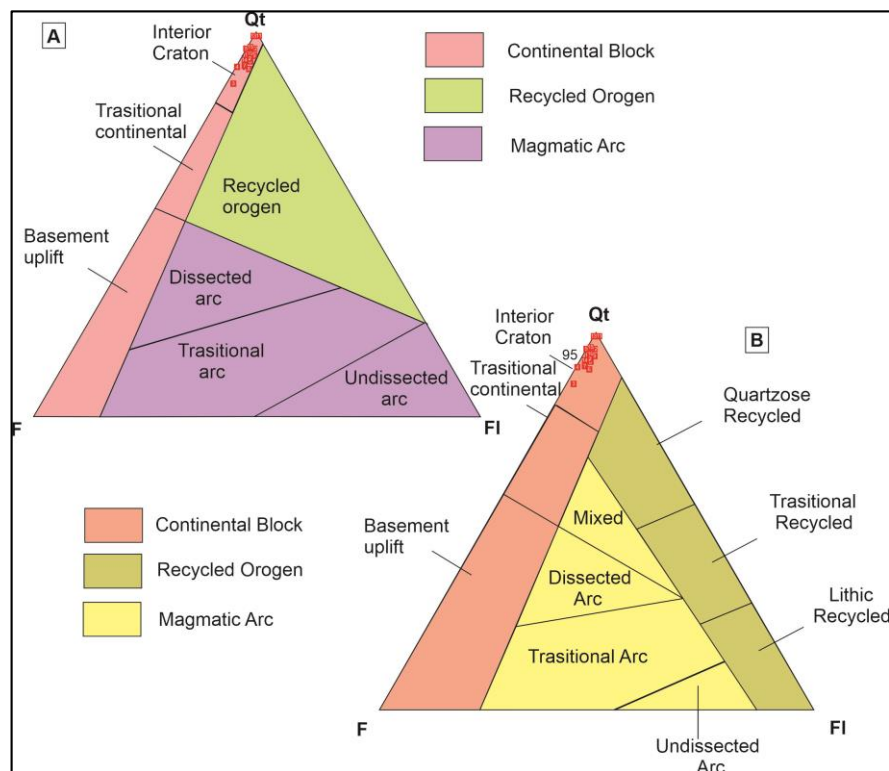


Figure 9 - Tectonic discrimination diagrams for the Poti Formation sandstones of the Parnaíba Basin. A) QmFLt triangular diagram. B) QtFLt triangular diagram. Both indicate craton interior field.

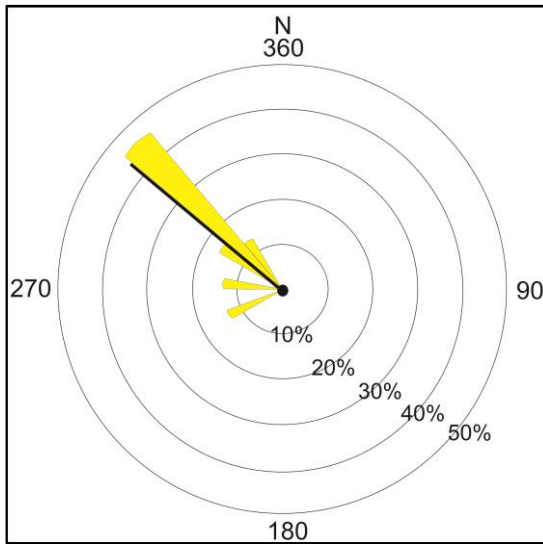


Figure 10 - Paleocurrents measured in the cross-stratified sandstones of the Poti Formation. The measurements show a predominance for NW and dispersion for W and SW, in all six stratigraphic logs. Number of measurements - 23.

The integration between petrography and XRD allowed the identification of feldspar types (potassium feldspar and plagioclase) and clays, represented by kaolinite and illite (Figure 11). The presence of plagioclases, zircon, epidote, amphibole, tourmaline, muscovite and hematite, in addition to the occurrence of metamorphic and sedimentary lithic fragments, indicate a probable metamorphic source. On the other hand, prismatic and euhedral grains of zircon, amphibole, tourmaline and titanite, as well as quartz grains with inclusions in the framework, indicate an igneous source. Figure 12 shows the main heavy mineral grains of the Formation.

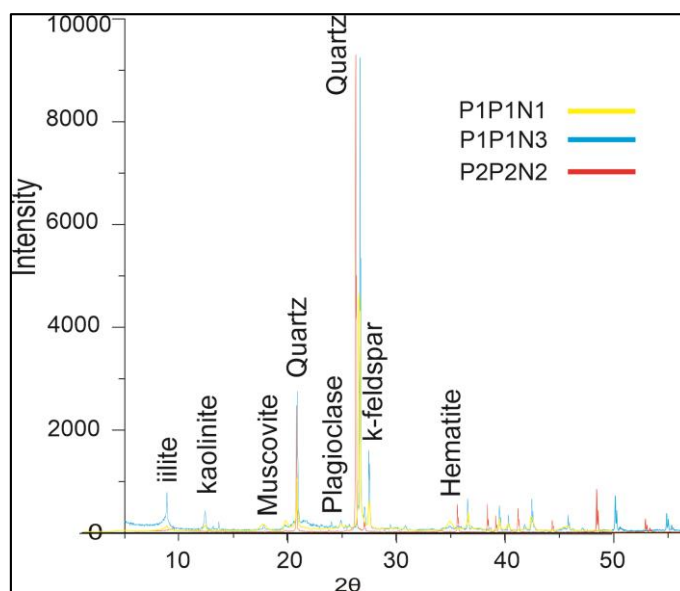


Figure 11 - Diffractograms exhibiting the most important mineral peaks identified.

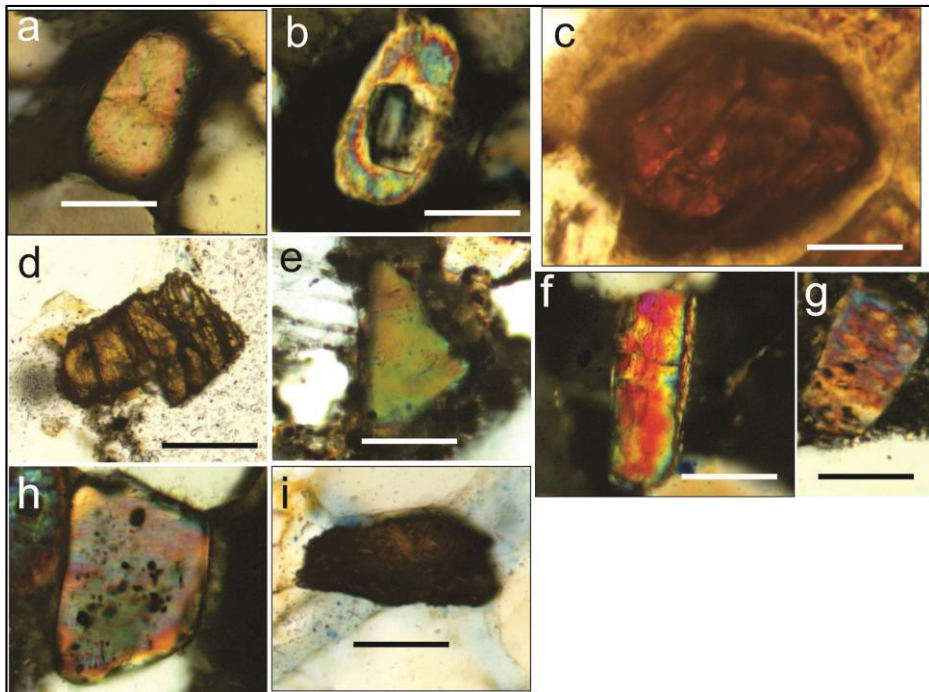


Figure 12 - A) High relief and interference colors in a rounded zircon grain. B) Rounded epidote grain with low relief and high interference color. C) Rounded rutile grains rarely alter to titanium oxide. D) Prismatic titanite grain with high relief. E) Sub-rounded amphibole grain with moderate relief. F) Prismatic and elongated zircon grain. G) Amphibole grain with moderate relief. H) Tourmaline grain with numerous inclusions showing high interference colors. I) Amphibole grain with corroded edges and rounded corners. The scale bar measures 60 micrometers.

The technique of cathodoluminescence and X-ray diffractometry provided an integrated perspective that, when combined, generate precise information about the rock provenance. The most used application of cathodoluminescence refers to diagenetic aspects and sediment provenance, as the minerals emit luminescence that allows the study of mineral alterations and their formation processes (Götze, 2002). This technique provides information about the diagenesis of sedimentary rocks, as it accurately differentiates the detrital and authigenic components, which can be clay infiltration, quartz and feldspar cementation (Pagel *et al.*, 2000). In addition, it distinguishes well the types of carbonate cement such as calcite and dolomite.

The results of cathodoluminescence in the Poti Formation sandstones show that quartz grains have brown, reddish brown and violet colors, while feldspars exhibits a bright blue color. Diagenetic and post-depositional products such as cementation and diagenetic clay do not show luminescence. These data indicate that the sources can be both metamorphic and igneous (Augustsson and Bahlbarg, 2003) and will be addressed in the discussion.

5 Discussion

5.1 Facies Analyses, Facies Associations, and Depositional System

In the studied successions of the Poti Formation, five sedimentary facies were recognized. Table 1 lists the main facies and characteristics of the succession, and all sedimentary facies are siliciclastic and arranged in ascending order of numbering.

The swaley cross-stratification sandstone facies (Facies 1), with fine-grained tabular layers, is interspersed with facies 2 and 3, being generated by a combination of oscillatory and unidirectional flows that generate shallow excavations, called swales (Dumas e Arnott, 2006; Jelby *et al.*, 2020; Vakarelov *et al.*, 2012). The presence of parallel layers below these structures may indicate the action of unidirectional currents superimposed on the oscillatory flows (Arnott e Southard, 1990). Therefore, facies 1 underwent storm wave reworking between the storm wave base line and the fair-weather wave base (Dumas e Arnott, 2006).

The hummocky cross-stratification sandstone (Facies 2) is fine-grained, exhibits tabular layers with great lateral extension, and is interspersed with facies 1, 3, 4 and 5. Oscillatory and combined flows form this facies under storm wave action that exceeds the wave base line action (Almoqaddam *et al.*, 2018; Feitosa *et al.*, 2019). The presence of straight crest waveforms (dunes) with paleocurrents flowing towards the NW direction is related to the occurrence of transitional unidirectional currents, usually associated to storms (Mutti *et al.*, 1996; Mutti, 1992; Bowman and Johnson, 2014);; in addition, structures generated by oscillatory flows, such as asymmetric 3D waveforms, were observed. Therefore, its deposition represents offshore environments with a predominance of oscillatory flows.

The sandstone with plane-undulating stratification (Facies 3) is fine-grained and composed of tabular layers. Unidirectional upper-regime flows of rip currents or high-energy wave action in deeper portions of a platform produces these stratifications (Collinson *et al.*, 2006). Symmetrical waveforms and flat to undulating laminations/stratifications characterizes the shoreface and these structures occurrence is common in this subenvironment (Plint, 2010; Maahs *et al.*, 2019).

The massive mudstone (Facies 5) is composed of clay and is interspersed with fine sandstones from Facies 2 and 4. Fine-grained laminated/stratified sandstones and very fine-grained siltstones intercalates with Facies 5, indicating two forms of deposition. In the first, the mudstones discontinuously intercalates with facies 4 or mixes with the silt grains in facies 4. Plane-undulating siltstones with small amounts of clay represents Facies 4. This distribution and facies relationship occurred due to the alternation in depositional energy, which provided

the deposition of sand and very fine silt, in periods of high energy, in transition zones on the shelf. (Basilici *et al.*, 2012)

In the second form of sedimentation, the predominance of low energy conditions provides mudstones deposition, which occurs on the top of Facies 2, interpreted as a product of deposition after the occurrence of storms, in calm environments or influenced by tides (Asurmend *et al.*, 2018; Angus *et al.*, 2020).

5.2 Facies Associations

The two facies associations that reflect the variety of processes that operated in each Poti Formation sedimentation environment were formed from the grouping of different sedimentary facies. The Upper Shoreface (FA1) and Lower Shoreface/Offshore (FA2) facies associations reflect a shallow marine platform environment dominated by storm waves.

5.2.1 Upper Shoreface (FA1)

In the study area, the occurrence of this facies association increases from southeast to northwest, reaching four meters of thickness. It is mainly composed of fine sandstones with swaley cross-stratification (Facies 1), plane-undulating stratified sandstones (Facies 3), and very fine siltstones with plane-undulating stratification/lamination (Facies 4), to a lesser extent. Subordinately, coarse-grained sandstones occur towards the top of this facies association; there is no significant presence of clay laminations (Facies 5) and small waveforms (ripples).does not occur.

Compared to the FA2 deposits, the upper shoreface is closer to the shoreline, being characterized by longshore currents and a wave-breaking zone (Cliff, 2006). In addition, it is more affected by the influence of storms and consequently has higher depositional energy; the constant interaction between waves and the seafloor above the fair-weather wave base characterizes the Upper Shoreface (Grundvag *et al.*, 2020; Grundvag and Olaussen, 2017).

Unidirectional, oscillatory currents, and combined flows generates the horizontal and low-angle structures in facies 1, 3, and 4 (Jelby *et al.*, 2020). The migration of longshore bars forms the cross-stratified sandstones on the shoreface, indicating the migration of dunes (Plint, 2010; Della Fávera, 2001).

5.2.2 Lower Shoreface /Offshore (FA2)

This facies association is mostly composed of fine-grained sandstones with hummocky cross stratification (Facies 2) and intercalations between the very fine-grained siltstones with plane-undulating stratification/lamination (Facies 4) and massive mudstones (Facies 5). Facies 2 and 3 show bioturbation produced by trace fossils of the *cruziana* facies.

The presence of hummocky cross-stratification and bioturbated deposits with presence of mud indicate a transition between shoreface and offshore. In distal portions of the platform, the low energy of sediment transport promotes the decanting process, which stops when high-energy process of storm events happen (Plint, 2010). The oscillatory flow creates hummocky cross-stratification, during periods of storms and below the wave base line, where aggradation rates help to preserve hummocks (Dumas e Arnott, 2006; Peters e Loss, 2012).

When the influence of storms ceases, these layers remain preserved in deeper portions of the shelf; and the occurrence of asymmetric waveforms at the base of facies 2 indicates the influence of oscillatory and unidirectional current flows (Xiao *et al.*, 2020; McCabe, 1985; Quin, 2011). The presence of thicker sandstone beds towards the top of this association indicates the transition to the upper shoreface, in which sedimentation occurs above the wave base line and under conditions of relative sea level fall (Santos *et al.*, 2015; Lee *et al.*, 2018).

5.3 Depositional System

The two facies associations that comprises the storm wave-dominated shallow marine depositional system exhibits representative facies variations, indicating a gradational transition between these associations. The sedimentary structures present in facies 1, 2, 3, 4 and 5 suggest the incidence of combined flows with a predominance of oscillatory current flow in the shallow platform environment, with frequent storm events. The integration of facies association data and depositional system resulted in a depositional model for the Poti Formation, composed of upper shoreface and transition between lower shoreface and offshore (Figure 13). The paleocurrent measurements, with NW direction, recorded in the Poti Formation in the Itaueira region reinforce a connection with the Paleotethys, indicated by the paleogeographic maps (Scotese, 2021).

Stratigraphic logs 3 and 4 exhibit a sudden variation among facies associations, in which lower shoreface/offshore (FA2) environments transition to upper shoreface (FA1). In this transition, the fine sandstones of FA2 grade to fine to coarse-grained sandstones of FA1, being the result of an increase in the sedimentary supply with the formation of finning-upwards logs.

From southeast to northwest, the lateral variation of facies exhibits less influence of storm waves, which resulted from the variation of the wave base line. The presence of clay clasts in profiles 3 and 4 may indicate tidal influence on sediment deposition or the excavation of FA2 deposits by higher energy processes with high sedimentary supply (Vakarelov *et al.*, 2012; Jelby *et al.*, 2020).

In the nineties, petrographic studies carried out in wells identified that very fine to medium-grained sandstones of subarkose to lithic composition predominate in the successions;

in addition, the processes of clay infiltration, secondary cements overgrowth, dissolution and mechanical and chemical compaction influenced the petrophysical characteristics of these rocks (Góes, 1995).

In the last decade, the research developed in outcrops and wells indicated that rocks of different facies associations and with the same composition (Arkoses) had variable diagenetic events intensities, due to relative sea level variations, since the Parnaíba Basin had a ramp with a gentle slope and, therefore, sensitive to these variations (Paiva, 2018; Araújo, 2018).

The most important mineral phases identified in the Poti Formation comprise monocrystalline quartz, plagioclase, potassium feldspar (microcline), muscovite, heavy minerals, hematite cement, illite and kaolinite. The formation of illite indicates the action of weathering processes that alter potassium-rich minerals; in addition, illite is the product of alteration of phyllosilicates under arid climate conditions (Thiry, 2000; Chamley, 1989; Betard, *et al*, 2009). Kaolinite is the main clay mineral identified and its formation results from the alteration of feldspars under humid climates, as well as the product of hydrothermal alteration at depths less than 1 km (Marfil, *et al*, 2003).

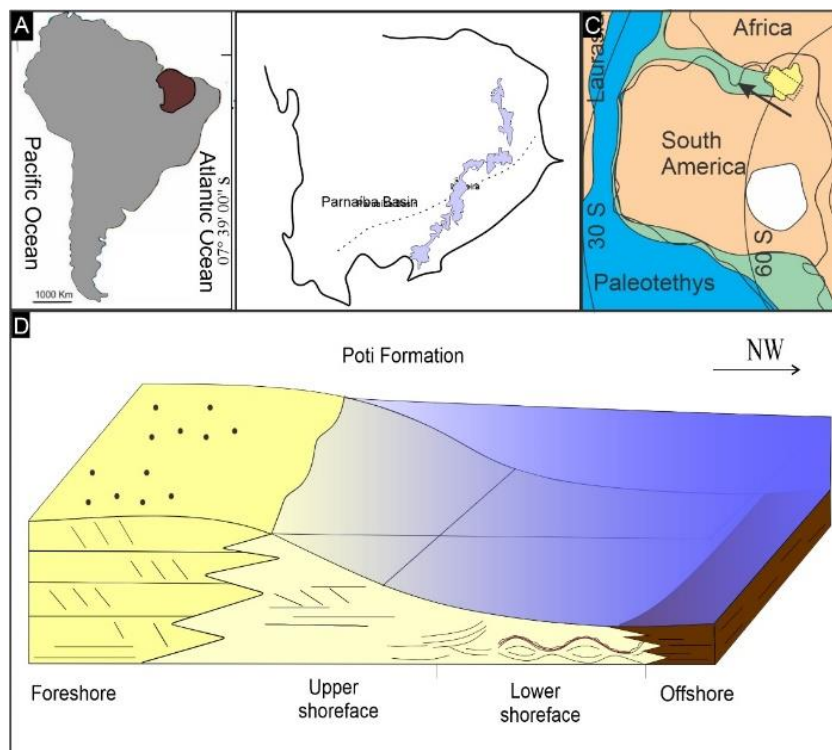


Figure 13 - A) Location of the Parnaíba Basin on the South American Platform. B) Geographical distribution of the Poti Formation in the Parnaíba Basin. C) Paleogeographic contextualization of the Parnaíba Basin in the Carboniferous. The arrow indicates the paleocurrent recorded in the field in accordance with the paleogeographic position; Parnaíba Basin in yellow; during this period, the Tethys Sea influenced in the rising epicontinentals seas on the basin. D) Depositional model of the Poti Formation and location of the main subenvironments of the storm wave-dominated shallow platform system.

5.4 Considerations about the Provenance of the Poti Formation

The integration and interpretation of field data, petrography, cathodoluminescence and X-ray diffractometry revealed information that allowed making inferences about the tectonic environment and sediment source area for the Poti Formation, central portion of the Parnaíba Basin. The plotted points in the Dicknson (1985) provenance diagram was based on different types of quartz, feldspar and rock fragments present in the samples and indicates provenance from continental blocks.

Paleocurrent measurements, performed on cross-stratified sandstones in the six stratigraphic logs of the Poti Formation, indicate a predominant direction to NW and secondarily to SW. Therefore, the source areas were to the southeast of the study area, characterized by crystalline terrains of the Borborema Province (Santos et al., 2018). Therefore, the source area may be composed of high-grade metamorphic rocks, metasediments and igneous rocks from this province.

The technique of cathodoluminescence and X-ray diffractometry were used to provide an integrated perspective that, when combined, generate more accurate information about the rocks provenance. The most used application of cathodoluminescence refers to diagenetic aspects and origin of sediments, because minerals emit luminescence that allows the study of mineral alterations and their formation processes (Götze, 2002).

Commonly, Quartz grains have their luminescence altered during the transport process from the source area, in the sedimentary basin, resulting in grains with varied luminescence colors. However, cathodoluminescence distinguishes the secondary or authigenic quartz and determines, therefore, the provenance of quartz grains (Götze, 2002; Augustsson and Bahlburg, 2003).

Quartz grains with bright red or blue luminescence indicate sources generated at high temperatures and with fast cooling, usually occurring in volcanic rocks or rocks affected by contact metamorphism. In contrast, plutonic rocks with low crystallization temperatures and slow cooling, the predominant luminescence is blue (Boggs *et al.*, 2002; Augustsson and Bahlburg, 2003). Brown and reddish brown colors indicate sources from metamorphic rocks with low-grade metamorphism or high temperature metamorphic rocks with slow cooling. Some authors point out that quartz of volcanic origin presents higher luminescence intensities compared to those of metamorphic origin, presenting bright red colors (Zinkemagel, 1978; Boggs e Krisley, 2006).

Violet colored grains indicate plutonic, volcanic, from quartz phenocrysts, and high-grade metamorphic sources with fast cooling; quartz grains from pegmatite show pale blue or green

luminescence. Finally, authigenic quartz grains and hydrothermal products do not have luminescence (Gotze, 2012; Augustsson and Bahlburg, 2003).

Cathodoluminescence images produced on the storm wave-dominated shallow platform deposits thin sections of the Carboniferous of the Parnaíba Basin show quartz with brown, reddish brown and violet colors (Figure 14A). Metamorphic rocks regionally metamorphosed with slow cooling and with plutonic or contact metamorphic rocks are sources associated with these colors. The siltstone fragments have the same brown color as the Poti Formation rock framework grains (Figure 14B), which may indicate that the source is intrabasinal. The feldspar grains are prismatic and exhibit a bright blue color (Figure 14C), while the kaolinite/illite matrix and silica cement do not show luminescence (Figure 14D). The integration of cathodoluminescence with petrography and heavy minerals refines the results, which determine the tectonic units as possible sources of sediments in the Borborema Province.

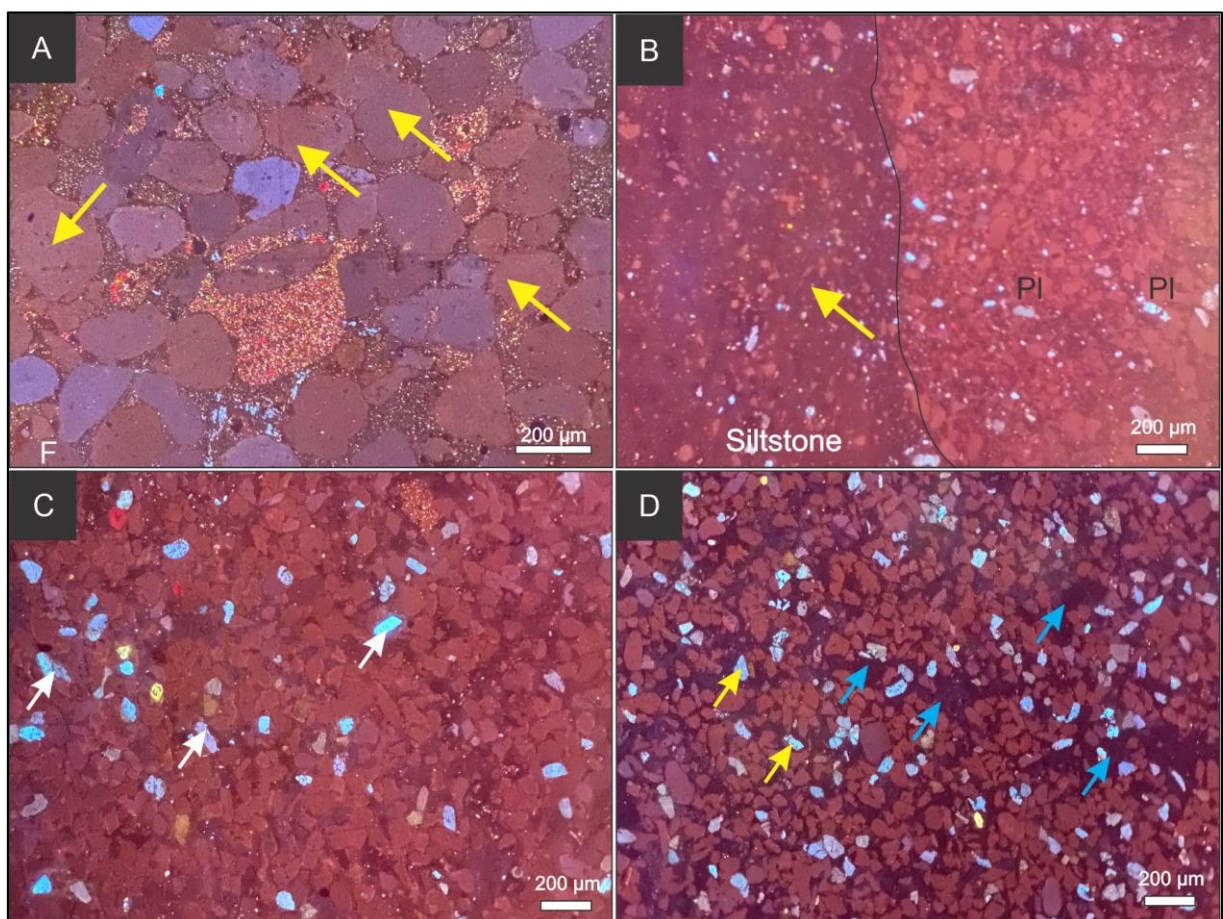


Figure 14 - Cathodoluminescence applied on quartz and feldspar grains from the Poti Formation. A) Brown quartz grains (yellow arrow). B) Fragment of siltstone exhibiting dark brown color (yellow arrow). C) Prismatic feldspar grains exhibiting bright blue color (white arrow). D) Clay and cements without luminescence (blue arrow) and feldspars with a bright blue color (yellow arrow).

Quartzarenites and subarkose sandstones have their origin related to inner craton blocks with a predominance of metamorphic and igneous rocks. However, due to the amount of feldspar, it is possible that the original environment was continental transition, since most of the feldspars altered to clay minerals or underwent a process of total dissolution in diagenesis, resulting in greater mineralogical maturity to the rock. Cratonic regions are portions of continental shelves bordered by orogenic belts and tectonically stabilized.

The Poti Formation sandstones are texturally immature, with subangular and moderately to poorly sorted grains, indicating greater proximity to the sediment source area, due to rapid transport and short periods of physical and chemical weathering. The low concentration of hematite cement may indicate that the contribution of volcanic rock fragments on sedimentation was minimal as a source of sediments (Dowey *et al.*, 2012; Haile *et al.*, 2018; Cardoso *et al.*, 2019).

Located to the southeast of the study area, the Borborema Province is the probable sediment source area for the Poti Formation. Collisional events that reactivated the Transbrasiliano Lineament, resulting in the approach and collision with the São Francisco Craton generated the Borborema Province (Araújo, 2014). The Brasiliano Cycle produced approximately 30% of the granitic magmatism in the province (Brito Neves *et al.*, 2003). The paleocurrent pattern and petrographic data defined the geotectonic unit's sediment source.

The Barra Bonita Formation, Serra da Aldeia Intrusive Suite, Lagoa Alegre Complex, Remanso Granitoid Body, Campos Sales-Assaré Pluton, Ipueirinha Group, Itaizinho Complex and Granjeiro Complex are the probable sources of the Poti Formation sediments. The Barra Bonita Formation and the Ipueirinha Group are composed of metasedimentary rocks such as phyllite and micaschists associated with feldspathic quartzite and marbles; the most abundant minerals are muscovite, biotite, plagioclase and accessory minerals such as sericite, garnet, kyanite, staurolite and cordierite (Caixito *et al.*, 2016; Basto *et al.*, 2019). The Alegre Complex is composed of metasedimentary rocks, migmatized gneisses, paragneisses, mafic rocks, banded iron formation and amphibolite dykes (Cid *et al.*, 2000).

The Sobradinho-Remanso and Itaizinho Complex are composed of migmatized TTG association rocks, metasediments with mafic rock enclaves and associations of iron formations (Garcia *et al.*, 2021; Melo e Vasconcelos, 1991). The Remanso granite, the Campos Sales-Assaré pluton and the Aldeia intrusive comprises potassium feldspar-rich granites, which is common for Proterozoic granites from the Borborema Province (Perpetuo *et al.*, 2016; Jesus *et al.*, 2022). The Granjeiro Complex has migmatized TTG composition and associations of

metasedimentary rocks of Archean age, being the oldest source of the associations (Silva *et al.*, 2002).

The Poti Formation rocks present a large contribution of quartz grains and feldspars, with the presence of lithic fragments of medium to high-grade metamorphic rocks, metasedimentary and igneous rocks, as indicated by the cathodoluminescence and the presence of inclusions in plutonic quartz grains. . The high occurrence of muscovite grains and microclines indicates that this source was rich in peraluminous and alkaline rocks, since the microcline is rich in potassium. In addition, the intrusive bodies next to the study area are rich in potassium feldspars, considered, therefore, a significant source of sediments. These rock associations are compatible with the data presented by cathodoluminescence and by the group of heavy minerals from the Poti Formation. Therefore, the most likely source is the Rio Grande do Norte Domain (Granjeiro Terrain), in the Borborema Province.

The reported ages for the syenogranitic orthogneisses in the Granjeiro Complex indicates ages of 2.6 Ga; These rocks are composed of metaluminous and peraluminous metagranites and syenogranites and rich in potassium (Vale, 2018).

Heavy minerals are of paramount importance in these integrated investigations since they are crucial for provenance analyses. However, the processes of weathering, transport, and diagenesis can make it difficult to identify source areas, because such minerals have its shape, density, physical resistance, and chemical stability modified (Morton, 1991; Morton & Hallsworth, 1994, 1999).

The identification of zircon grains, prismatic and rounded epidote, subrounded rutile, prismatic and rounded titanite, amphiboles, and tourmaline supports the hypothesis that the sources are medium- to high-grade metamorphic. The presence of prismatic and euhedral grains of zircon, amphibole and tourmaline suggest igneous rocks sources, associated with the Proterozoic granites of the Brasiliano. The upper shoreface facies associations contains the majority of the heavy minerals, which may be due to the higher depositional energy of these environments compared to the lower shoreface/offshore facies association sandstones.

6 Conclusions

The identification of five sedimentary facies allowed the faciological analyses, which is composed of sandstone with swaley cross-stratification (Facies 1), sandstone with hummocky cross-stratification (Facies 2), sandstone with plane-undulating stratification (Facies 3), siltstone with plane-undulating stratification/lamination (Facies 4), and massive mudstone (Facies 5). Oscillatory, unidirectional, or combination of both types of flows formed these deposits

The analysis and facies associations of the Poti formation indicates that the sediments were deposited on the upper shoreface (FA1) and lower shoreface/offshore (FA2) in a storm wave-dominated shallow platform environment under humid to arid climatic variations that constantly changed the fair-weather wave base line.

The Poti Formation sandstones plotted into the quartzarenites and subarkose sandstones fields with silt-grained and fine to coarse-grained sandstones with moderately to poorly sorted, subangular, and subrounded grains with low sphericity. They are texturally immature with less than 5% clay matrix in the composition; however, these sandstones are compositionally mature, since they have more than 90% quartz in their framework. These rocks are grain-supported and exhibits weak packing. Punctual contacts predominates, followed by sharp contacts.

From the integration of the data, it is possible to suggest that the Poti Formation is composed of sediments from the Granjeiro Territory, contained in the Rio Grande do Norte Domain, in the Borborema Province.

Through the results of X-ray diffractometry and diagenetic analysis, it was possible to determine the types of plagioclases, cements and mechanically infiltrated clays (kaolinite and illite). Infiltration of clay and cementation by hematite are the most significant diagenetic aspects identified, and both reduced the porosity of the Poti Formation rocks, especially in the basal layers of the study area.

Based on the modal composition that considers mono and polycrystalline quartz grains, feldspars, and rock fragments, we suggest that the primary sources of sediments for the Poti Formation were medium to high-grade metamorphic rocks, metasedimentary rocks and igneous rocks that occurs on the southeast of the Parnaíba Basin, next to Itaueira city in the State of Piauí. Continental blocks in interior craton are the possible source of sediments; it is possible that diagenetic processes altered the original composition of the rock; however, the textural features showed that the sediments underwent rapid transport and little reworking.

Finally, the integration of petrography, cathodoluminescence and X-ray diffractometry data proved to be extremely important, as the results were consistent with the inference and considerations about sediment provenance and climate. The application of sedimentary facies study and paleocurrent measurements provided inferences about the depositional environment of the Poti Formation in the Upper Carboniferous Period and its probable connection with the Tethys Sea to the northwest, as shown on the depositional model.

Acknowledgments

The first author is grateful to the Human Resources Program in analogous petroleum system and simulation of reservoirs in sedimentary basins (PRH47-Finep) of the Brazilian

National Agency for Petroleum Natural Gas and Biofuels for the postgraduation scholarship [grant number 00467281203]. All authors are also grateful to the Geosciences Postgraduation Program (PPGEOC) of the Federal University of Pernambuco and Federal University of Alagoas (UFAL-CETEC) for the support. We also thank to CNPQ (National Council for Scientific and Technological Development) for all the financial support and postgraduation scholarship (grant number 143630/2019-9). We would like to thank Valdielly Larisse Silva for the English review, Virgínia Neuman, and LAGESE (Laboratory of Sedimentary Geology) for the laboratory support, as well as CETENE (Northeast Technology Center), for x-Ray diffractometry analysis; and FADE (UFPE Development Support Foundation for the support) , during the work development.

References

- Almoqaddam, R.O., Darwish, M., Barkooky, C., Clerk, C. 2018. Sedimentary facies of the Upper Bahariya sandstone reservoir in East Bahariya C area, North Western Desert, Egypt. E. Journ. OF Petrol. 27, pp. 1103-1112.
- Augustsson, C., Bahlburg, H., 2003. Cathodoluminescence spectra of detrital quartz as provenance indicators for Paleozoic metasediments in southern Andean Patagonia. J. South Am. Earth Sci. 16, 15–26. [https://doi.org/10.1016/S0895-9811\(03\)00016-6](https://doi.org/10.1016/S0895-9811(03)00016-6)
- Angus, L., Hampson, G.J., Palci, F., Fraser, A.J. 2020. Characteristics and context of high-energy, tidally modulated, barred Shoreface deposits: Kimmeridgian-Tithonian sandstones, Weald Basin, Southern U.K. and Northern France. J. of Sed. Resear. 90, pp. 313-335. DOI: <http://dx.doi.org/10.2110/jsr.2020.19>.
- Araújo, C. E. G., Weinberg, R. F, Cordani, U. G. 2014. Extruding the Borborema Province (NE-Brazil): a two-stage Neoproterozoic collision process. Terra Nov. 26, pp 157–168.
- Araújo, V.B.V. 2018. Sedimentação, estratigrafia e diagênese dos reservatórios da Formação Poti, Viseano, Bacia do Parnaíba. Universidade de Brasília. pp. 152.
- Armitage J.J. & Allen P.A. 2010. Cratonic basins and the long-term subsidence history of continental interiors. Journal of the Geological Society of London **167**, 61–70. <https://doi.org/10.1144/0016-76492009-108>.
- Arnott, R.W., Southard, J.B., 1990. Exploratory flow duct experiments on combined flow bed configurations and some implications for interpreting storm event stratification. J. Sediment. Petrol. 60, 21 l-219.
- Asurmendi, E., Sanchez, M.L., Heredia, S. 2018. Stratigraphy and facies analysis of the La Chica Formation, Central Precordillera: Insights on the postglacial Ordovician-Silurian boundary and Early Silurian deposits from Argentina. DOI: [10.1002/gj.3390](https://doi.org/10.1002/gj.3390).
- Basilici, G., Luca, P.H.V., Oliveira, E.P. 2012. A Depositional model for a wave-dominated open-coast tidal flat, based on analyses of the Cambrian-Ordovician Lagarto and Palmares formation, northeastern Brazil. Sedimentology 59, pp. 1613-1639. doi: [10.1111/j.1365-3091.2011.01318.x](https://doi.org/10.1111/j.1365-3091.2011.01318.x).
- Basto, C.F., Caixito, F.A., Vale, J.A.R., Silveira, D.A., Rodrigues, J.B., Alkmim, A.R., Valeriano, C.M., Santos, E.J. 2019. Na Eodiacaran back-arc basin preserved in the Transversal Zone of the Borborema Province: Evidence from geochemistry, geochronology and isotope systematics of the Ipueirinha Group, NE Brazil. Prec. Res. 230, pp. 213-231. <https://doi.org/10.1016/j.precamres.2018.11.002>.

Betard, F., Caner, L., Gunnell, Y., Bourgeon, G. 2009. Ililite neoformation in plagioclase during weathering: Evidence from semi-arid, Northeast Brazil. *Geoderma* 152, 53-62. <https://doi.org/10.1016/j.geoderma.2009.05.016>.

Blakey, R.C., 2003. Carboniferous-Permian paleogeography of the assembly of Pangea. XVth International Congress on Carboniferous and Permian Stratigraphy.

Boggs, S., Krinsley, D., 2006. Application to Cathodoluminescence Imaging to the Study of Sedimentary Rocks. Cambridge University Press, Cambridge, UK. <https://doi.org/10.1017/CBO9780511535475>.

Boggs S. Jr., Kwon Y.-I., Goles G.G., Rusk B.G., Krinsley D., Seyedolali A. 2002. Is quartz cathodoluminescence color a reliable provenance tool? A quantitative examination. *Journal of Sedimentary Research*, 72:408–415.

Boggs, S., Krinsley, D., 2006. Application of Cathodoluminescence Imaging to the Study of Sedimentary Rocks. Cambridge University Press. <https://doi.org/10.1017/CBO9780511535475>.

Boggs, S., Jr., 2009. Petrology of Sedimentary Rocks. New York: Cambridge University Press. <https://doi.org/10.1002/gj.1241>.

Bowman, A.P., Johnson, H.D., 2014. Storm-dominated shelf-edge delta successions in a high accommodation setting: The palaeo-Orinoco Delta (Mayaro Formation), Columbus Basin, South-East Trinidad. *Sedimentology* 61, 792–835.

Brito-Neves, B.B., Fuck, R.A., Cordani, U.G., Thomaz Filho, A., 1984. Influence of basement structures on the evolution of the major sedimentary basins of Brazil: A case of tectonic heritage. *J. of Geodynamics* 1, 495-510. [https://doi.org/10.1016/0264-3707\(84\)90021-8](https://doi.org/10.1016/0264-3707(84)90021-8).

Brito Neves, B. de B., Passarelli, C. R., Basei, M. A. S., & Santos, E. J. 2003. Idades U-Pb em zircão de alguns granitos clássicos da Província Borborema. *Geologia USP. Série Científica*, 3, 25-38. <https://doi.org/10.5327/S1519-874X2003000100003>.

Bruckmann, M.P., Philipp, R.P., Scherer, C.M.S., Espíndola, E., Halfen, L. 2019. Análise petrográfica e proveniência do Arenito Pedreira, Jurássico Superior da Bacia do Paraná, sul do Brasil. *Pesquisa em Geoc.* V 46, n 3. doi.org/10.22456/1807-9806.97380.

Caxito, F.A., Uhlein, A., Dantas, E.L., Stevenson, R., Salgado, S.S., Dussin, I.A., Sial, A. N., 2016. A complete Wilson Cycle recorded within the Riacho do Pontal Orogen, NE Brazil: Implications for the Neoproterozoic evolution of the Borborema Province at the heart of West Gondwana. *Pre. Res* 282, 97–120. <https://doi.org/10.1016/j.precamres.2016.07.001>.

- Caputo, M.V. 1984. Stratigraphy, tectonics, paleoclimatology and paleogeography of northern basins of Brazil (Doctorate thesis). University of California, Santa Barbara, USA.
- Cardoso, A.R., Nogueira, A.C.R., Rabelo, C.E.N., Soares, J.L., Góes, A.M. 2019. Multi-approach provenance in stratigraphy: Implications for the Upper Mesozoic evolution of the Parnaíba Basin, NE Brazil. *Journal of South American Earth Sciences* 96, pp. 102386. <https://doi.org/10.1016/j.sames.2019.102386>.
- Cesero, P.; Mauro, L.M.; Deros, L.F. 1989. Técnicas de preparação de lâminas petrográficas e de moldes de poros na Petrobrás. *Boletim de Geociências da Petrobrás*, n.3, p.105-116.
- Coelho, D.L.O., Julià, J., Rodríguez-Tribaldos, V., White, N., 2018. Deep crustal architecture of the Parnaíba basin of NE Brazil from receiver function analysis: Implications for basin subsidence, in: Geological Society Special Publication. Geological Society of London, pp. 83–99. <https://doi.org/10.1144/SP472.8>.
- Collinson, J. D.; Mountney, P.D; Thompson, D. B. 2006. *Sedimentary structures*, 3th ed.: Chapman and Hall, London, 280p
- Corrêa-Martins, F.J., Mendes, J.C., Bertolino, C., De, J., Mendonça, O., n.d. *Petrografia, Diagênese e Considerações sobre Proveniência da Formação Itapecuru no Norte do Maranhão (Cretáceo Inferior, Bacia do Parnaíba, NE Brasil)*.
- Chamley, H., 1989. *Clay Sedimentology*. Springer Verlag, Berlin, 623 pp.
- Costa, C.Z., Remus, M.V. 2016. Proveniência dos arenitos da Bacia de Campos (Andar Alagoas), por meio da composição da granada. *Geol. Serie cient. USP* 16, pp. 83-100. DOI: 10.11606/issn.2316-9095.v16i2p83-100.
- Cid, J.P., Nardi, L.V.S., Conceição, H., Bonin, B., Jardim de Sá, E.F. 2000. The alcaline silica-saturated ultrapotassic magmatism of the Riacho do Potntal Fold Belt, NE Brazil: an example of syenite-granite Neoproterozoic association. *Journal of S. Amer. Earth Sci.* 13, pp. 661-683. [https://doi.org/10.1016/S0895-9811\(00\)00047-X](https://doi.org/10.1016/S0895-9811(00)00047-X).
- Daly, M.C., Fuck, R.A., Julià, J., Macdonald, D.I.M., Watts, A.B., 2018. Cratonic basin formation: A case study of the Parnaíba Basin of Brazil, in: Geological Society Special Publication. Geological Society of London, pp. 1–15. <https://doi.org/10.1144/SP472.20>.
- Della Fávera, J.C., 2001. *Fundamentos de estratigrafia moderna*. Editora Moderna, Rio de Janeiro.

Dickinson, W.R., 1985. Interpreting provenance relations from detrital modes of sandstones. In: Zuffa, G.G. (Ed.), Provenance of Arenites. Reidel, 148. NATO ASI Series, Dordrecht, pp. 333-361.

Dowey, P.J., Hodgson, D.M., Worden, R.H., 2012. Pre-requisites, processes, and prediction of chlorite grain coatings in petroleum reservoirs: A review of subsurface examples. *Marine and Petroleum Geology* 32, 63-75. [10.1016/j.marpetgeo.2011.11.007](https://doi.org/10.1016/j.marpetgeo.2011.11.007).

Dumas, S., Arnott, R.W.C., 2006. Origin of hummocky and swaley cross-stratification. The controlling influence of unidirectional current strength and aggradation rate. *Geology* 34, 1073–1076. <https://doi.org/10.1130/G22930A.1>.

Dutra, V.P.L. 2011. Análise faciológica e petrográfica da Formação Poti (Mississipiano, Bacia do Parnaíba) em testemunhos de sondagem (Conclusion monography). Universidade Federal do Rio de Janeiro. pp. 82.

Fan, A.P., Sun, S.N., Yang, R.C., Zhang, Z., De, S., Nenzhelele, J.D.N., Li, Y., Liu, H.P., Zhou, Y.Q., Yuan, J., 2020. Provenance analysis of the Cretaceous Laiyang Group on Lingshan Island (western Yellow Sea, China) and its tectono-sedimentary implications. *Australian Journal of Earth Sciences* 67, 361–377. <https://doi.org/10.1080/08120099.2019.1661285>.

Feitosa, I.L., Alvarenga, C.J.S., Martinho, C.T. 2019. Litofácies, ambientes deposicionais e ciclicidade do Grupo Paranoá: exemplo de região da Serra de São Domingos, Minas Gerais. *Geol. Série Científica da USP* 19 (1), pp. 153-170. DOI: 10.11606/issn.2316-9095.v19-140467.

Ferraz, N.C., Cóbora, V.C., Sousa, D.C. 2017. Análise estratigráfica da sequência Mesodevoniana-Eocarbonífera da Bacia do Parnaíba, Nordeste do Brasil. *Geociências*, UNESP, 36, n1, 154-172. <https://doi.org/10.5016/geociencias.v36i1.12302>.

Garcia, P.M.P., Carriño, E.L.V., Ribeiro, B.P., Misi, A., Sá, J.H.S., Rios, D.C. 2021. Geology, petrogenesis and geochronology of the Rio Salitre Complex: Implications for the Paleoproterozoic evolution of the northern São Francisco Craton, Brazil. *J. of South Amer. Earth Sci.* 107, pp. 103112. <https://doi.org/10.1016/j.jsames.2020.103112>.

Góes A. M. & Feijó F. J. 1994. Bacia do Parnaíba. Boletim de Geociências da Petrobras, 8 (1), p.57-67.

Góes, A. M. 1995. A Formação Poti (Carbonífero Inferior) da Bacia do Parnaíba. TS Universidade de São Paulo. Instituto de Geociências. São Paulo. 171p.

Gotze, J., 2002. Potential of cathodoluminescence (cl) microscopy and spectroscopy for the analyses of minerals and material, in: Analytical and Bioanalytical Chemistry. pp. 703-708. <https://doi.org/10.1007/s00216-002-1461-1>.

Gotze, J., 2012. Application of cathodoluminescence microscopy in geosciences, in: Microscopy and Microanalyses 8, pp. 1270-1284. <https://doi.org/10.1017/S1431927612001122>

Grundvåg, S.A., Jelby, M.E., Olaussen, S., Śliwińska, K.K., 2021. The role of shelf morphology on storm-bed variability and stratigraphic architecture, Lower Cretaceous, Svalbard. *Sedimentology* 68, 196–237. <https://doi.org/10.1111/sed.12791>.

Grundvåg, S.A., Olaussen, S., 2017. Sedimentology of the Lower Cretaceous at Kikutoddan and Keilhaufjellet, southern Spitsbergen: Implications for an onshore-offshore link. *Polar Research* 36. <https://doi.org/10.1080/17518369.2017.1302124>.

Haile, B.G., Czarniecka, U., Xi, K., Smyrak-Sikora, A., Jahren, J., Braathen, A., Hellevang, H., 2019. Hydrothermally induced diagenesis: Evidence from shallow marine-deltaic sediments, Wilhelmøya, Svalbard. *Geoscience Frontiers* 10, 629–649. <https://doi.org/10.1016/j.gsf.2018.02.015>.

Hasui, Y., Carneiro C. D. R., Almeida F. F. M. De Bartorelli A. 2012. Eds. *Geologia do Brasil*. São Paulo: Ed Beca. 900p.

Jelby, M.E., Grundvåg, S.A., Helland-Hansen, W., Olaussen, S., Stemmerik, L., 2020. Tempestite facies variability and storm-depositional processes across a wide ramp: Towards a polygenetic model for hummocky cross-stratification. *Sedimentology* 67, 742–781. <https://doi.org/10.1111/sed.12671>.

Jesus, J.V.M., Almeida, C.N.A., Schitt, R.S., Vilhena, J.F.M. 2022. Shoshonitic magmatism in the Southwestern Borborema Province (NE Brazil): The plutons of Campos Sales-Assaré and Padre Marcos. *J. of South Amer. Earth Sci.* 116, pp. 103833. <https://doi.org/10.1016/j.james.2022.103833>.

Lee, H.S., Chen, J., Han, Z., Chough, S.K., 2018. Depositional processes and environmental changes during initial flooding of an epeiric platform: Liguan Formation (Cambrian Series 2), Shandong Province, China. *Geosciences Journal* 22, 903–919. <https://doi.org/10.1007/s12303-018-0027-y>

Lima, E. A. M. & Leite J. F. 1978. Projeto estudo Global dos Recursos Minerais da Bacia do Parnaíba: Integração geológico-metalogenética. Relatório Final da Etapa III. DNPM – Departamento Nacional de Produção Mineral, CPRM – Companhia de Pesquisa de Recursos Minerais. Recife, pp. 212.

Loboziak, S., Melo, J.H.G., 2000. Miospore events from late Early to Late Devonian strata of Western Gondwana. *Geobios* 33, 399–407. [https://doi.org/10.1016/S0016-6995\(00\)80072-8](https://doi.org/10.1016/S0016-6995(00)80072-8).

- Lorentzen, S., Braut, T., Augustsson, C., Nystuen, J.P., Jahren, J., Schovsbo, N.H., 2020. Provenance of lower Cambrian quartz arenite on southwestern Baltica: Weathering versus recycling. *Journal of Sedimentary Research* 90, 493–512. <https://doi.org/10.2110/JSR.2020.20>
- Maahs, R., Kuchle, J. Scherer, C.M.S., Alvarenga, R.S. 2019. Sequence stratigraphy of fluvial to shallow-marine deposits: The case of the early Permian Rio Bonito Formation, Paraná Basin, southernmost Brazil. *Brazilian Journal of Geology* 49 (4). DOI: 10.1590/2317-4889201920190059.
- Marfil, R., Delgado, A., Rossi, C., Iglesia, A.L., Ramseyer, K. 2003. Origin and diagenetic evolution of kaolin in reservoir sandstones and associated shales of the Jurassic and Cretaceous, Salam Field, Western Desert (Egypt). *Inst. Assoc. Sediment. Special Puc 34*, pp. 319-342. 10.1002/9781444304336.ch14.
- McCabe P.J. 1985. Depositional environments of coal and coal-bearing strata. In: Rahmani R.A., Flores R.M. (Eds.), *Sedimentology of coal and coal- bearing sequences*. Oxford, IAS, Special Publication, 7, 13-42.
- Melo, F., Vasconcelos, A.M., 1991. Mapa Geológico da Folha Patos (SC.24-V-A-V), escala 1:100.000. Departamento Nacional de Produção Mineral (DNPM)/Companhia de Pesquisa de Recursos Minerais (CPRM/SGB), Brasília, Programa Levantamentos Geológicos Básicos do Brasil
- Memória, S. C., Netto, R. G., de Andrade, L. S., Sedorko, D., Cisneros, J. C., & Agostinho, S. M. (2021). Ichnofauna from the Silurian–Devonian beds of the Parnaíba Basin at Poti River Canyon (Piauí State, NE Brazil). *Journal of South American Earth Sciences*, 110. <https://doi.org/10.1016/j.jsames.2021.103376>.
- Mesner, C.J., Wooldridge, C.P., 1964. Maranhão Paleozoic basin and Cretaceous coastal basin, north Brazil. *Bull. Am. Assoc. Petroleum Geology* 48 (9), 1475-1512. DOI: 10.1306/BC743D99-11D7-8645000102C1865D.
- Morad, S., Al-Ramadan, K., Ketzer, J.M., de Ros, L.F., 2010. The impact of diagenesis on the heterogeneity of sandstone reservoirs: A review of the role of depositional fades and sequence stratigraphy. *American Association of Petroleum Geologists Bulletin*. <https://doi.org/10.1306/04211009178>.
- Morton, A.C., 1991. Geochemical studies of detrital heavy minerals and their application to provenance research. *Geological Society Special Publication* 57, 31–45. <https://doi.org/10.1144/GSL.SP.1991.057.01.04>.

- Morton, A. C. & Hallsworth, C. 1994. Identifying provenience-specific features of detrital heavy mineral assemblages in sandstones. *Sed. Geology*, 90. pp.241-256. [https://doi.org/10.1016/0037-0738\(94\)90041-8](https://doi.org/10.1016/0037-0738(94)90041-8).
- Morton, A. C. & Hallsworth, C. 1999. Processes controlling the composition of heavy mineral assemblages in sandstones. *Sedimentary Geology* 124, pp.3-29. [https://doi.org/10.1016/S0037-0738\(98\)00118-3](https://doi.org/10.1016/S0037-0738(98)00118-3).
- Mutti, E., 1992. Turbidite sandstones. San Donato Milanese. AGIP – Istituto di Geologia, Università di Parma, pp. 275.
- Mutti, E., Davoli, G., Tinterri, R., Zavala, C., 1996. The importante of Fluvio-Deltaic Systems Dominated by Catastrophic Flooding in Tectonically active Basins, 48. *Memorie di Scienze Geologiche*, Universita di Padova, pp. 233-291.
- Ocampo-Díaz, Y.Z.E., Sosa-Ceballos, G., Saucedo, R., Macías, J.L., Bolós, X., Radilla-Albarrán, U.A., Martínez-Paco, M., Salinas-Ocampo, U., Cisneros-Máximo, G., 2021. Provenance and compositional variations of intra-caldera lake sediments at La Primavera, Jalisco, Western Mexico. *Journal of South American Earth Sciences* 110. <https://doi.org/10.1016/j.jsames.2021.103335>.
- Oliveira, D.C., Mohriak, W.U., 2003. Jaibaras trough: An important element in the early tectonic evolution of the Parnaíba interior sag basin, Northen Brazil. *Marine and Petroleum Geology* 20, 352-383. [https://doi.org/10.1016/S0264-8172\(03\)00044-8](https://doi.org/10.1016/S0264-8172(03)00044-8)
- Paiva, R.G. 2018. Estratigrafia de sequências aplicada à Formação Poti, Viseano da Bacia do Parnaíba (Mater's dissertation). Universidade de Brasília. pp. 104.
- Pasquo, M., Iannuzzi, R. 2014. New Palynological information from the Poti Formation (upper Visean) at the Roncador creek, Parnaíba Basin, northeastern Brazil. *Boletin Geológico y Minero*, 125(4), 405-435.
- Perpetuo, M.P., Amaral, W.S., Costa, F.C., Uchoa Filho, E.C., Sousa, D.F.M. 2016. Geochemistry of the Serra das Melancias Pluton in the Serra da Aldeia Suite: a classic post-collisional high Ba-Sr granite in the Riacho do Pontal Fold Belt, NE Brazil. *Braz. J. Geol.* 46 (2), 221-237. <https://doi.org/10.1590/2317-4889201620160002>.
- Peters, S.E., Loss, D.P., 2012. Storm and fair-weather wave base: a relevant distinction? *Geology* 40, 511–514. <https://doi.org/10.1130/G32791.1>.
- Plint A.G. 2010. Wave- and storm-dominated shoreline and shallowmarine systems. In: James N.P., Dalrymple R. W. (Eds.), *Facies models 4. Newfoundland & Labrador, Geological Association of Canada Publications*, 4, p. 167-199.

- Quin, J.G., 2011. Is most hummocky cross-stratification formed by large-scale ripples? *Sedimentology* 58, 1414–1433. <https://doi.org/10.1111/j.1365-3091.2010.01219.x>.
- Santos, M.N., Jr Chemale, F., Dussin, I.A., Martins, M.S., Queiroga, G., Pinto, R.T.R., Santos, A.N., Armstrong, R. 2015. Provenance and paleogeographyc reconstruction of a mesoproterozoic intracratonic sag basin (Upper Es'pinhaço Basin, Brazil). *Sedimentary Geology* 318, 40-57.
- Santos, F.H., Amaral, W., Luvizotto, G.L., Sousa, D.F.M. 2018. P-T evolution of metasedimentary rocks of the Santa Filomena Complex, Riacho do Pontal Orogen, Borborema Province (NE Brazil): Geothermobarometry and metamorphic modelling. *J. Of S. Amer. Eart Sci.* 82, pp. 91-107. <https://doi.org/10.1016/j.jsames.2017.12.013>.
- Santos, M.E.C.M., Carvalho, M.S., 2009. Paleontologia das Bacias do Parnaíba, Grajaú e São Luís – Reconstituições Paleobiologicas. Companhia de Pesquisa de Recursos Minerais (CPRM), Rio de Janeiro, p. 212.
- Scotese, C.R., 2021. An Atlas of Phanerozoic Paleogeographic Maps: The Seas Come In and the Seas Go Out. *Annual review of Earth and Planetary Sciences* 49, 669-718.
- Soares, J.E.P., Stephenson, R., Fuck, R.A., de Lima, M.V.A.G., de Araújo, V.C.M., Lima, F.T., Rocha, F.A.S., da Trindade, C.R., 2018. Structure of the crust and upper mantle beneath the Parnaíba Basin, Brazil, from wide-angle reflection-refraction data. *Geological Society, London, Special Publications*, 472. <https://doi.org/10.6084/m9.figshare.c.4058582>
- Thiry, M., Francé, F., 2000. Palaeoclimatic interpretation of clay minerals in marine deposits: an outlook from the continental origin, *Earth-Science Reviews* 49. pp. 201-221. [https://doi.org/10.1016/S0012-8252\(99\)00054-9](https://doi.org/10.1016/S0012-8252(99)00054-9)
- Tucker, M.E., 2001. *Sedimentary Petrology: Na introduction to the origin of Sedimentary Rock*. Blackwell Science, Oxford.
- Vakarelov, B.K., Ainsworth, R.B., MacEachern, J.A., 2012. Recognition of wave-dominated, tide-influenced shoreline systems in the rock record: Variations from a microtidal shoreline model. *Sedimentary Geology* 279, 23–41. <https://doi.org/10.1016/j.sedgeo.2011.03.004>.
- Vale, J.A.R., 2018. Caracterização geoquímica e geocronológica ´ do Complexo Granjeiro, Província Borborema, NE Brasil: Implicações para a evolução paleoarqueana do distrito ferrífero de Curral Novo do Piauí. MSc Dissertaton, Universidade de São Paulo, São Paulo, p. 110p.
- Vaz, P.T., Resende, N.G.A.M., Wanderley Filho, J.R., Travassos, W.A., 2007. Bacia do Parnaíba. *Bol. Geociências Petrobras* 15, 253–263.

Worden, R.H., Armitage, P.J., Butcher, A.R., Churchill, J.M., Csoma, A.E., Hollis, C., Lander, R.H., Omma, J.E., 2018. Petroleum reservoir quality prediction: Overview and contrasting approaches from sandstone and carbonate communities, in: Geological Society Special Publication. Geological Society of London, pp. 1–31. <https://doi.org/10.1144/SP435.21>

Xiao, Q., She, G., Wang, G., Li, Y., Ouyang, G., Cao, K., Manson, R., Du, Y. 2020. Terminal Ediacaran carbonate tempestites in the eastern Yangtze Gorges, South China. *Paleogeography, Paleoclimatology, Paleoecology* 547. <https://doi.org/10.1016/j.palaeo.2020.109681>.

Zinkernagel U. 1978. Cathodoluminescence of quartz and its application to sandstone petrology. *Contributions to Sedimentology*, 8, pp. 1-69.

5.2 ARTIGO 2 - PETROGRAPHY, DIAGENESIS, AND CONSIDERATIONS ABOUT THE RESERVOIR QUALITY OF THE POTI FORMATION SANDSTONES, PARNAÍBA BASIN, NORTHEASTERN BRAZIL

João Vicente Tavares Calandrini de Azevedo^{a,*}, Mário Ferreira de Lima Filho^a, Zenilda Vieira Batista^b, Sônia Maria Oliveira Agostinho da Silva^a, Emmanuel Franco Neto^a, Valdielly Larisse Silva^a

^a Federal University of Pernambuco, Post-graduation Program, Department of Geology, Av. Da Arquitetura, S/N, Recife, Pernambuco, 52740030, Brazil.

^b Federal University of Alagoas, Center of Technology, Av. Lourival Melo Mota, S/N, Alagoas, Maceió, 57072-900, Brazil.

* Corresponding author:
joaovince2015@gmail.com (J.V. Azevedo)

ABSTRACT

The focus of this research was to characterize the Poti Formation sandstones in the Parnaíba Basin in terms of their petrographic and diagenetic constituents, in the Itaueira region (Piauí State). Therefore, the following materials and techniques were used: petrography, X-ray diffraction (XRD), and hot cathodoluminescence (CL). The analyses allowed characterizing diagenetic events and their effects on Poti Formation rocks, thereby inferring reservoir quality. According to previous work, the studied succession represents a storm wave-dominated platform environment, divided into two facies associations: Lower Shoreface/Offshore (FA1) and Upper Shoreface (FA2). The sandstones are composed of silt and fine to coarse-grained quartzarenites and subarkosian sandstones with subangular to angular and poorly sorted grains; these rocks are texturally immature with weak packing index. Both associations are texturally homogeneous, but they differ in grain-size, subenvironment, and diagenetic events that affected reservoir quality. The identified diagenetic processes are mechanical infiltration of clay, mechanical and chemical compaction, cementation of silica and hematite, alteration of unstable grains, dissolution, and substitution. With an average porosity of 11%, intergranular, intragranular, moldic, and large pore types, formed by feldspar dissolution, mechanical compaction and fracturing processes, represents these rocks. Clay and iron cement had a negative impact on reservoir quality, particularly in the lower shoreface/offshore and basal layers, where porosity and permeability decreased. In contrast, the low occurrence of these events in the upper beds and upper shoreface facies associations had no major impact on reservoir quality and maintained the porosity. The Sardinha Formation acid hydrothermalism contributed to the formation of large pores and increased the generation of secondary porosity, with a maximum value of 4.0 %. According to the data, the upper shoreface facies association and the upper beds of the succession exhibits the best reservoir qualities.

KEYWORDS: Reservoir rock; Parnaíba Basin; Poti Formation; Sandstone diagenesis; Porosity

1 Introduction

Inserted in the Canindé Group, the Visean Poti Formation has extensive exposures in the Parnaíba Basin's north, central, and southeast areas (Melo and Loboziak, 2000; Vaz *et al.*, 2007). This unit is in gradational contact with the underlying platform deposits of the Longá Formation, while its upper contact with the overlying Piauí Formation is regionally discordant (Lima and Leite, 1978; Santos and Carvalho, 2009).

The Poti Formation is composed of conglomerates and sandstones interbedded with siltstones and shales, deposited in storm-wave-dominated platforms, fluvial channels, deltaic, and tidal flat environments, reaching a maximum thickness of 320 meters (Ferraz *et al.*, 2016; Góes e Feijó, 1994; Oliveira e Moura, 2018).

The Coal Exploration Program (1975 - 1981) conducted several studies at the Poti Formation during the seventies. However, this unit still lacks detailed petrographic, diagenetic and faciological studies that could provide more information and contribute to future studies on the quality of Poti sandstones as a hydrocarbon reservoir, since this unit occurs to a large extent in the Parnaíba Basin. Regarded as a rock reservoir, along with the Cabeças and Piauí formations, the Poti Formation exhibits good porosity (average of 18%) and permeability (values exceeding 240 mD) (Soares and Borghi, 2014; Soares, 2007; Miranda *et al.*, 2018).

By selling blocks to exploitation, The Brazilian National Agency for Petroleum Natural Gas and Biofuels (ANP) has attracted many scientific and exploratory studies in recent decades, and this investment has resulted in a production of 5% of total gas generated in the country (Abelha *et al.*, 2018).

A series of studies involving petrophysical characterization and facies associations were conducted with the intention of assessing the Poti Formation's reservoir capacity (Dutra, 2011; Paiva, 2018). Furthermore, the application of sequence stratigraphy and diagenetic processes studies are critical for determining the changes in reservoir rocks of petroleum systems. (Araújo, 2018; Ferraz *et al.*, 2016).

The depositional and diagenetic events directly affect the reservoirs quality, modifying porosity and permeability as a function of depth and facies variation (Taylor *et al.*, 2010; Arlebrand *et al.*, 2021). Therefore, it is important to understand the heterogeneities of sandy bodies, as reservoir analogues, as well as the processes that affect their petrophysical characteristics, such as diagenesis (Sech *et al.*, 2009; Morad *et al.*, 2000; Worden *et al.*, 2018; Qian *et al.*, 2020). To comprehend the diagenetic mechanisms that influence reservoir quality and heterogeneity is crucial, for maximizing hydrocarbon recovery from mature producing oilfields (Morad *et al.*, 2010; Zhao *et al.*, 2022).

The constituents and diagenetic processes that occur in Poti Formation sandstones still need investigation, as well as their implications for the quality of these rocks as hydrocarbon reservoirs,. Therefore, this work aims to produce a petrographic and diagenetic characterization, to access the diagenetic processes and constituents that affected the porosity and original permeability of the studied sandstones.

This study contributed to a better comprehension of the diagenetic implications in the reservoir sandstones of the studied succession and to complement future works that will be carried out in the study area. Furthermore, petrographic and diagenetic aspects, in combination with nanomineralogical analysis (X-ray diffractometry and cathodoluminescence), will aid in understanding the mineral transformations during diagenesis, as well as identifying the clay mineral phases, increasing the geological knowledge of the studied unit.

2 Geological Setting

The Parnaíba Basin is an intracratonic basin, which covers an area of approximately 600.000 Km² and can achieve 3.500 m-thick of Paleozoic sedimentary successions in its depocenter (Figure 01; Vaz *et al*, 2007; Coelho *et al*, 2018; Daly *et al*, 2018). Geographically, the research area is in the Southwest of the Itaueira city, State of Piauí, Northeast Brazil (Figure 2).

The Parnaíba Basin basement origin relates to the formation and stabilization of the South-American Platform, which registered the deformational and orogenic events of the Brasiliano Cycle, and the development of transtensional rift events of the Jaibaras Basin (Oliveira and Moriak, 2003; Brito Neves and Fuck, 2013; Brito Neves, 1984; Brito Neves *et al.*, 2014). In the Paleozoic sedimentary basins of Brazil, such as Parnaíba, Paraná, and Amazonas, a phase of intracratonic sedimentation began, recording many depositional cycles, as soon as the Gondwana supercontinent stabilized. (Almeida et al., 2000; Carneiro & Almeida, 2004; Milani et al., 2007).

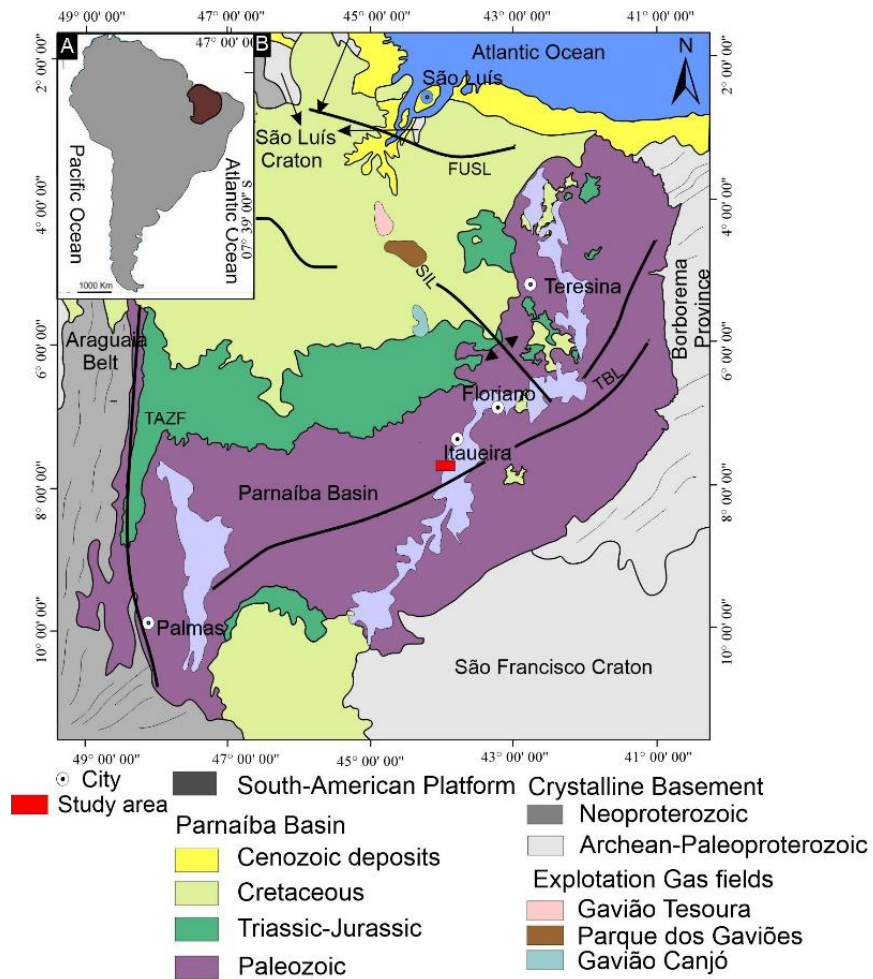


Figure 1 - A) Localization of the Parnaíba Basin contextualized in the South-American Platform. B) Simplified geological map of the Parnaíba Basin and the basement tectonic subdivision. TOAA: Tocantins-Araguaia Lineament; FUSL: Ferrer-Urbano Santos Lineament; PSIL: Picos-Santa Inês Lineament; TBL: Transbrasiliano Lineament. Modified of CPRM (2004).

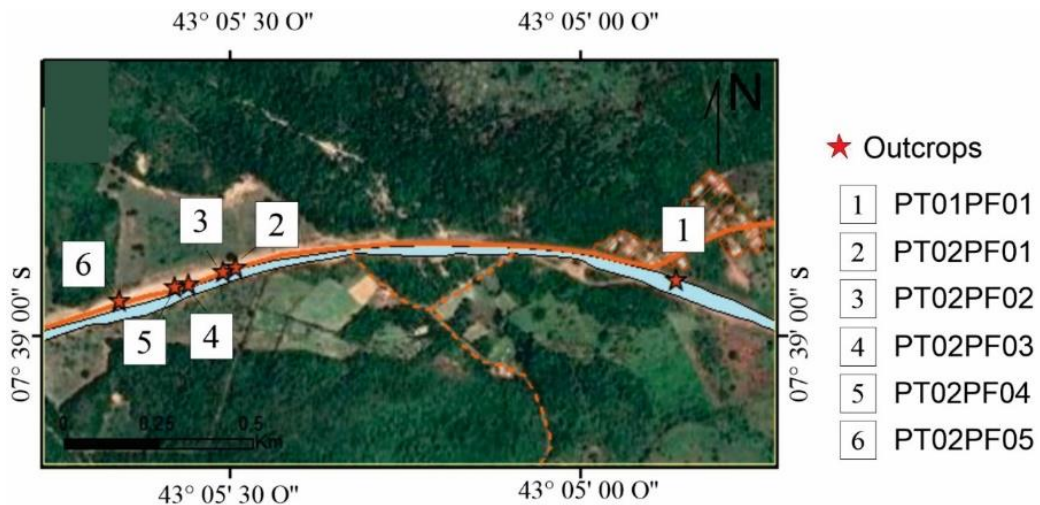


Figure 2 - Localization map of the study area and stratigraphic logs of the Poti Formation

The Parnaíba Basin sedimentary succession is divided into five supersequences, comprising siliciclastic and carbonate rocks ranging from the Silurian to the Cretaceous

(Tribaldos and White, 2018; Góes and Feijó, 1994). The first three supersequences (Serra Grande, Canindé, and Balsas Groups) is composed of neritic rocks with deposition induced by eustatic changes in sea level, and register a depocenter migration from the middle part of the basin to the N-NW region during the Cretaceous (Soares *et al.*, 2018; Brito Neves *et al.*, 1984). In the Gondwana active edge, the Parnaíba Basin and other Brazilian syneclysis had their erosive contacts and regional unconformities formed by epirogenic movements (Almeida and Carneiro, 2004; Cordani *et al.*, 1984; Cordani *et al.*, 2009; Oliveira *et al.*, 2018).

The Poti Formation belongs to the Canindé Group (Figure 3; Mesodevonian-Eocarboniferous Sequence), which represents the most important transgressive-regressive cycle in the Parnaíba Basin (Vaz et al, 2007; Della Fávera 1990). These rocks deposition occurred in deltaic, platform, neritic environments influenced by storm waves, and periglacial environments (Lima and Leite, 1978; Caputo, 1984; Jaju *et al.*, 2018).

The Poti Formation studied succession is composed of sandstone with swaley cross-stratification, sandstone with hummocky cross-stratification, sandstone with parallel to undulating stratification, siltstone with parallel to undulating stratification/lamination, and massive mudstone (Azevedo *et al.*, 2022). These facies grouping produced two faciological associations (AF): Lower Shoreface/Offshore (FA1) and Upper Shoreface (FA2).

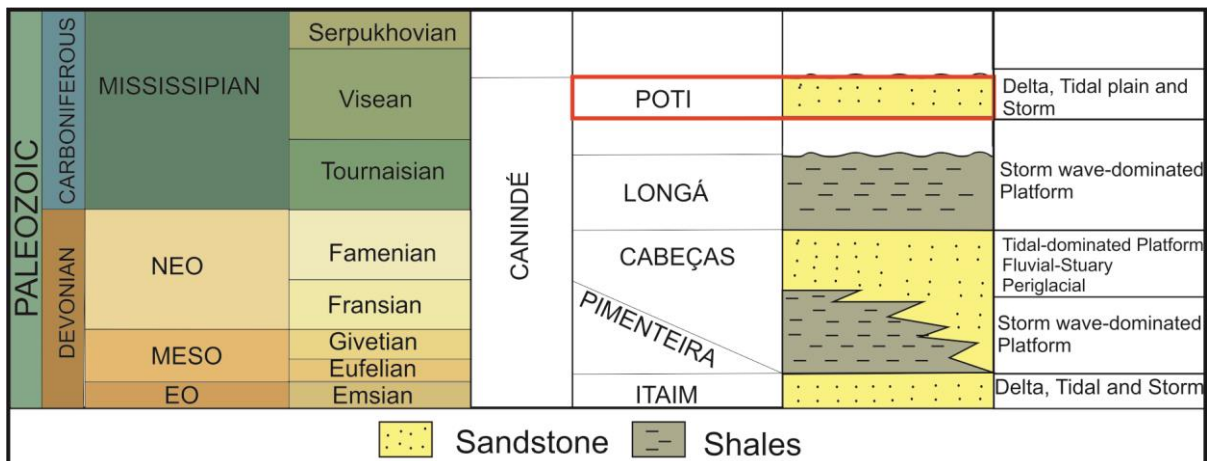


Figure 3 - Simplified chronostratigraphic chart of the Parnaíba Basin, Canindé Group. Adapted from Vaz *et al* (2007).

3 Material and Methods

The field research was carried out in the central portion of the Parnaíba Basin and six outcrops were analyzed in detail (Figure 4). For petrographic analysis, 15 samples were collected; grain size, texture, mineralogical composition, porosity type, primary and diagenetic constituents, diagenetic sequence, contact between grains, and packing level (Kahn, 1956). were all determined using a petrographic microscope (model Axioslop with a digital camera).

According to Cesere *et al.* (1989), thin sections of the studied rocks were previously impregnated with blue epoxy resin in order to identify and characterize the porosity, as well as to study the mineralogical composition and classification of the samples. The Folk (1968) classification, which takes into consideration the total content of quartz, feldspars, and rock fragments, was applied. According to Gazzi-Dickson method, the constituent quantification considered the counting of 300 points per thin section along three perpendicular crossings to the rock's structure and framework (Dickson, 1985).

In order to identify the clay content and other mineral phases, four sample of the studied sandstones were powdered in fractions smaller than $2\mu\text{m}$ and analyzed by X-ray diffraction at the Northeast Technology Center (CETENE). The diffractometer utilized was a Bruker model D8 Advance A25-X1 that operated using the Bragg-Brentano method at ambient temperature and humidity (24.30/37 %). The angular interval was 5° - 80° ; step: 0.02° ; time per step: 1.0 s; primary slit: 0.1 mm; Secondary slit: 5.0 mm; rotation speed: 15 /min. The data treatment was made by software X'PertHighScore, version 2.1b, which includes the PCPDFWIN (Powder Diffraction File-International Centre for Diffraction Data), from PANanalytical, as well.

In six samples, hot cathodoluminescence allowed the determination of carbonatic cements type, diagenetic constituents, and other minerals not visible under a conventional microscope. The experiment operated with an acceleration voltage of 10 Kv and $100\mu\text{A}$ current, vacuum between 0.003 and 0.05Pa, exposure time firstly of 10–15s and, afterwards, 40s. Images were taken by Nikon FDX-35, connected to a Axioskop microscop, in the Sedimentary Geology Laboratory (LAGESE), located at the Petroleum and Energy Institute of Research (LITPEG) The luminescence pattern was interpreted in accordance with Bernet & Bassett (2014), Augustsson (2012), Oliveira *et al.* (2017), and Boggs and Krinsley (2006).

The arithmetic average of the porosities per thin section from the petrographic study was used to calculate the average porosity. According to Morad *et al.* (2010), the diagenetic stages are defined as follows: eodiagenesis includes processes that occur under the influence of depositional fluids, at shallow depths, and at low temperatures (between 30 and 70°C , with a burial depth of 2.0 km);

Mesodiagenesis includes processes and reactions involving the reaction on minerals with acid water under effective burial conditions and relative high temperature (70° to 200°C). Mesodiagenesis can be shallow and deep: shallow mesodiagenesis corresponds to depths between 2 and 3 km and temperatures between 70 and 100°C ; deep mesodiagenesis extends from depths around 3 km and temperatures around 100°C till the limit of metamorphism; The

processes of uplift and re-exposure of sedimentary rocks to surface conditions, with meteoric conditions, are referred as telodiagenesis.

4 Results

4.1 Facies associations brief review

Although paleoenvironmental analyses are not within the scope of this work, this section provides a brief review of the faciological data, improving the understanding of the studied sandstone composition. The Upper Carboniferous Poti Formation succession is composed of five sedimentary facies grouped into two facies associations that represents a storm wave-dominated shallow platform environment: Upper Shoreface (FA1) and Lower Shoreface/Offshore (FA2). Figure 4 exhibits the overall framework of these deposits, in the Itaueira region. The Poti Formation studied succession is composed of sandstone with swaley cross-stratification, sandstone with hummocky cross-stratification, sandstone with parallel to undulating stratification, siltstone with parallel to undulating stratification/lamination, and massive mudstone.

These successions are composed of fine-grained sandstones with subangular and moderately to poorly sorted grains. The layers exhibit tabular geometry, and their depositional pattern and sedimentary structures show a constant variation of the fair-weather wave base, due to the influence of storms and eustatic sea level changes on shallow platforms, in arid to temperate climates. The paleocurrent measurements indicated NW and subordinately SW direction. The detailed sedimentological description can be found in Vaz *et al.* (2007), Góes (1995), Góes and Feijó (1994), Azevedo *et al.* (2022) e Soares and Borghi (2014).



Figure 4 - Panoramic view of the Poti Formation sandstones in the Itaueira region, Parnaíba Basin and vertical distribution of the sedimentary facies. The blue line represents an unconformity between the Poti Formation and the overlying Piauí Formation.

4.2 Petrography characterization of the Poti Formation

4.2.1 Texture, composition and fabric

Poti Formation is composed of silt and fine to coarse-grained sandstones, with subrounded to rounded and poorly to moderately sorted grains, exhibiting low sphericity. The grains presents preferential orientation with parallel and/or imbricated stratification, and fining-upward pattern (Figure 5A). However, in some samples the orientation is homogeneous and random (Figure 5B).

The primary constituents of these sandstones are quartz grains, feldspars, rock fragments, micas, and heavy minerals. Furthermore, diagenetic constituents such as infiltrated clay, mechanical and chemical compaction, partial or total grain replacement, and mineral authigenesis (clay and diagenetic cements) occur, filling the rock pore spaces.

In the framework, monocrystalline quartz grains predominate, which vary between 90 and 98%, exhibiting straight and undulose extinction (Figure 5C). Polycrystalline quartz grains are rounded and display internal contacts that range from long to concave-convex and its occurrence is rare (Figure 5D).

Feldspar grains may be divided into two types: plagioclase (average of 1.8 %) with albite twinning (Figure 5E) and potassium feldspar (average of 0.4%) with crosshatched twinning pattern (Figure 5F). Among rock fragments, the most common is quartzite fragment, which shows oriented and concave-convex internal contacts between grains (Figure 6A). In a lesser proportion, fragments of siltstones (Figure 8B), gneiss and chert are also common. Zircon, epidote, muscovite, hematite, rutile, amphibole, tourmaline (Figure 6C; D; E; F); titanite and biotite represent the accessory minerals.

Punctual and straight contacts predominate, with concave-convex contact occurring less frequently, resulting in a grain-supported framework, with weak packing and an average primary porosity of 11%. (With a minimum porosity of 0.35 % and maximum of 28 %).

According to Folk's classification scheme (1968), sandstones were classified as quartzarenites and subarkose sandstones (Figure 7). Table 01 exhibits the composition and petrographic characteristics of these sandstones. The occurrence of more than 98% of quartz and chert in some samples, as well as more than 12 % of feldspar and lithic fragments provides a supermature and submature mineralogical maturity to these rocks. In terms of stratigraphic positioning, subarkosian sandstones are generally found at the base of the layers, while quartzarenites are observed at the top (Figure 8).

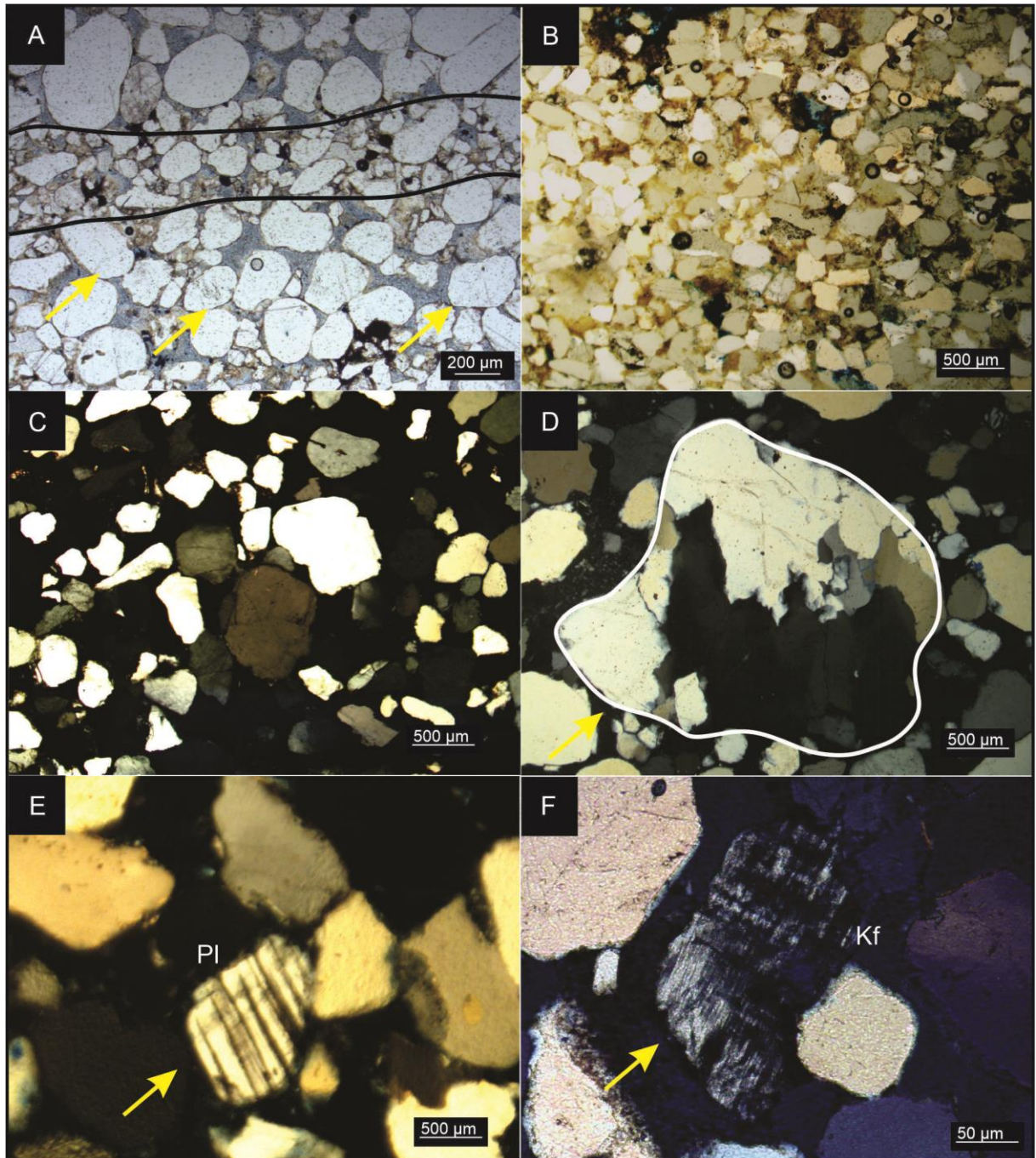


Figure 5 - A) Fine-grained sandstone exhibiting fining-upward stratifications/laminations. The quartz grain is rounded to subrounded and bimodal (P//). B) Fine-grained sandstone with subrounded and well-sorted grains, which show homogeneous framework without orientation (P//). C) Fine-grained sandstone with subrounded and poorly sorted quartz grains, exhibiting straight extinction, predominantly (PX). D) Polycrystalline quartz grain with internal sutured contacts between grains (PX). E) Plagioclase grain with poorly preserved albite twinning (PX). F) Poorly preserved Potassium feldspar with crosshatched twinning, exhibiting border limit slightly replaced by clay minerals (PX).

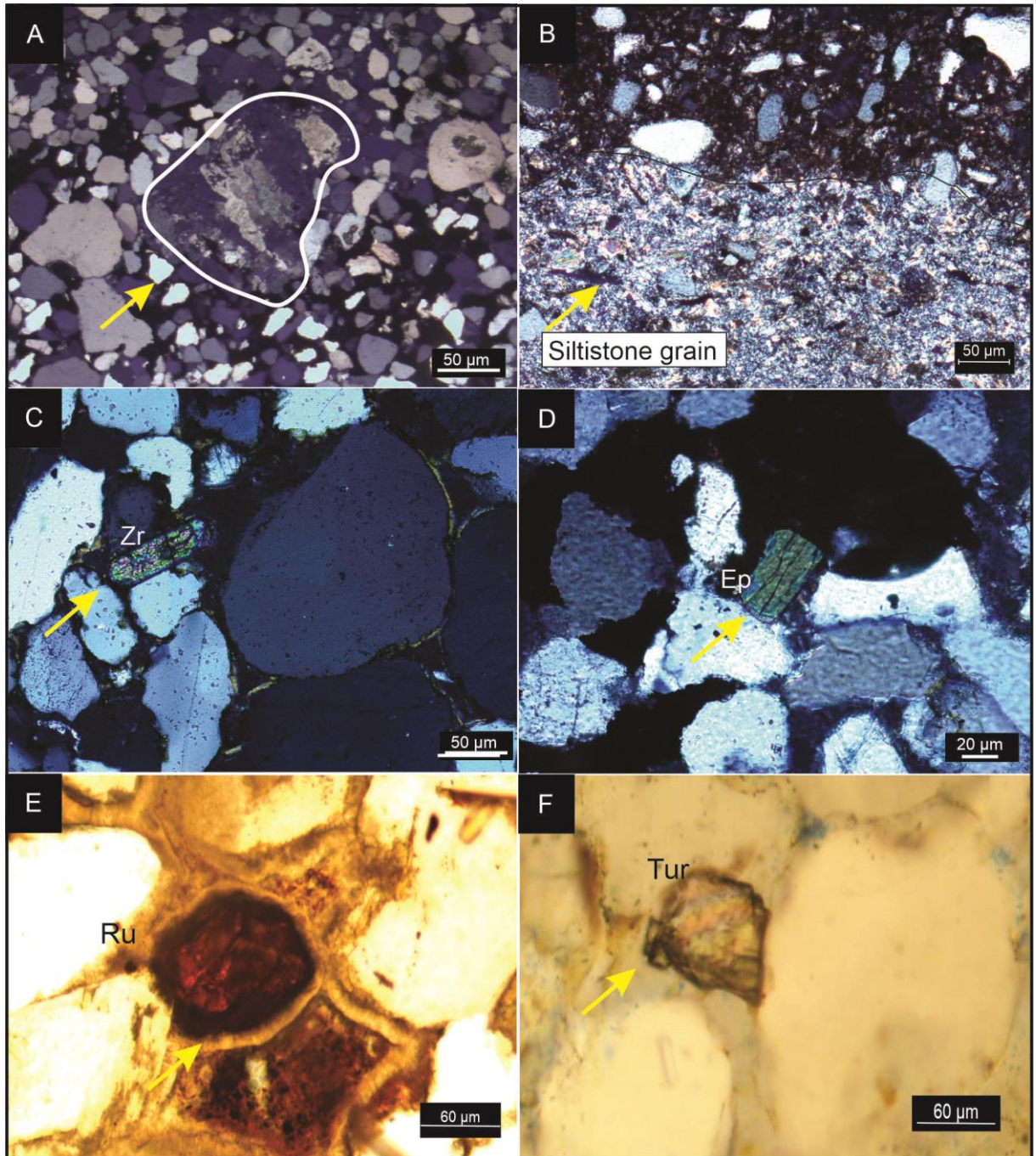


Figure 6 - A) Subrounded quartzite grain with sutered grains and preferential orientation (PX). B) Rounded siltstone lithic fragment. C) Prismatic zircon grain, exhibiting high interference colors. D) Prismatic epidote grain with high, intermediate interference colors, and a smaller relief compared to zircon grains (PX). E) Rutile grain showing darker borders and dark red interference colors. F) Tourmaline grain with medium relief and dark borders, being common the presence of inclusions (PX). Zr- Zircon; Ru- Rutile; Ep- Epidote; Tur- Tourmaline.

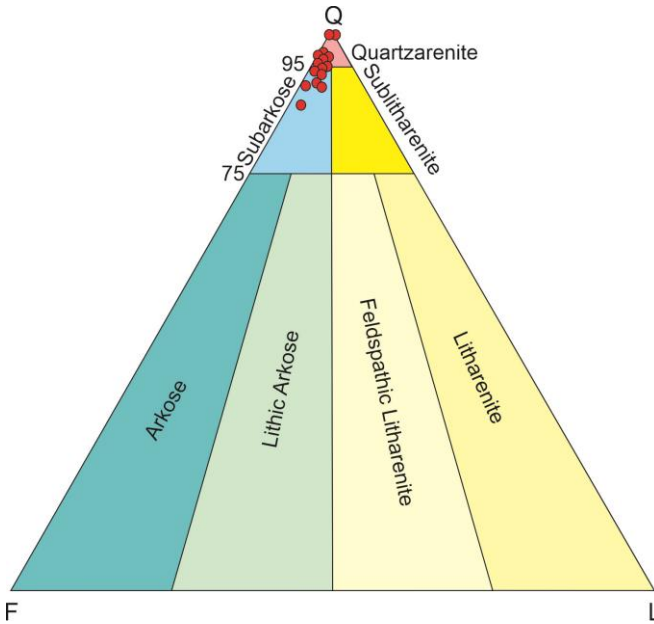


Figure 7 - Classification of the Poti Formation sandstones, according to Folk (1968).

Table 1 - Composition and petrographic features of the Poti Formation.

Symbol	Mineral component	Description
Qm	Monocrystalline quartz	Rounded to subrounded grains with straight extinction. It is the most abundant constituent in the sandstones of the Poti Formation
Qp	Polycrystalline quartz	Subrounded stable grains. This component is rare in the rock composition.
Pl	Plagioclase	Subrounded to rounded grains, exhibiting poorly preserved albite twinning
Kf	Feldspar	Subrounded grains with crosshatching twinning.
L	Lithic grains	Metamorphic quartzite subrounded grains with undulose extinction. In less proportion, the sedimentary mudstone grains are rounded to subrounded (L), chert and gneiss
Mc	Minor constituents	Muscovite, epidote (prismatic, rounded), angular amphiboles, zircon (prismatic, rounded and zoned), prismatic tourmaline (with inclusions), rutile (rounded grains), titanite, hematite and opaque minerals.
Ft	Total feldspar	The total feldspar grains are composed of plagioclase and potassium feldspar (Pl+KF)

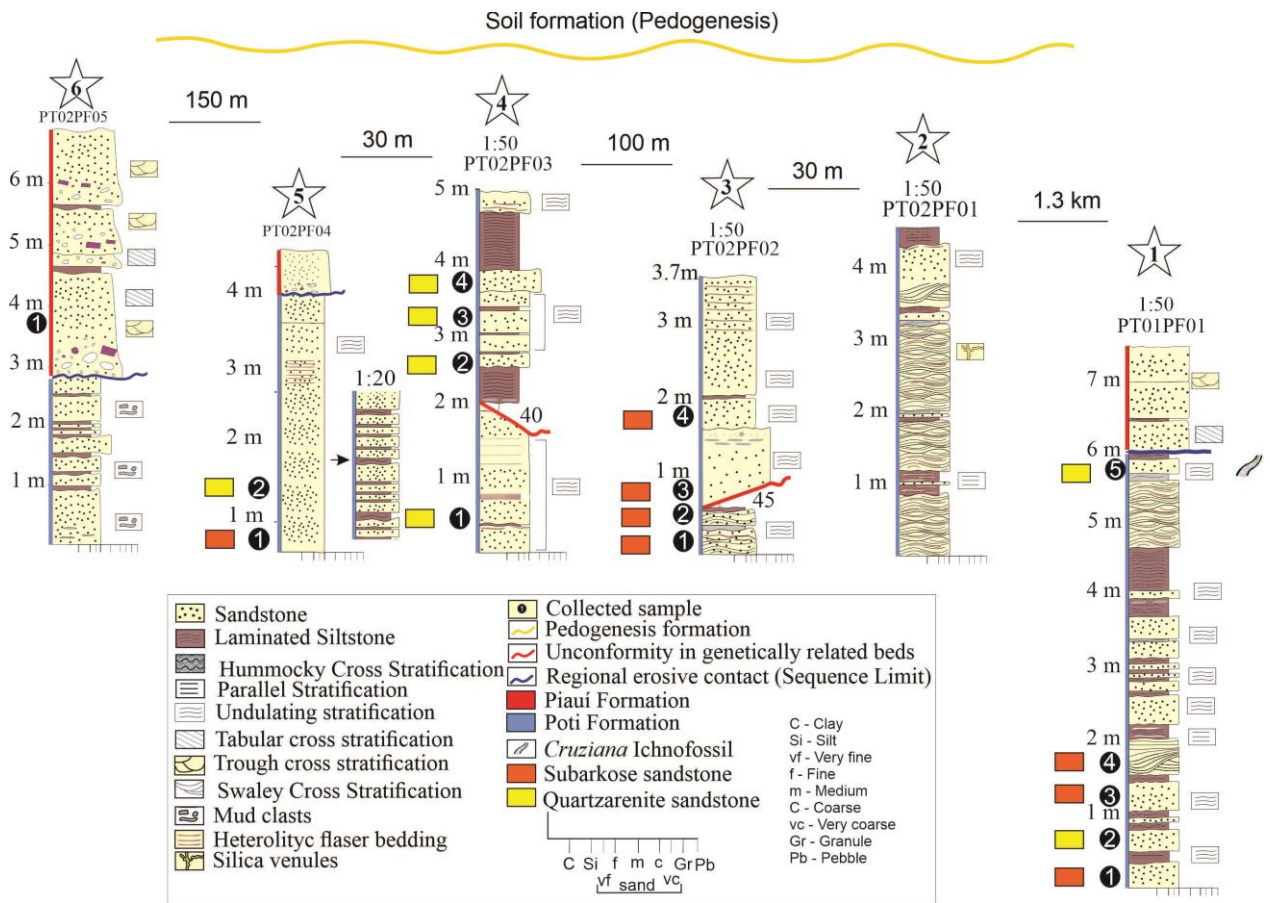


Figure 8 - Stratigraphic logs of the Poti Formation exhibiting sedimentary structures, main lithology and collected sample of each log. Horizontal scale is 1:50.

The clay matrix content percentage is greater than 5 % in thirteen analyzed samples and smaller than 5% in two samples. Mechanical infiltrated clay represents this matrix; however, there is diagenetic clay as a substitution product of silicates in the rock framework. Because of clay grain-size, the mineral phases could only be identified using X-ray diffraction, which revealed quartz, muscovite, kaolinite, and illite minerals. The detrital matrix occurs primarily in the basal portions of stratigraphic profiles and ranges from 1.0 to 13%. The majority of the sandstone samples are texturally immature, based on grain roundness degree and detrital matrix content.

The clay mineral phases identified in the six stratigraphic logs in the Poti Formation, register kaolinite as the most common clay, with peaks of 9.95, followed by illite, which is less common and presents peaks of 7.13. (Figure 9).

Silica and hematite are the cement content that predominates, appearing as syntaxial overgrowth and filling intergranular primary spaces, respectively. As indicated by the

cathodoluminescence images, the carbonatic cement appears as isolated and small concentrations.

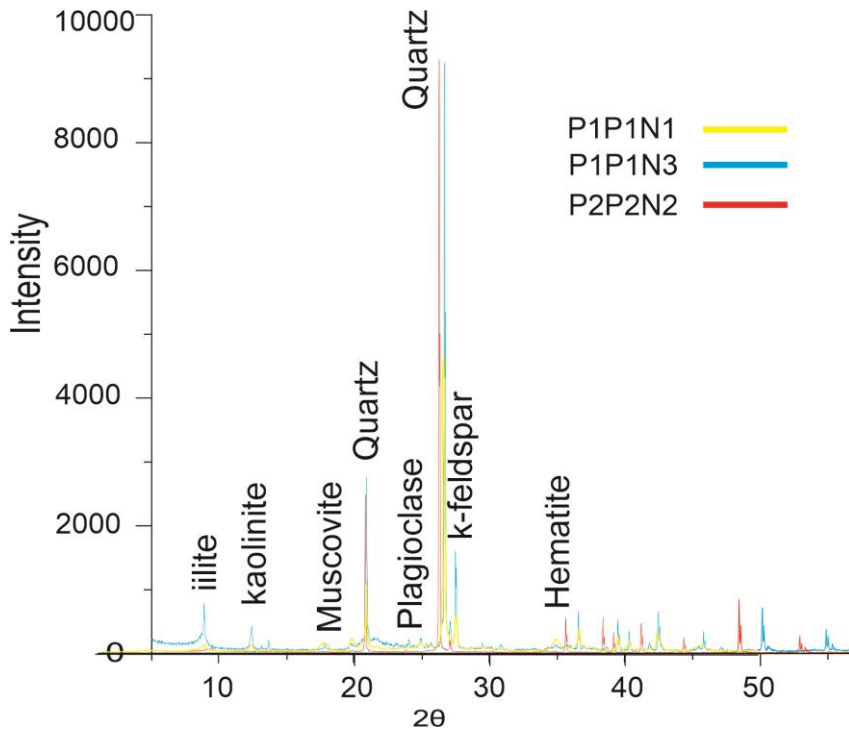


Figure 9 - Diffractograms of the Poti Formation. Emphasis in the illite and kaolinite peaks. Different colors identify the samples.

4.3 Diagenesis of the Poti Formation

Diagenesis refers to a group of physical, chemical, and biological processes that occur after sediment deposition, influenced by the fluids chemistry found in interstitial pores, as well as by increasing temperature and pressure, due to progressive burial depth (Worden & Morad, 2003; Li *et al.*, 2022; Worden *et al.*, 2018; 2009).

Different diagenetic processes operated on the Poti Formation sandstones, with varying intensities (some more active, others less active, and sometimes absent) that influenced the reservoir characteristics of this unit.

4.3.1 Constituents and diagenetic processes

Through thin section description, it was possible to identify the diagenetic processes, mineralogical composition, and the relationship between the mineralogical components, identifying, therefore, what modified the original composition of the studied rock. Mechanical infiltration of clay; mechanical compaction; chemical compaction; silica cement as secondary quartz overgrowth; kaolinite/illite cement, grain dissolution; grain alteration; grain replacement by clay minerals; and hematite, titanium oxide, and carbonate cement formation constitute the diagenetic processes and constituents identified.

4.3.2 Mechanical infiltration of clay

The mechanical infiltrated clay found in the studied sandstones are the most significant diagenetic process recognized. The clay occurs as discontinuous and fine coatings that covers the grain surface (Figure 10A), aggregates (Figure 10B), meniscus (Figure 10C), and pendulous aggregates (Figure 10D), reducing the primary porosity. According to XRD analysis, these clays are kaolinite and illite.

4.3.3 Mechanical and chemical compaction

Mica grains and other ductile particles are bent and deformed (Figure 10E), whereas quartz grains have little fracture evidence (Figure 10F). Mechanical compaction reduces primary porosity; however, this process acted with little intensity in the Poti Formation rocks, resulting in the preservation of porosity.

The dissolution of quartz grains forms concave-convex and sutured contacts as the pressure generated by the overlying layers increases, indicating chemical compaction (Figure 10G). The Poti Formation mechanical compaction process intensity is evidenced by loose packing, slightly deformed muscovites, predominance of punctual contacts followed by straight contacts (Figure 10H).

4.3.4 Hematite cement

Iron oxide and hydroxide cement is the most abundant, and occurs filling intergranular spaces, mainly as aggregates that partially or totally occupies the pores (Figure 11A). Hematite also occurs as a result of biotite and amphibole alteration, but in negligible amounts (Figure 11B).

This cement occurs at an average of 8% in the Poti Formation, with minimum and maximum values ranging from 1% to 23%, respectively. This proportion decreases from the lower to the upper beds in the stratigraphic logs, and hematite cementation happens after silica cementation, clay infiltration, dissolution, and grain replacement, as evidenced by petrography. The XRD analysis confirmed the presence of hematite oxide.

4.3.5 Silica cement

Silica cement is formed continuously and discontinuously between the quartz grains (Figure 11C), and as prismatic shapes at the grains edges, as well (Figure 11D). A dust line distinguishes this cementation, which occurs in late-eodiagenesis and early-mesodiagenesis. In the studied samples, quartz cement have small decrease from the lower to the upper beds in the stratigraphic logs, with an average of 9% (with a maximum of 15 % and a minimum of 2.5 %).

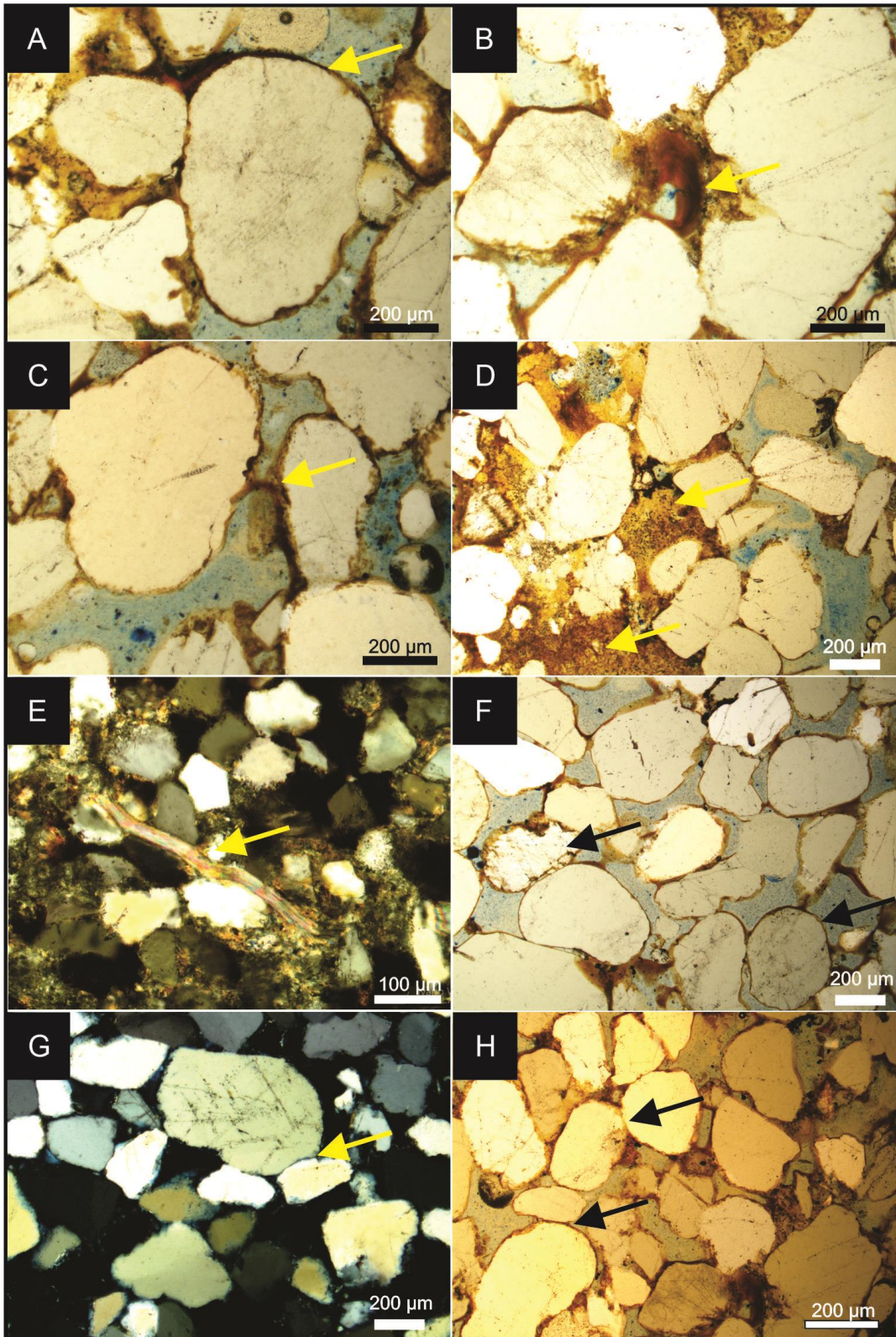


Figure 10 - A) Clay in the form of discontinuous cuticles (arrow) enveloping the quartz grain - (P//). B) Occurrence of pendular aggregates (arrow), which are typical in the vadose zone infiltration - (P//). C) Infiltrated clay with a meniscus habit (arrow), which is characteristic of vadose zones - (P//). D) Clay aggregate morphology occupying the primary porosity spaces (arrow) - (P//). E) Muscovite grain slightly bent and exhibiting altered edges (arrow) - (PX). F) Fractured quartz grain (arrow), indicating the mechanical compaction degree. Note the infiltrated clay within the open fractures (P//). G) Poti Formation sandstones exhibiting low proportions of concave-convex contacts between quartz grains (arrow) - (PX). H) Occurrence of punctual contacts (arrows) - (P//). PX-Crossed polarizers; P// - Parallel polarizers.

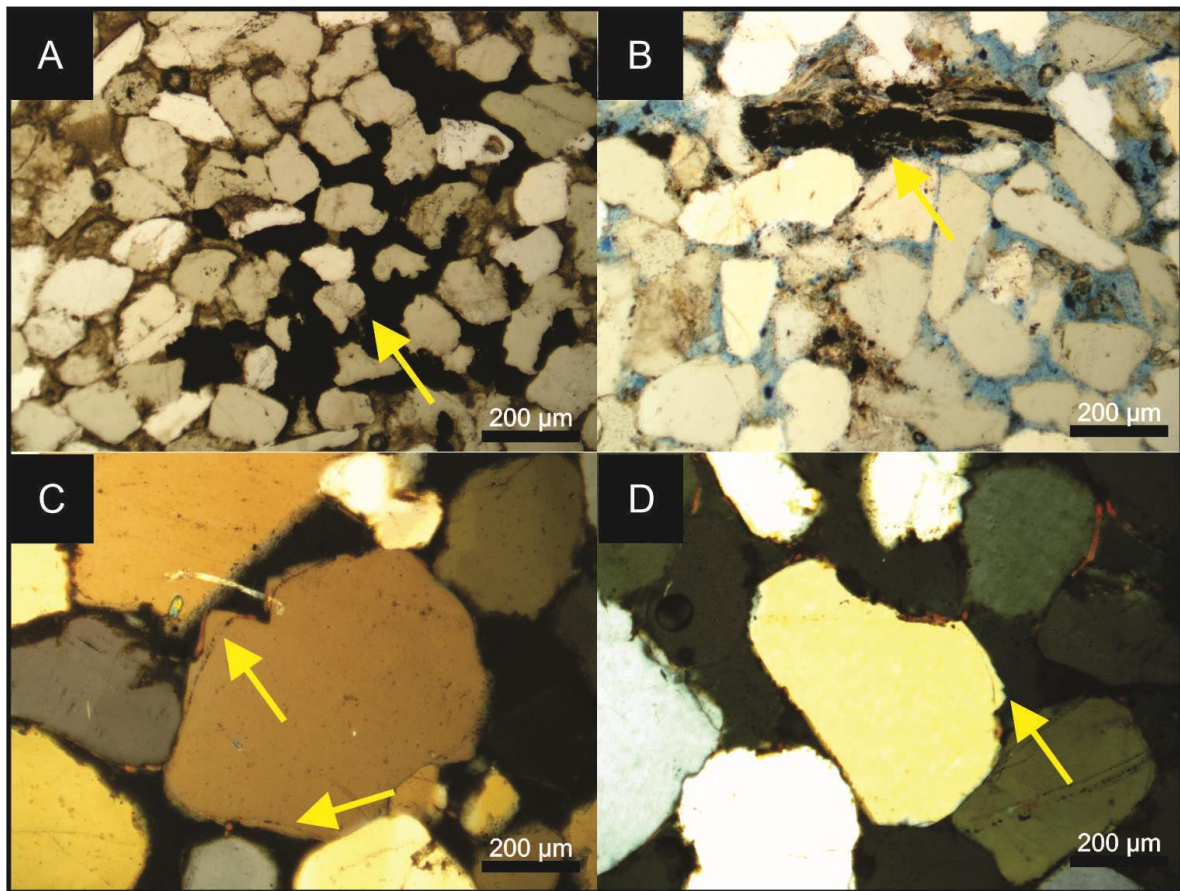


Figure 11 - A) Hematite cement as aggregates filling primary porosity (yellow arrow) - P//. B) Biotite grain being replaced by Fe oxides at the cleavage orientations (black arrow) - P//. C) Discontinuous quartz overgrowth on the grain surface (yellow arrow) - PX. D) Silica overgrowth on the surface of quartz grains with prismatic forms (arrow) - PX.

4.3.6 Carbonate cement

The petrographic analyses did not identify calcite and dolomite carbonate cement, which occurs as trace amounts. However, cathodoluminescence analysis indicated points with characteristic colors of carbonates (Figure 12A; B; calcite and dolomite).

4.3.7 Titanium oxide cement

Titanium oxide cement took place as an authigenic phase in the form of intergranular aggregates around accessory minerals such as titanite and rutile (Figure 12C; D). This type of cement is uncommon, and its concentration in the Poti Formation sandstones is minimal.

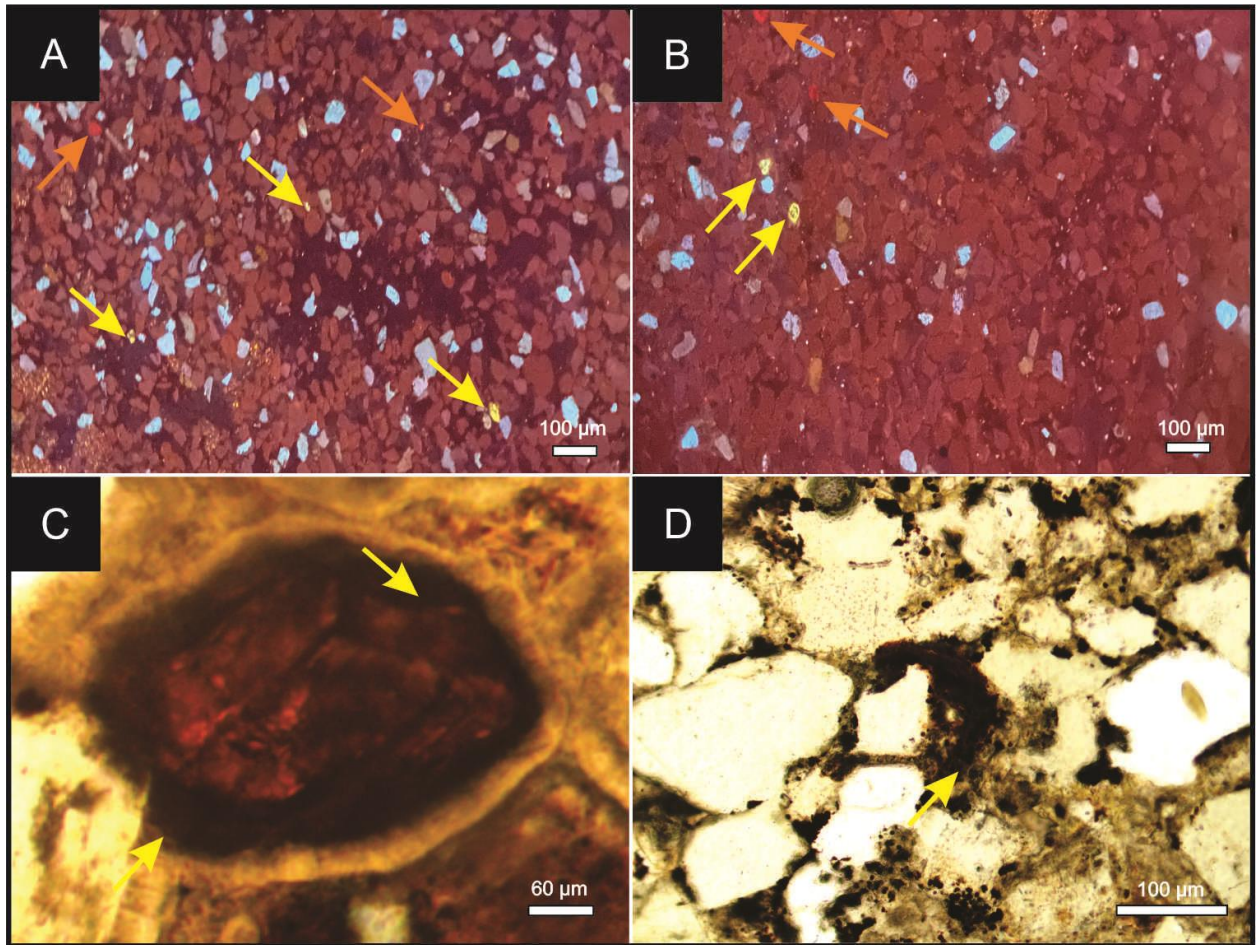


Figure 12 - Cathodoluminescence of the Poti Formation sandstones. A and B) The yellow and orange arrow indicate low presence of calcite and dolomite minerals in the rock framework, respectively. C and D) Rutile grains altering to titanium oxide along its borders limit (arrows).

4.3.8 Kaolinite and illite

Some samples contain kaolinite, which fills the primary pores and contributes to the reduction of porosity. It also occurs as lamellar shapes, replacing muscovite grains (Figure 13A), replacing potassium feldspar and plagioclase grains (Figure 13B). Kaolinite and illite happens as authigenic and detrital aggregates in the intergranular pore spaces and as continuous coatings around grains.

The authigenic illite occurs continuously as fringes and cuticles involving primary grains, and as a feldspar substitution mineral, reducing the porosity and permeability of the rocks. Illite is identified in the optical microscope by its fibrous appearance, being the clay mineral with the highest occurrence after kaolinite.

4.3.9 Alteration of unstable grains

The grain alteration process is present in accessory minerals such as muscovite, biotite, and titanite, but it also occurred in essential minerals such as feldspars in the studied sandstones.

A few samples, particularly those in the basal layers, contain biotite and altered titanite, which produced oxidizing cement (Figure 13C).

4.3.10 Dissolution

Partial dissolution of Poti Formation feldspar grains occurs preferentially in the cleavage planes or central region of the grains. Since microcline is more resistant to alteration than plagioclase, dissolution process produces secondary porosity more easily in the latter (Figure 13D). Dissolution also occurred in quartz grain borders and heavy mineral grains in the analyzed sandstones.

4.3.11 Substitution

It is common for kaolinite and illite clay minerals to replace muscovite and feldspars in these sandstones (Figure 13E;F). These processes take place during eodiagenesis and mesodiagenesis, resulting in the partial or total substitution of these constituents. Fan-shaped edges and open lamellae on muscovite grains distinguishes this phyllosilicates, when replaced by kaolinite/illite. There are iron oxides replacing biotite grains, but no chloritization process or chlorite cement was found in these rocks.

4.4 Porosity

The most common types of pores found in the analyzed samples by optical microscope are intergranular (Figure 14A), intragranular (Figure 14B), moldic (Figure 14C), and fractured grains (Figure 14D). With an average of 11%, intergranular porosity is the most frequent (with minimum and maximum values of 0.5 and 28 %, respectively) and occurs in all studied samples. However, the intergranular porosity is concentrated in upper beds on fine and coarse-grained sandstones.

The intragranular porosity occurs with an average of 0.25 % (with minimum and maximum values of 0.1 and 1.3 %, respectively) due to total or partial dissolution, of plagioclase and potassium feldspar grains. Moldic porosity is 0.7 % on average (with minimum and maximum values of 0.1 and 3.0 %, respectively.) The large pores occur in the stratigraphic logs closer to the Sardinha Formation basaltic intrusion, with an average of 0.7 % and a maximum value of 4.0 %. The pores produced by fracturing process are not significant. The total volume of secondary porosity evaluated under a petrographic microscope ranges from less than 1.0 % to 32 %, with an average of 13.5 %.

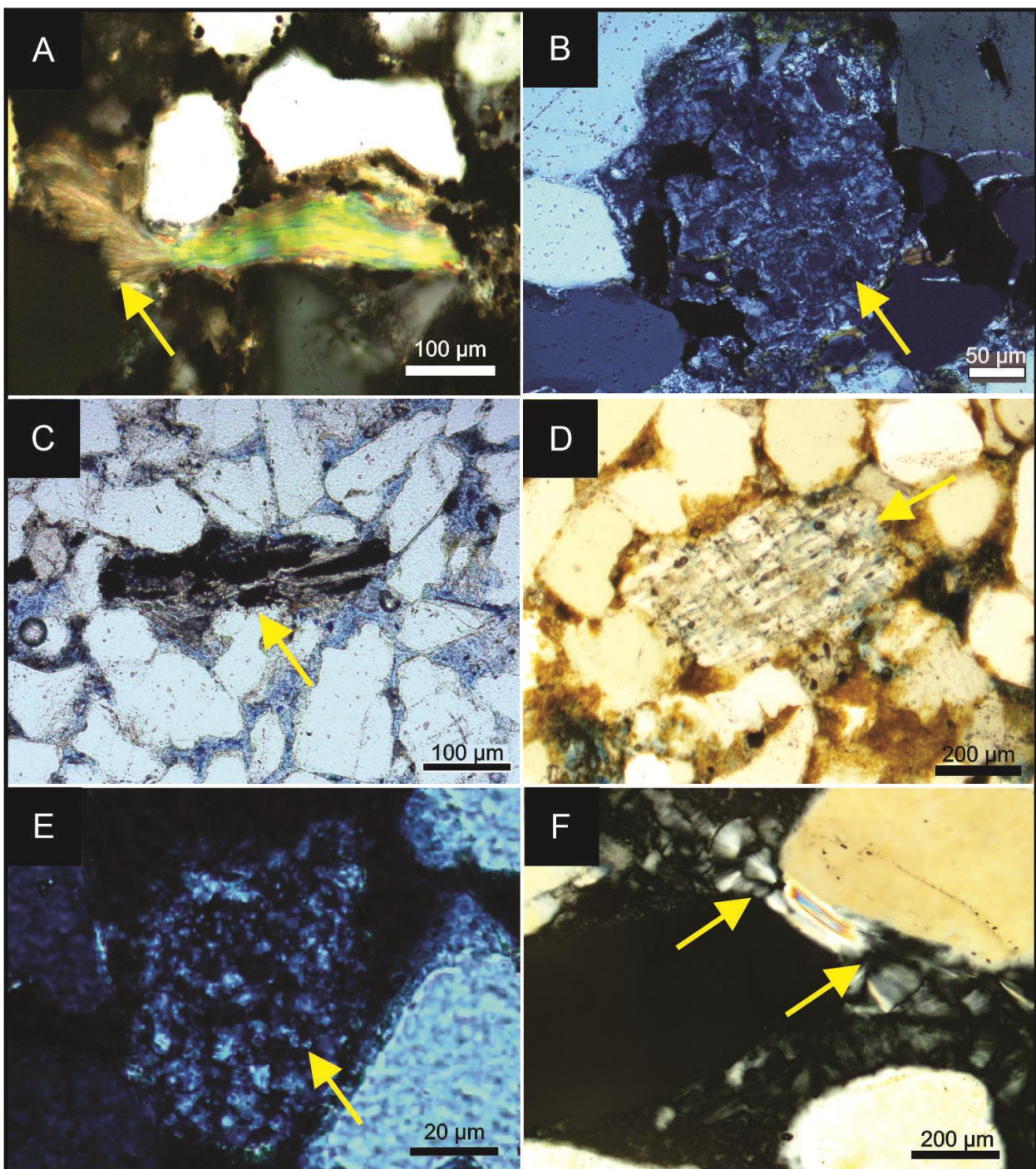


Figure 13 - A) Authigenic clay replacing muscovite grain on the expanded lamellae's edges (arrow) - PX. B) Total replacement of plagioclase grain to kaolinite (arrow) - PX. C) Alteration process on biotite grain, forming oxide Fe cement (arrow) - PX. D) Secondary porosity formation due to partial dissolution of potassium feldspar grain (arrow) - P//. E) Substitution process acting on plagioclase grains that forms kaolinite (arrow) - PX. F) Total substitution process on muscovite grain, resulting in booklet-shaped kaolinite cement (arrows) - PX.

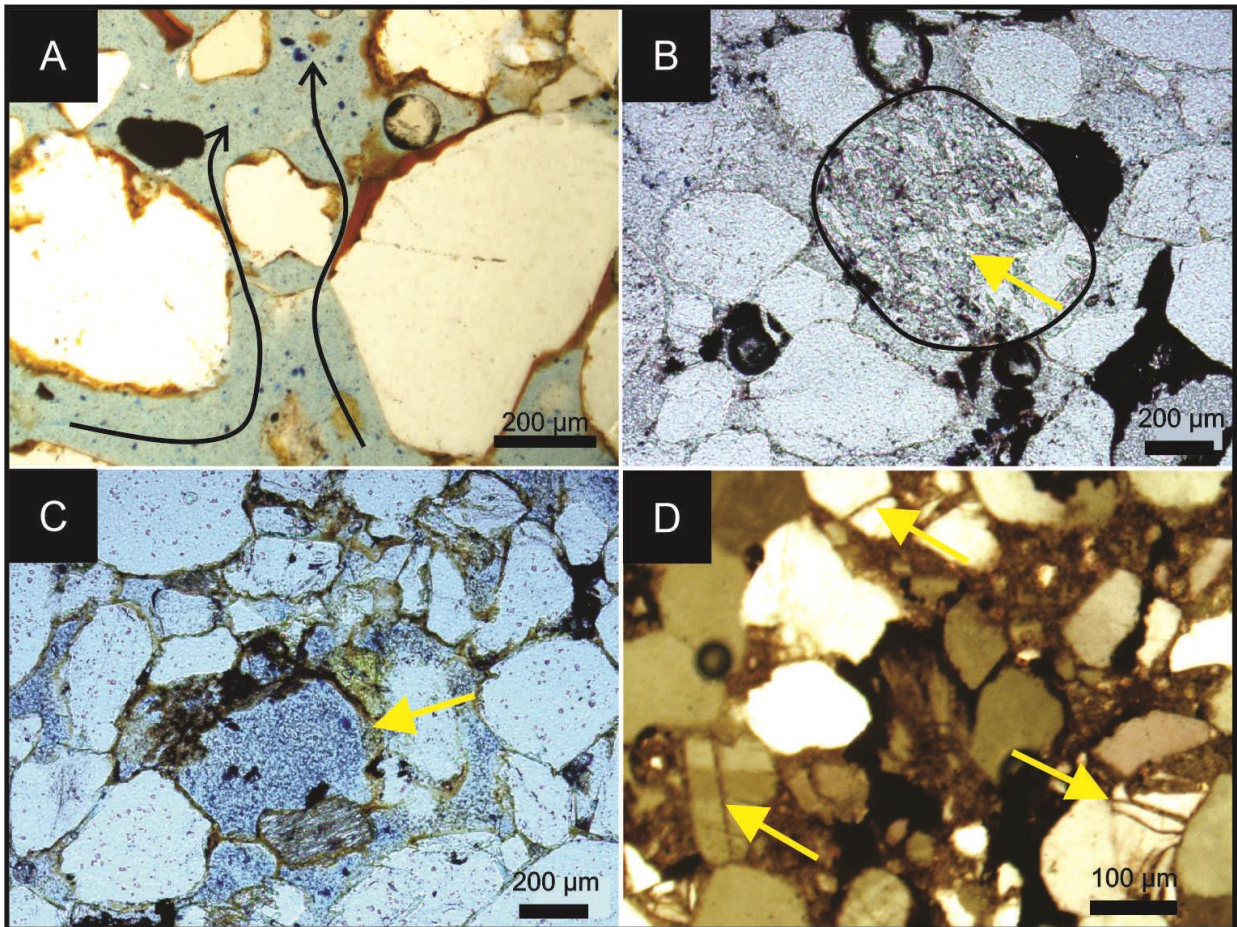


Figure 14 - A) The primary intergranular porosity. Detail of permeability based on petrographic analyses in fine-grained sandstones (black arrows; P//). B) Secondary porosity within feldspar grains (P//). C) Moldic porosity caused by increasing mechanical compaction that produces total grain substitution (yellow arrow; P//). D) Fracturing porosity induced by mechanical compaction and filled with infiltrated clay (yellow arrow; PX).

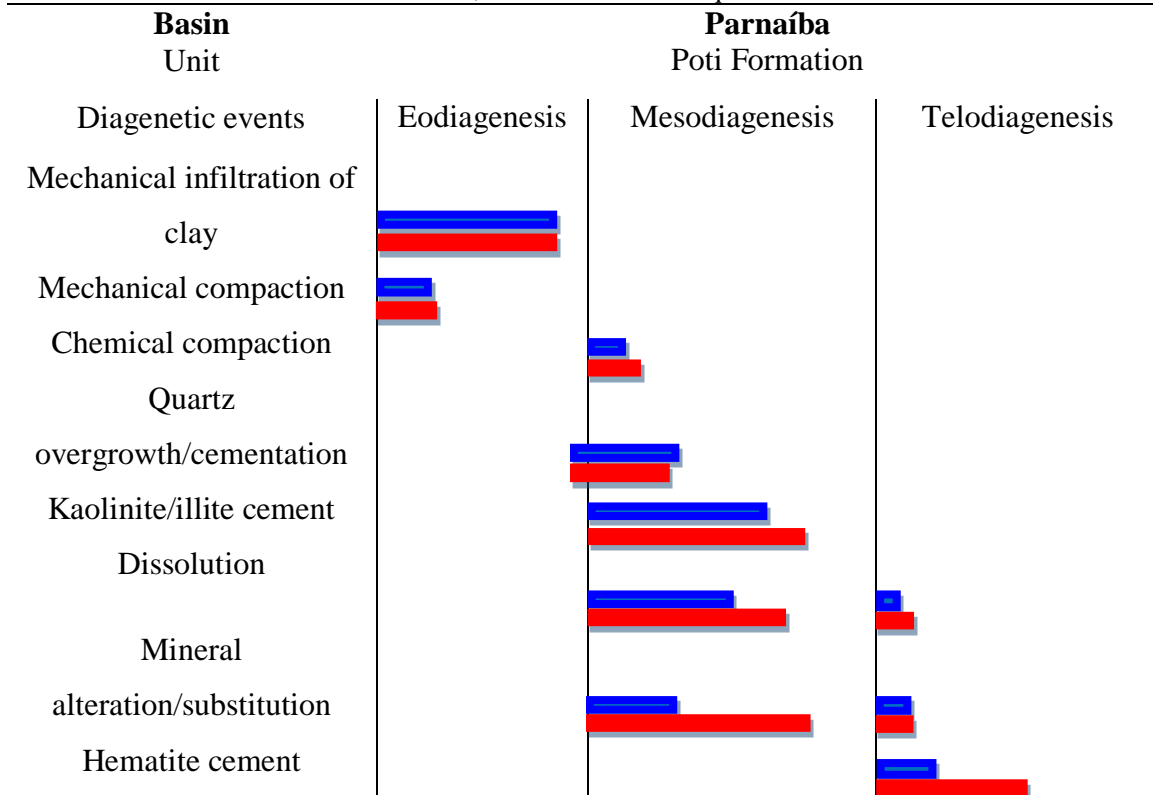
5 Discussion

5.1 Diagenetic events

Eight different diagenetic process have affected the Poti Formation sandstones and according to the temporal relations among these events, it was possible to provide a diagenetic sequence evolution that comprises eodiagenesis, mesodiagenesis, and telodiagenesis (Table 2).

The total amount of clay varies from 6.5 to 28 %, and its most noticeable effect is the reduction of primary porosity caused by mechanical infiltration, as well as the substitution of feldspar and muscovite grains to clay minerals. Clays with textures such as cuticles, meniscus, and pendulous usually occurs in the vadose zone, which is distinguished by greater proximity to the depositional surface and presence of eodiagenetic processes at temperatures less than 70 °C and depths smaller than 2.0 km (Xu *et al.*, 2021).

Table 2 - Diagenetic events that occurred in the Poti Formation. The red thick line represents subarkose sandstones, while the blue is the quartzarenites.



Kaolinite can be formed as a result of feldspar and muscovite alteration and substitution, and can be found mixed with infiltrated clay (Bhuiyan and Hossain, 2020; Khalifa and Morad, 2012). The penetration of meteoric waters produce kaolinite, by removing K⁺ ions of silicates at shallow burial depths that produces large amounts of this clay (Lanson *et al.*, 2002; Betard *et al.*, 2009).

Water accumulates and evaporates above the water table in the vadose zone, where clay infiltrates. The depth of penetration determines the amount of infiltrated clay, possibly introduced by episodic floods following a drought period, and if the water table decreases, these floods can infiltrate the permo-porous deposits (Caetano Chang and Wu, 2003).

The water meniscus accumulation forms the meniscus clay textures due to capillary pressure, which preserve these fluids, providing clay deposition mainly next to the contact between grains (Costa *et al.*, 2014; Bernard and Carrio-Schaffhauser, 2003). Clay bridge connections between grains, intergranular massive aggregates, and/or clay coatings oriented parallel to the grain surface distinguish these clays, which obliterate porosity.

Mechanical and chemical compaction occur as burial depth increases; the mechanical compaction occurs shortly after sediment deposition, whereas chemical compaction occurs at greater depths. Closed packing, rotation of elongated bioclasts (grains), fractured grains, and

pseudomatrix formation are all indicators of mechanical compaction (Bjørlykke, 2014; Dar *et al.*, 2022; Bjørlykke *et al.*, 2017). Fractured grains, when present, occurs filled with infiltrated and diagenetic clay, reducing the secondary porosity in these rocks (Liu *et al.*, 2022; Okunuadje *et al.*, 2020).

Chemical compaction evidences the end of eodiagenesis and the start of mesodiagenesis, while the mechanical compaction occurs in the early eodiagenesis (Gordon *et al.*, 2022; Lima and De Ross, 2002; Paz *et al.*, 2022). Through dissolution pressure, the chemical compaction produces dissolution and stiolite features along grains contacts; however, the presence of concave-convex contacts is poorly preserved in the studied succession. The cements of silica and clay infiltration can inhibit the advance of chemical compaction, because it provides more resistance to the rock framework (Bello *et al.*, 2022; Costa *et al.*, 2014)

Related to the level of burial depth, the intensity of mechanical and chemical compaction in quartzarenites and subarkose sandstones was similar. Some authors established that the silica overgrowth around grains reduces the intensity in which compaction acts on quartz and microcline grains (Quasim *et al.*, 2018; 2021 Khan *et al.*, 2018). However, the shallow burial depth, cementation, and clay infiltration must be the cause of low intensity of mechanical and chemical compaction in the Poti Formation. The muscovite and biotite grains are slightly deformed and the more resistant grains, such as quartz and quartzite fragments, do not exhibit fractures in the majority of these grains. Cathodoluminescence images also evidences the low impact of mechanical compaction, which do not produce fractured grains, especially on quartz grains.

The possible sources of silica cementation include pressure dissolution on grain contacts, meteoric solutions between pores, silica dust, the presence of silicates, biogenic silica, and groundwater (Alam *et al.*, 2022; Worden and Morad, 2003). Quartz cement is thought to have formed in the Poti Formation due to dissolution of potassium feldspars, phyllosilicates such as muscovites, and partial silicate alteration (Worden and Morad, 2003; Sajid *et al.*, 2020).

Primary porosity decreases due to the filling of silica cement, in the intergranular spaces, and syntaxial quartz overgrowths around the grains in a continuous and discontinuous pattern (Sayem *et al.*, 2022; Lawan *et al.*, 2021). However, the mechanical infiltration of clay inhibited the quartz overgrowth, especially in samples with a great amount of clay textures. When this growth is continuous and discontinuous, it suggests two stages of cementation: one before intense chemical compaction, in middle to late-eodiagenesis (probably near the end), and other after intense mechanical compaction, in mesodiagenesis at greater burial depths (Batista *et al.*, 2021; Wang *et al.*, 2020).

The carbonatic cement may have gone through dissolution processes due to the entry of hydrothermal fluids associated with the Sardinha Formation igneous intrusion, dissolving both feldspars and carbonates (Rong *et al.*, 2021). Dolomite and calcite are the only type of carbonate cement and its occurrence is not relevant to affect the reservoir sandstones of the Poti Formation. Calcite precipitation is influenced by water chemistry, specifically the Mg/Ca ratio, Eh, pH, temperature, and PCO₂ (Klein and Mizusaki, 2007). The dissolution of ferromagnesian and titanium silicates such as magnetite, ilmenite, biotite, amphibole, pyroxene, and rutile probably gave rise to titanium oxide (Nogueira *et al.*, 2021; De Ros, 1985).

The expansive clay texture and the common association to muscovites and feldspars distinguishes the lamellar kaolinite. The low birefringence in crossed nicols, in the gray order color, identifies the authigenic kaolinite, generally related to feldspars alteration. Kaolinite, as an authigenic alteration product, may have its origins connected to percolation of acidic fluids that corroded unstable silicate grains during the eodiagenetic stage, causing partial or total dissolution (Baoquan *et al.*, 2021; Marfil *et al.*, 2003). Feldspar dissolution/substitution processes accelerates as the temperature, depth, and CO₂ content of the formation waters arise (Duan *et al.*, 2018; Huang *et al.*, 2020).

Illite may be present as a result of kaolinite alteration, which dissolves at temperatures above 120°C, producing ions that contribute to authigenic illite formation, and as a product of sericite alteration, which is common in feldspars (Worden and Morad, 2003; Michelli, 2003; Huang *et al.*, 2020). The XRD and petrographic analysis show that potassium feldspar (microcline) predominates in the samples, implying that this reaction is probable to happen.

As clay mineral instability and burial depth increase, the alteration of muscovite and feldspar to kaolinite and illite takes place. These minerals alter to more stable phases, reaching the point of stability, and the concentration of certain chemical elements in the interstitial fluids influence the unstable grain alteration process to happen more efficiently (Costa *et al.*, 2014; Silva-Telles, 1991). This process varies on different portions of the sedimentary succession and occurs due to fluid percolation and burial depth increase in the early mesodiagenesis, especially on basal layers (Rong *et al.*, 2021; Morad *et al.*, 2010).

Dissolution contributes around 2% to porosity increasing and occurs at the end of eodiagenesis and during mesodiagenesis, mainly in feldspar grains. Hydrothermal fluids trigger the formation of large pores in the deepest parts of some stratigraphic logs.

Considering that the mechanical and chemical compaction were weak, the influence of basaltic dykes of the Sardinha Formation caused total dissolution of unstable minerals and

substitution of kaolinite or even smectite by illite due to acid hydrothermal fluids with temperatures above 120°C (Huang *et al.*, 2007; Ding *et al.*, 2011; Shu *et al.*, 2021).

When kaolinized, feldspar and muscovite grains alters to illite and this process occurs because of the burial depth increase (Costa *et al.*, 2014). Crystalline structure, Al/Si ratio, Ph, temperatures, organic acids, and chemical affinities in the environment influence feldspar dissolution or replacement (Wu *et al.*, 2022; Yuan *et al.*, 2019).

Because subarkose sandstones contain more feldspar in the rock framework, the process of alteration and replacement of these grains occurred more intensely, with kaolinite being the most common product. Kaolinite replaces feldspars grains and fills the primary porosity with different textures (Lawan *et al.*, 2021).

In the telodiagenesis phase, dissolution and alteration of ferromagnesian and silicate minerals during weathering and pedogenic processes, forms iron oxide cement (Carvalho *et al.*, 2018; Luo *et al.*, 2009). When this cement appears as thin coatings, surrounding the grains and filling pores, it may indicate two phases: 1) coatings covering quartz grains at the beginning of eodiagenesis; 2) precipitation of this cement filling the intergranular pores in telodiagenesis; however, the second hypothesis is the most likely to have happened in the Poti Formation sandstones. Iron oxide cement filling intergranular pores is typical of telodiagenesis, a stage in which meteoric waters can influence hematite precipitation (Tucker, 2001; Nogueira *et al.*, 2021; Batista *et al.*, 2021).

5.2 Porosity variations, Diagenetic constituents and Reservoir Quality

Among the diagenetic processes identified, some had a greater impact than others did in reducing and preserving the original porosity of the rock and in different facies associations

The samples with the highest porosity percentages have fine to coarse sand granulometry and are of primary and diagenetic origin. Diagenetic processes and constituents such as mechanical infiltrated clay, cementation of silica and iron oxide, and diagenetic alteration of feldspars and muscovites to clay kaolinite and illite, reduced the porosity by occupying the primary pore spaces.

Generated by the feldspar dissolution process, the intragranular secondary porosity is not expressive in the analyzed samples. The authigenic silica filling porosity, iron oxide, calcite, and iron oxide cementation in some samples reduced significantly the primary porosity of the rocks, particularly in stratigraphic logs distant from the Sardinha Formation igneous intrusion.

It is possible to establish a relationship between dissolution, silica cement, and hematite cement along the studied profiles, in relation to the igneous intrusion's proximity (Figure 15). Hematite cementation is higher in log 1 (samples 1–5), resulting in lower porosity; from sample

6 to 9, there is a significant increase in porosity, which varies, more or less, in samples 10 to 15 that are less than 100 meters apart from each other. The hydrothermalism possibly increased porosity in the mentioned range. The release of CO₂ changes the properties of the fluids, by making them more acidic, dissolving most of the silica and hematite cement, soluble grains, and authigenic clays (Boaquan *et al.*, 2021; Rong *et al.*, 2021).

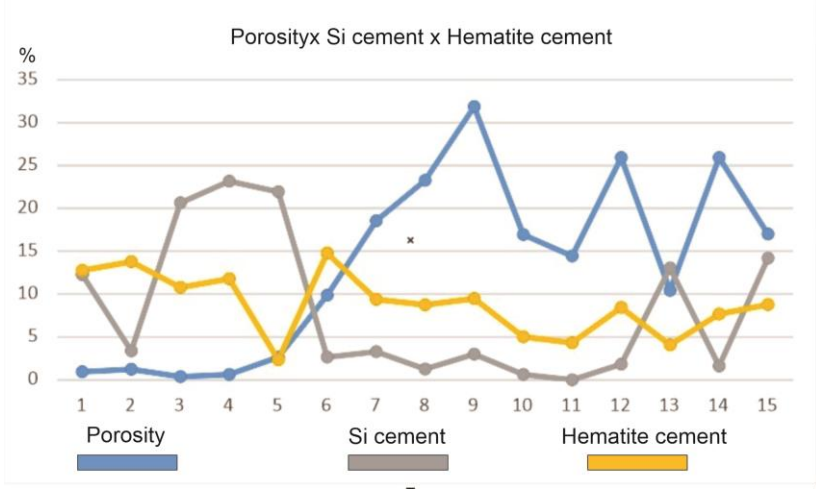


Figure 15 - Association between vertical and lateral porosity variation, silica cementation and hematite cementation, in the Poti Formation stratigraphic logs. Log 1 (samples 1 - 5); log 2 (samples 6 - 9); log 3 (samples 10 - 13), log 4 (samples 14 - 15).

Mechanical compaction had little impact on porosity reduction, as evidenced by the low fracturing of resistant grains such as quartz and feldspar, the low deformation of muscovites, the weak packing of most sandstones, and the silica cementation in the early to late-eclogogenesis, which provided greater rock resistance. Therefore, there was little porosity reduction at low burial depths (< 2.0 km; Worden, 2018; Morad *et al.*, 2010).

The impact of cementation and compaction processes on primary porosity reduction reveals that clay cementation seems to have more control over pore reduction than compaction. In addition, because the secondary quartz overgrowths in the studied sandstones are not well developed, they do not destroy but rather preserve the pore throats. This indicates that this process had no negative impact on the quality of the sandstone reservoir. The cementation of iron oxides that fills the pores, on the other hand, may have caused pore throat obstruction, which is negative to reservoir quality.

Therefore, the precipitation of iron oxides, mechanical infiltration of clays, and the formation of diagenetic minerals such as kaolinite all contributed to the reduction of the Poti Formation primary porosity. The influence of hydrothermal fluids associated with intrusions, in contrast, possibly increased secondary porosity due to total dissolution processes, resulting

in large pores. Furthermore, the high prevalence of fractures and normal movement faults probably formed or contributed to the development of these features (Figure 16).

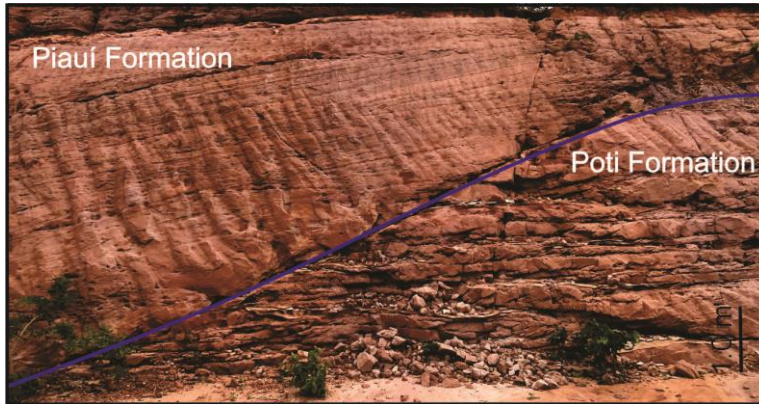


Figure 16 - Contact between the Poti and Piauí formations, emphasizing the general characteristics of faults and fractures, already studied by previous hydrocarbon generation models in the Parnaíba Basin.

Although the distribution of sedimentary facies controls conventional reservoirs, diagenetic events can modify their original characteristics, preserving or destroying sandstone porosity and permeability (Schrank *et al.*, 2017; Okunuwadje *et al.*, 2020). Consequently, diagenetic events recorded in Poti Formation sandstones could have increased or decreased the porosity. Furthermore, the intrusion of igneous bodies can alter the petrophysical properties of these rocks (Higgs *et al.*, 2021).

Silicate grain dissolution and alteration processes result in moldic and intergranular pores, as well as large pores (Figure 17A; Haile *et al.*, 2019; Shi *et al.*, 2021). The pores formed by grain fracturing are closed, but when opened, clay fills this pore spaces, indicating that clay infiltration also occurred at the beginning of mesodiagenesis. This clay content must be the result of feldspar alteration, dissolution pressure, in the chemical compaction, and meteoric acid waters infiltration through faults and fractures (Jesus 2004; Michelli, 2003).

Porosity values generated by dissolution are typically less than 2.0 %; therefore, the contribution of diagenetic processes and igneous intrusion is of paramount importance as an indicator of reservoirs with excellent petrophysical properties. The effects of intrusions in geological models for the Parnaíba Basin are widely accepted and the surface data in this study reinforces this model (Miranda *et al.*, 2018; Góes and Feijó, 1994). Hematite and silica cementation, as well as clay content, are higher in the transitional environments between lower shoreface and offshore (Figure 17B; C). The upper shoreface facies associations, on the other hand, demonstrated the best reservoir qualities. Therefore, the effects of diagenesis and the Sardinha Formation basaltic intrusion were extremely crucial in increasing porosity and permeability (Figure 17D).

Through total quantification carried out by the petrographic study, the lateral and vertical variation of porosity and its relationship with the intrusion of the Sardinha Formation is noticeable in the stratigraphic logs (Figure 18).

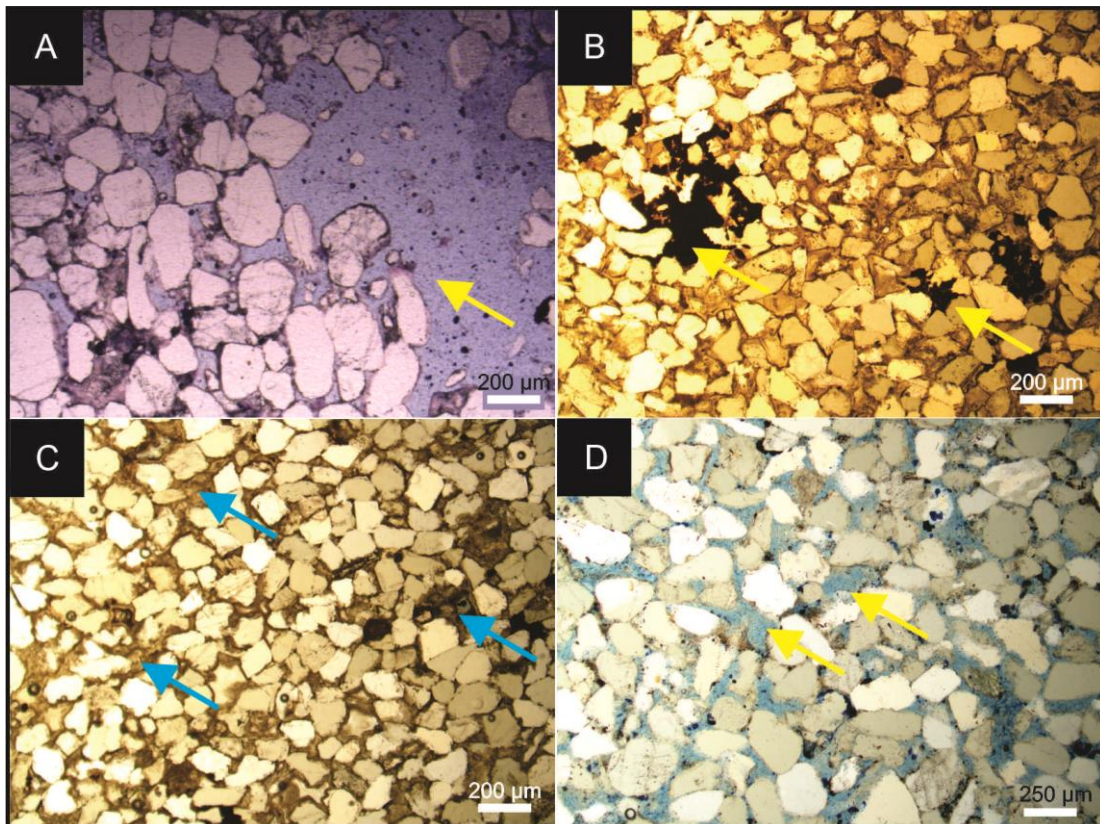


Figure 17 - A) Lower cement and clay values characterize the large pores in the sandstones next to the intrusion of the Sardinha Formation. B and C) Lower shoreface/Offshore sandstones, characterized by a greater amount of infiltrated clay (arrows), silica, and hematite cementation (blue arrows). D) Upper shoreface sandstones exhibiting good porosity and permeability (arrows).

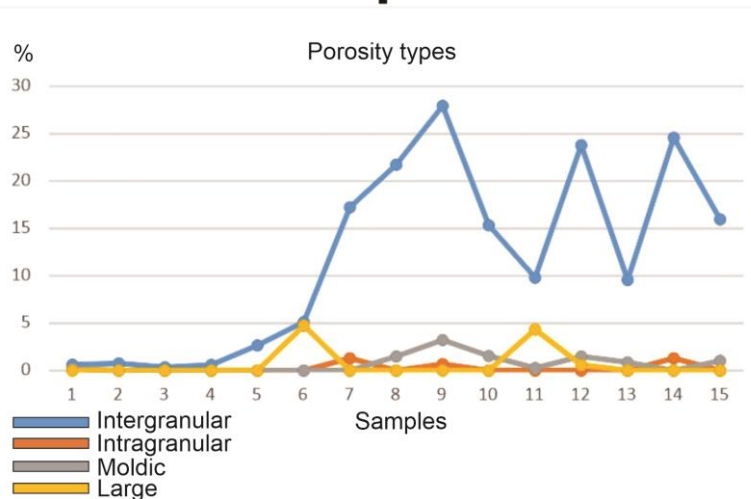


Figure 18 - Porosity types and modal quantities identified by petrographic analyses. From sample 6 to 9, the increase on porosity is noticeable, due to the predominance of upper shoreface facies association. The rise in porosity occurs particularly towards the top of the stratigraphic logs, and next to the influence of the Sardinha Formation, where the process of secondary porosity generation is more prominent, reaching a maximum value of 4.0 %.

6 Conclusions

Mechanical infiltration of clay, mechanical and chemical compaction represents the processes that occurred in the eodiagenesis; the mesodiagenesis processes comprises silica cementation, authigenic kaolinite/illite formation, dissolution, and substitution. The hematite cements occurs in telodiagenesis.

The sedimentary succession analyzed in the study area is composed of two facies associations embracing storm wave-dominated platform environment, represented by lower shoreface/offshore (AF-1) and upper shoreface (AF-2) subenvironments, which contain sand bodies that form reservoirs of different thicknesses and lateral continuity. These rocks are classified as quartzarenites and subarkose sandstones with high compositional maturity, low textural maturity, and weak packing level. The sediment source area, climate, depositional systems, and diagenetic processes influenced the detrital and authigenic components origin.

From the petrographic analysis, it was possible to identify the diagenetic controls in the reservoir sandstones quality of the studied unit. The upper shoreface sandstones represents the best reservoirs, and the sandstones of the lower shoreface/offshore association were the most affected by diagenetic processes and constituents such as hematite cementation, mineral alteration and mechanical infiltration and kaolinite/illite cement.

Because clay infiltration, silica and hematite cementation is more noticeable in the lower shoreface/offshore facies associations, the porosity is smaller. In the upper shoreface facies associations, these diagenetic events are less intense in proportion, and porosity is better preserved. However, diagenetic events and hydrothermal fluids may have altered these properties and reservoir quality.

According to the diagenetic analysis, the mechanically infiltrated clay and hematite cement had the biggest negative impact on the primary porosity of the studied sandstones. Petrography, on the other hand, revealed that the detrital composition also influenced the change in primary porosity, because the dissolution process modified some unstable primary constituents, as feldspars, producing cement, while others generated clay minerals as a product of alteration, and secondary porosity.

The intergranular pores, with a higher occurrence, and large pores represents the most important porosity types. Secondary porosity, on the contrary, is low and grain dissolution is the main diagenetic process, responsible for its formation.

According to the data integration, diagenetic processes, particularly the fine-grained sandstones of the lower layers of the lower shoreface/offshore facies associations, significantly influenced the Poti Formation sandstones petrophysical properties. The fine to coarse-grained

sandstones of the upper shoreface facies associations and the upper beds of the sedimentary succession, on the other hand, exhibits the best hydrocarbon reservoir quality.

The different depositional environments and diagenesis modified or maintained the porosity, permeability, and textural properties of the Poti Formation rocks. More research on different points of the Parnaíba Basin is required and recommended to better constrain the diagenetic evolution of other depositional environments and the influence of igneous intrusions. The analyses of drill core data is also highly suggest.

Acknowledgments

The first author is grateful to the Human Resources Program in analogous petroleum system and simulation of reservoirs in sedimentary basins (PRH47-Finep) of the Brazilian National Agency for Petroleum Natural Gas and Biofuel. The Brazilian National Agency for Petroleum Natural Gas and Biofuels (ANP) for the postgraduation scholarship [grant number 00467281203]. All authors are also grateful to the Geosciences Postgraduation Program (PPGEOC) of the Federal University of Pernambuco and Federal University of Alagoas (UFAL-CETEC) for the support. We also thank to CNPQ (National Council for Scientific and Technological Development) for all the financial support and postgraduation scholarship (grant number 143630/2019-9). We would like to thank Valdielly Larisse Silva for the English review and Virgínia Neuman and LAGESE (Laboratory of Sedimentary Geology) for the laboratory support, located at Petroleum and Energy Research Institute (LITPEG), as well as CETENE (Northeast Technology Center), for x-Ray diffractometry analysis.

References

- Abelha, M., Petersohn, E., Bastos, G., Araújo, D., 2018. New insights into the Parnaíba Basin: Results of investments by the Brazilian National Petroleum Agency, in: Geological Society Special Publication. Geological Society of London, pp. 361–366. <https://doi.org/10.1144/SP472.13>.
- Alam, K., Abdullatif, O., El-Husseiny, A., Babalola, L., 2022. Depositional and diagenetic controls on reservoir heterogeneity and quality of the Bhuban formation, Neogene Surma Group, Srikail Gas Field, Bengal Basin, Bangladesh. Journal of Asian Earth Sciences 223. <https://doi.org/10.1016/j.jseaes.2021.104985>.
- Araújo, V.B.V. 2018. Sedimentação, estratigrafia e diagênese dos reservatórios da Formação Poti, Viseano, Bacia do Parnaíba. Universidade de Brasília. pp. 152
- Almeida, F.F.M., Carneiro, C.D.R., 2004. Inundações marinhas fanerozóicas no Brasil e recursos minerais associados. In: Mantesso-Neto, V., Bartorelli, A., Carneiro, C.D.R., Brito-Neves, B.B., Geologia do Continente Sul Americano: Evolução da obra de Fernando Flávio Marques de Almeida. Beca, pp 43-58.
- Augustsson, C., Bahlburg, H., 2003. Cathodoluminescence spectra of detrital quartz as provenance indicators for Paleozoic metasediments in southern Andean Patagonia. J. South Am. Earth Sci. 16, 15–26. [https://doi.org/10.1016/S0895-9811\(03\)00016-6](https://doi.org/10.1016/S0895-9811(03)00016-6)
- Augustsson, C., Reker, A., 2012. Cathodoluminescence spectra of quartz as provenance indicators revisited. Journal of Sedimentary Research. 82 (8), 559-570. <http://dx.doi.org/10.2110/jsr.2012.51>.
- Almeida, EEM. de., Brito Neves, B.B. de. and Carneiro, C.D.R. (2000) The origin and evolution of the South American Platform. Earth Science. Reviews v. 50, 77-111. [https://doi.org/10.1016/S0012-8252\(99\)00072-0](https://doi.org/10.1016/S0012-8252(99)00072-0).
- Ärlebrand, A., Augustsson, C., Escalona, A., Grundvåg, S.A., Marín, D., 2021. Provenance, depositional setting and diagenesis as keys to reservoir quality of the Lower Cretaceous in the SW Barents Sea. Marine and Petroleum Geology 132. <https://doi.org/10.1016/j.marpetgeo.2021.105217>.
- Batista, V.Z., Ferreira de Lima Filho, M., Rodrigues de Andrade Freitas, W., Marques Vieira, M., Oliveira Agostinho da Silva, S.M., Silva, V.L., 2021. Influência dos processos diagenéticos na porosidade dos arenitos da formação iborepi, Bacia de Lavras da Mangabeira, Estado do Ceará. Revista de Geociências do Nordeste 282–294. <https://doi.org/10.21680/2447-3359.2021v7n2id22226>.

Baoquan, M., Shumin, C., Weilin, Y., Chengyan, L., Hong, Z., Zhifeng, S., Jiandong, Z., Ya, W., Shangxin, W., Jingyan, W., 2021. Pore structure evaluation of low permeability clastic reservoirs based on sedimentation diagenesis: A case study of the Chang 8 reservoirs in the Zhenbei region, Ordos Basin. *Journal of Petroleum Science and Engineering* 196. <https://doi.org/10.1016/j.petrol.2020.107841>.

Bello, A.M., Usman, M.B., Abubakar, U., Al-Ramadan, K., Babalola, L.O., Amao, A.O., Sarki Yandoka, B.M., Kachalla, A., Kwami, I.A., Ismail, M.A., Umar, U.S., Kimayim, A., 2022. Role of diagenetic alterations on porosity evolution in the cretaceous (Albian-Aptian) Bima Sandstone, a case study from the Northern Benue Trough, NE Nigeria. *Mar Pet Geol* 145. <https://doi.org/10.1016/j.marpetgeo.2022.105851>.

Bernard, X. D; Carrio-Schaffhauser E. 2003. Kaolinic meniscus bridges as an indicator of early diagenesis in Nabian sandstones, Sinai, Egypt. *Sedimentology*, 50,1221-1229.

Bernet, M., Bassett, K., 2005. Provenance analysis by single quartz grain SEM-CL/optical microscopy. *J. Sediment. Res.* 3, 496-504. <https://doi.org/10.2110/jsr.2005.038>.

Betard, F., Caner, L. Gunnell, Y., Bourgeon, G. 2009. Illite neoformation in plagioclase during weathering: Evidence from semi-arid, Northeast Brazil. *Geoderma* 152, 53-62. <https://doi.org/10.1016/j.geoderma.2009.05.016>.

Bhuiyan, A.H., Hossain, S. 2020. Petrographic characterization and diagenetic evaluation of reservoir sandstones from Smorbukk and Heidrum fields, offshore Norway. *Journal of Natural Gas Geosciences* 5, pp. 11-20. <https://doi.org/10.1016/j.jnggs.2019.12.001>.

Bjørlykke, K., 2014. Relationships between depositional environments, burial history and rock properties. Some principal aspects of diagenetic process in sedimentary basins. *Sediment. Geol.* 301, 1–14. <https://doi.org/10.1016/j.sedgeo.2013.12.002>.

Bjørlykke, K., Line, L.H., Jahren, J., Mondol, N.H., Aagaard, P., Hellevang, H. 2017. Compaction of sand and clay: constraints from experimental compaction, chemical reactions and fluid flow during burial-an overview (ext.abs). In: AAPG Annual Convention & Exhibition, Houston, Texas, Search and Discovery article. pp.17.

Boggs, S., Krinsley, D., 2006. Application of Cathodoluminescence Imaging to the Study of Sedimentary Rocks. Cambridge University Press. <https://doi.org/10.1017/CBO9780511535475>.

Brito-Neves, B.B., Fuck, R.A., Cordani, U.G., Thomaz Filho, A., 1984. Influence of basement structures on the evolution of the major sedimentary basins of Brazil: A case of tectonic heritage. *J. of Geodynamics* 1, 495-510. [https://doi.org/10.1016/0264-3707\(84\)90021-8](https://doi.org/10.1016/0264-3707(84)90021-8)

Brito Neves B.B., Fuck R.A. 2013. Neoproterozoic evolution of the South-American platform. *Journal of South American Earth Sciences*, 47, 72-89. <https://doi.org/10.1016/j.jsames.2013.04.005>.

Brito Neves, B.B., Fuck, R.A., Pimentel, M.M., 2014. The Brasiliano collage in South America: A review. *Brazilian Journal of Geology*. <https://doi.org/10.5327/Z2317-4889201400030010>

Caetano-Chang, M., Tai W.f. 2003. Diagênese de Arenitos da Formação Pirambóia no centro-leste paulista. *Revista de Geociências, UNESP* 22, pp. 33-39.

Caputo, M.V. 1984. Stratigraphy, tectonics, paleoclimatology and paleogeography of northern basins of Brazil (Doctorate thesis). University of California, Santa Barbara, USA.

Carvalho, R.R. de, Neumann, V.H., Fambrini, G.L., Assine, M.L., Vieira, M.M., Rocha, D.E.G.A. da, Ramos, G.M.S., 2018. The basal siliciclastic Silurian-Devonian Tacaratu formation of the Jatobá basin: Analysis of facies, provenance and palaeocurrents. *Journal of South American Earth Sciences* 88, 94–106. <https://doi.org/10.1016/j.jsames.2018.07.004>.

Coelho, D.L.O., Julià, J., Rodríguez-Tribaldos, V., White, N., 2018. Deep crustal architecture of the Parnaíba basin of NE Brazil from receiver function analysis: Implications for basin subsidence, in: *Geological Society Special Publication*. Geological Society of London, pp. 83–99. <https://doi.org/10.1144/SP472.8>.

Cordani, U.G., Neves, B.B.B., Fuck, R.A., Porto, R.; Thomaz Filho, A., Cunha, F.M.B. 1984. Estudo preliminar de integração do Pré-Cambriano com os eventos tectônicos das bacias sedimentares brasileiras. *Série Ciência-Técnica-Petróleo* 15, pp.70.

Cordani U.G., Neves B.B.B., Thomaz Filho A. 2009. Estudo preliminar de integração do Pré-Cambriano com os eventos tectônicos das bacias sedimentares brasileiras. *Boletim de Geociências da Petrobrás*, 17(1), 205-219.

Costa, A.B.S., Córdoba, V.C., Sá, E.F.J., Scherer, C.M.S. 2014. Diagênese dos arenitos da tecnosseuência rift da Bacia do Araripe, NE do Brasil. *Brazilian Journal of Geology* v44 (n3). pp 457-470. DOI: 10.5327-4889201400030008.

Daly, M.C., Fuck, R.A., Julià, J., Macdonald, D.I.M., Watts, A.B., 2018. Cratonic basin formation: A case study of the Parnaíba Basin of Brazil, in: *Geological Society Special Publication*. Geological Society of London, pp. 1–15. <https://doi.org/10.1144/SP472.20>.

Dar, Q.U.Z., Pu, R., Baiyegunhi, C., Shabeer, G., Ali, R.I., Ashraf, U., Sajid, Z., Mehmood, M., 2022. The impact of diagenesis on the reservoir quality of the early Cretaceous

Lower Goru sandstones in the Lower Indus Basin, Pakistan. Journal of Petroleum Exploration and Production Technology 12, 1437–1452. <https://doi.org/10.1007/s13202-021-01415-8>

De Ros, L. F. 1985. Petrologia e características dos reservatórios da Formação Sergi (Jurássico) no Campo de Sesmaria, Bacia do recôncavo, Brasil (Master dissertation). Universidade Federal de Ouro Preto, Ouro Preto. p.107.

De Ros, L. F., 1998 Heterogeneous generation and evolution of diagenetic quartzarenites in the Siluro-Devonian Furnas Formation of the Paraná Basin, Southeer Brazil. Sedimentary Geology, 116, p.99-128.

Ding, C., Chen, G., Zhang, H., Yang, F., Mao, X., 2011. Geochemical characterostics and geological environment of Zijinshan complex in the Eastern Ordos Basin. J. Mineral. Petrol. 31, 74–81

Duan, W., Li, C., Luo, C., Chen, X.G., Bao, X. 2018. Effect of formation overpressure on the reservoir diagenesis and its petroleum geological significance for the DF11 Block of the Yinggehai Basin, the South China Sea. Marine and Petroleum Geol. V97, 49-65. <https://doi.org/10.1016/j.marpetgeo.2018.06.033>.

Dutra, V.P.L. 2011. Análise faciológica e petrográfica da Formação Poti (Mississipiano, Bacia do Parnaíba) em testemunhos de sondagem (Conclusion Course). Universidade Federal do Rio de Janeiro, Brasil. pp. 82.

Ferraz, N.C., Cóbora, V.C., Sousa, D.C. 2017. Análise estratigráfica da sequência Mesodevoniana-Eocarbonífera da Bacia do Parnaíba, Nordeste do Brasil. Geociências, UNESP, 36, n1, 154-172. <https://doi.org/10.5016/geociencias.v36i1.12302>.

Folk, R.L., 1968. In: Petrology of Sedimentary Rocks. Hemphil's Public., Austin, Texas, p. 107.

Góes A. M. & Feijó F. J. 1994. Bacia do Parnaíba. Boletim de Geociências da Petrobras, 8 (1), p.57-67.

Góes, A. M. 1995. A Formação Poti (Carbonífero Inferior) da Bacia do Parnaíba. TS Universidade de São Paulo. Instituto de Geociências. São Paulo. 171p.

Gordon, J.B., Sanei, H., Pedersen, P.K., 2022. Secondary porosity development in incised valley sandstones from two wells from the Flemish Pass area, offshore Newfoundland. Marine and Petroleum Geology 140. <https://doi.org/10.1016/j.marpetgeo.2022.105644>.

Haile, B.G., Czarniecka, U., Xi, K., Smyrak-Sikora, A., Jahren, J., Braathen, A., Hellevang, H., 2019. Hydrothermally induced diagenesis: Evidence from shallow marine-deltaic sediments, Wilhelmøya, Svalbard. Geoscience Frontiers 10, 629–649. <https://doi.org/10.1016/j.gsf.2018.02.015>.

Higgs, K.E., Funnell, R.H., Browne, G.H., 2021. A multidisciplinary study of diagenesis and pore fluid evolution in frontier basins; an example from Canterbury and Great South basins, New Zealand. *Marine and Petroleum Geology* 124. <https://doi.org/10.1016/j.marpetgeo.2020.104817>.

Huang, S., Huang, P., Wang, Q., Liu, H., Wu, M., Zou, M. 2007. The significance of cementation in porosity preservation in deep-buried sandstones. *Lithologic Reser.* 19, pp. 7-13.

Huang, Y., Kane, I.A., Zhao, Y., 2020. Effects of sedimentary processes and diagenesis on reservoir quality of submarine lobes of the Huangliu Formation in the Yinggehai Basin, China. *Marine and Petroleum Geology* 120. <https://doi.org/10.1016/j.marpetgeo.2020.104526>.

Jaju, M.M., Mort, H.P., Nader, F.H., Filho, M.L., Macdonald, D.I.M., 2018. Palaeogeographical and palaeoclimatic evolution of the intracratonic Parnaíba Basin, NE Brazil using GPlates plate tectonic reconstructions and chemostratigraphic tools. <https://doi.org/10.6084/m9.figshare.c.4100348>.

Jesus, C. M. 2004. Petrografia das Rochas Siliciclásticas da Formação Urucutuca, Bacia de Almada / Porção Emersa - BA. Rio de Janeiro (Master's Dissertation). Universidade Estadual do Rio Grande do Sul (UERG). pp.134.

Kahn, J.S., 1956a. The analysis and distribution of the properties of packing in sand-size sediments1: On the measurement of packing in sandstones. *The Journal of Geology* 64, 385-395. <https://doi.org/10.1086/626372>.

Khan, Z., Ahmad, A.H.M., Sachan, H.K., Quasim, M.A., 2018. The Effects of Diagenesis on the Reservoir Characters in Ridge sandstone of Jurassic Jumara dome, Kachchh, Western India. *Journal of the Geological Society of India* 92, 145–156. <https://doi.org/10.1007/s12594-018-0973-z>.

Khalifa, M., Morad, S., 2012. Impact of structural setting on diagenesis of fluvial and tidal sandstones: The Bahi Formation, Upper Cretaceous, NW Sirt Basin, North Central Libya. *Marine and Petroleum Geology* 38, 211–231. <https://doi.org/10.1016/j.marpetgeo.2011.05.006>.

Klein, C.; Mizusaki, A. M. P. 2007. Cimentação Carbonática Em Reservatórios Siliciclásticos - O Papel Da Dolomita -. *pesqui geocienc*, 34, 91-108.

Lanson, B., Beaufort, D., Berger, G., Bauer, A., Cassagnabère, A., Meunier, A., 2002. Authigenic kaolin and illitic minerals during burial diagenesis of sandstones: a review. *Clay Minerals* 37, 1–22. <https://doi.org/10.1180/0009855023710014>.

Lawan, A.Y., Worden, R.H., Utley, J.E.P., Crowley, S.F., 2021. Sedimentological and diagenetic controls on the reservoir quality of marginal marine sandstones buried to moderate

depths and temperatures: Brent Province, UK North Sea. *Marine and Petroleum Geology* 128. <https://doi.org/10.1016/j.marpetgeo.2021.104993>.

Li, Y., Fan, A., Yang, R., Sun, Y., Lenhardt, N., 2022. Braided deltas and diagenetic control on tight sandstone reservoirs: A case study on the Permian Lower Shihezi Formation in the southern Ordos Basin (central China). *Sedimentary Geology* 435. <https://doi.org/10.1016/j.sedgeo.2022.106156>.

Lima, R.D., De Ros, L.F. 2002. The role of Depositional setting and diagenesis on the reservoir quality of Devonian sandstones from the Solimões Basin, Brazilian Amazonia. *Marine and Petroleum Geol.* 19, pp. 1047-1071. [https://doi.org/10.1016/S0264-8172\(03\)00002-3](https://doi.org/10.1016/S0264-8172(03)00002-3).

Lima, E. A. M. & Leite J. F. 1978. Projeto estudo Global dos Recursos Minerais da Bacia do Parnaíba: Integração geológico-metalogenética. Relatório Final da Etapa III. DNPM – Departamento Nacional de Produção Mineral, CPRM – Companhia de Pesquisa de Recursos Minerais. Recife, pp. 212.

Lina, L.H., Jahren, J., Hellevang, H., 2018. Mechanical compaction in chlorite-coated sandstone reservoirs – Examples from Middle – Late Triassic channels in the southwestern Barents Sea. *Marine and Petroleum Geology* 96, 348–370. <https://doi.org/10.1016/j.marpetgeo.2018.05.025>.

Liu, L., Dong, H., Wu, Y., Fan, R., Sun, Z., Huang, R., Zhang, J., 2022. Sedimentary and diagenetic characteristics of the Z21 field in the Huizhou depression, Pearl River Mouth basin, South China Sea. *Scientific Reports* 12. <https://doi.org/10.1038/s41598-022-09532-y>.

Liu, J.L., Salem, A., Ketzer, J.M., Lei, X.L., Guo, D.Y., Hlal, O. 2009. Impact of diagenesis on reservoir-quality evolution in fluvial and lacustrine-deltaic sandstones: Evidence from Jurassic and Triassic sandstones from Ordos Basin, China. *Journal of Petroleum Geol.* 32, pp. 79-102. <https://doi.org/10.1111/j.1747-5457.2009.00436.x>.

Melo, J.H.G., Loboziak, S., 2000. Visean miospore biostratigraphy and correlation of the Poti Formation (Parnaíba Basin, northern Brazil). *Review of Paleobotany and Palinology* 112, 147-165. [https://doi.org/10.1016/S0034-6667\(00\)00043-9](https://doi.org/10.1016/S0034-6667(00)00043-9).

Marfil, R., Delgado, A., Rossi, C., Iglesia, A.L., Ramseyer, K. 2003. Origin and diagenetic evolution of kaolin in reservoir sandstones and associated shales of the Jurassic and Cretaceous, Salam Field, Western Desert (Egypt). *Inst. Assoc. Sediment. Special Puc* 34, pp. 319-342. [10.1002/9781444304336.ch14](https://doi.org/10.1002/9781444304336.ch14).

Michelli, M. J. 2003. Argilominerais e Ostracodes da Formação Alagamar (Cretáceo Inferior), Bacia Potiguar, NE - Brasil: Paleoambiente e Indicadores Térmicos (Mater's

Dissertation). Universidade Federal do Rio Grande do Sul, Porto Alegre. pp. 111. <http://hdl.handle.net/10183/1943>

Milani, E.J., Melo, J.H.G., Souza, P.A., Fernandes, L.A., França, A.B., 2007. Bacia do Parana. *Bol. Geociencias Petrobras* 15 (2), 265–287.

Miranda, F.S., Vettorazzi, A.L., Cunha, P.R.D.C., Aragão, F.B., Michelon, D., Caldeira, J.L., Porsche, E., Martins, C., Ribeiro, R.B., Vilela, A.F., Corrêa, J.R., Silveira, L.S., Andreola, K., 2018. Atypical igneous-sedimentary petroleum systems of the Parnaíba Basin, Brazil: Seismic, well logs and cores, in: Geological Society Special Publication. Geological Society of London, pp. 341–360. <https://doi.org/10.1144/SP472.15>.

Morad, S., Ketzer, J.M., de Ros, L.R., 2000. Spatial and temporal distribution of diagenetic alterations in siliciclastic rocks: Implications for mass transfer in sedimentary basins. *Sedimentology*. <https://doi.org/10.1046/j.1365-3091.2000.00007.x>

Morad, S., Al-Ramadan, K., Ketzer, J.M., de Ros, L.F., 2010. The impact of diagenesis on the heterogeneity of sandstone reservoirs: A review of the role of depositional fades and sequence stratigraphy. *American Association of Petroleum Geologists Bulletin*. <https://doi.org/10.1306/04211009178>.

Nogueira, A.C.R., Rabelo, C.E.N., Góes, A.M., Cardoso, A.R., Bandeira, J., Rezende, G.L., dos Santos, R.F., Truckenbrodt, W., 2021. Evolution of Jurassic intertrap deposits in the Parnaíba Basin, northern Brazil: The last sediment-lava interaction linked to the CAMP in West Gondwana. *Palaeogeography, Palaeoclimatology, Palaeoecology* 572. <https://doi.org/10.1016/j.palaeo.2021.110370>.

Okunuwadje, S.E., MacDonald, D., Bowden, S., 2020. Diagenetic and Reservoir Quality Variation of Miocene Sandstone Reservoir Analogues from Three Basins of Southern California, USA. *Journal of Earth Science* 31, 930–949. <https://doi.org/10.1007/s12583-020-1289-7>.

Oliveira, D.C., Mohriak, W.U., 2003. Jaibaras trough: An important element in the early tectonic evolution of the Parnaíba interior sag basin, Northern Brazil. *Marine and Petroleum Geology* 20, 352–383. [https://doi.org/10.1016/S0264-8172\(03\)00044-8](https://doi.org/10.1016/S0264-8172(03)00044-8)

Oliveira, C.E., Pe-Piper, G., Piper, D.J.W., Zhang, Y., Corney, R., 2017. Integrated methodology for determining provenance of detrital quartz using optical petrographic microscopy and cathodoluminescence (CL) properties. *Marine and Petroleum Geology* 88, 41–53. <https://doi.org/10.1016/j.marpetgeo.2017.07.031>.

Oliveira, C.V., Moura, C.A.V. 2018. Provenance of detrital zircons of the Canindé Group (Parnaíba Basin), northeastern Brazil. *Journal of South American Earth Sciences* 90, 162-180. <https://doi.org/10.1016/j.jsames.2018.12.009>.

Oliveira, A.L., Pimentel, M.M., Fuck, R.A., Oliveira, D.C., 2018. Petrology of Jurassic and Cretaceous basaltic formations from the Parnaíba Basin, NE Brazil: correlations and associations with large igneous provinces. *Geological Society, London, Special Publications*, 472. <https://doi.org/10.6084/m9.figshare.c.3985437>.

Okunuwadje, S.E., MacDonald, D., Bowden, S., 2020. Diagenetic and reservoir quality variation of miocene sandstone reservoir analogues from three basins of southern California, USA. *J. Earth Sci.* 31, 930–949. <https://doi.org/10.1007/s12583-020-1289-7>.

Paiva, R.G. 2018. Estratigrafia de sequências aplicada à Formação Poti, Viseano da Bacia do Parnaíba (Mater's dissertation). Universidade de Brasília. pp. 104.

Paz, D., Gómez-Dacal, A.R., Varela, A.N., Comerio, M., Muñoz-Olivero, T.M., Bucher, J., Richiano, S., Poiré, D.G., 2022. Controls on composition and diagenesis of wave- and river-dominated deltas: impacts on reservoir properties. An example from the La Anita Formation (Argentina). *Marine and Petroleum Geology* 138. <https://doi.org/10.1016/j.marpetgeo.2022.105571>.

Quasim, M.A., Ghosh, S.K. and Ahmad, A.H.M. 2018. Petrography and diagenetic evolution of the Proterozoic Kaimur Group Sandstones, Son Valley, India: implicand Tripathi, S.C. (Ed.). *Geol. Evol. Prec. Indian Shield*. Springer International Publishing, AG, part of Springer Nature, pp.515-550. [10.1007/978-3-319-89698-4_20](https://doi.org/10.1007/978-3-319-89698-4_20).

Quasim, M.A., Khan, S., Srivastava, V.K., Ghaznavi, A.A., Ahmad, A.H.M., 2021. Role of cementation and compaction in controlling the reservoir quality of the Middle to Late Jurassic Sandstones, Jara dome, Kachchh Basin, western India. *Geological Journal* 56, 976–994. <https://doi.org/10.1002/gj.3989>.

Qian, W., Yin, T., Zhang, C., Hou, G., He, M., 2020. Diagenesis and diagenetic stages prediction of Ed2 reservoir in the west of Bozhong sag. *Petroleum* 6, 23–30. <https://doi.org/10.1016/j.petlm.2019.04.003>

Rong, H., Jiao, Y., Wu, L., Zhao, X., Cao, M., Liu, W., 2021. Effects of igneous intrusions on diagenesis and reservoir quality of sandstone in the Songliao Basin, China. *Marine and Petroleum Geology* 127. <https://doi.org/10.1016/j.marpetgeo.2021.104980>.

Sajid Z, Ismail MS, Zakariah MNA, Tsegab H, Gámez Vintaned JA, Hanif T, Ahmed N 2020 Impact of Paleosalinity, Paleoredox, Paleoproductivity/Preservation on the Organic

Matter Enrichment in Black Shales from Triassic Turbidites of Semanggol Basin, Peninsular Malaysia. Minerals 10(10):915. 10.3390/min10100915.

Santos, M.E.C.M., Carvalho, M.S., 2009. Paleontologia das Bacias do Parnaíba, Grajaú e São Luís – Reconstituições Paleobiológicas. Companhia de Pesquisa de Recursos Minerais (CPRM), Rio de Janeiro, p. 212. .

Sayem, A.S.M., Rahman, M.J.J., Abdullah, R., Azim, K.M.R., 2022. Diagenetic history of the Miocene Surma Group sandstones from the Eastern Fold Belt of the Bengal Basin. J. of Asian Earth Sci. 7, pp.100098. <https://doi.org/10.1016/j.jaesx.2022.100098>.

Schrank, A.B.S., Altenhofen, S.D., de Ros, L.F., 2017. Diagenetic preservation and modification of porosity in aptian lithic reservoirs from the sergipe-alagoas basin, Ne Brazil. Journal of Sedimentary Research 87, 1156–1175. <https://doi.org/10.2110/jsr.2017.64>.

Scherer, C.M.S. and De Ros, L.F. 2009. Heterogeneidades dos reservatórios flúvio-eólicos da Formação Sergi na Bacia do Recôncavo. Boletim de Geociências da Petrobras 17(2), 249–271.

Sech, R. P., Jackson, M. D. & Hampson, G. J. 2009. Three-dimensional modeling of a shoreface-shelf parasequence reservoir analog: part 1. Surface-based modeling to capture high-resolution facies architecture. American Association of Petroleum Geologists Bulletin, 93, 1155–1181. DOI:10.1306/05110908144.

Soares, G.L., 2007. Análise estratigráfica de alta resolução no intervalo do limite formacional Longá/Poti (Neodevoniano/Eocarbonífero) em testemunhos de sondagem da Bacia do Parnaíba (Conclusion monography). pp. 112.

Soares, G.L., Borghi, L. 2014. Estratigrafia de sequências do contato formacional Longá/Poti (Carbonífero Inferior) em testemunhos de sondagem da Bacia do Parnaíba. Boletim de Geociências da Petrobras 22 (2), pp. 213-235.

Soares, J.E.P., Stephenson, R., Fuck, R.A., de Lima, M.V.A.G., de Araújo, V.C.M., Lima, F.T., Rocha, F.A.S., da Trindade, C.R., 2018. Structure of the crust and upper mantle beneath the Parnaíba Basin, Brazil, from wide-angle reflection-refraction data. Geological Society, London, Special Publications, 472. <https://doi.org/10.6084/m9.figshare.c.4058582>

Shi, J., Lin, Y., Zhao, A., Wang, X., An, K., Zhong, X., Hu, K., Zhu, Y., Liu, L. 2021. Diagenetic features and porosity dense evolution of Chang 8 tight sandstones reservoir in Hujianshan área, Ordos Basin. Journal of P. Exploration and Prod. 11, pp. 1037-1051. 10.1007/s13202-021-01092-7.

Shu, Y., Sang, S.X., Lin, Y.X., Zhou, X.Z., Wang, H., Wang, Z.L. 2021. The influence of magmatic- hydrothermal activities on porosity and permeability of sandstones reservoirs in

the Linxing area, Ordos Basin, Northern China. *J. of A. Earth Sci.* 213, pp. 104741. <https://doi.org/10.1016/j.jseaes.2021.104741>.

Silva-Telles Jr., A.C., Arai M., Coimbra J.C. 1991. Biocronostratigrafia e paleocologia da Bacia do Araripe. In: Ponte F.C., Dino R., Arai M., Silva-Telles Jr A.C. *Geologia das Bacias Sedimentares Mesozoicas do Interior do Nordeste Brasil*. Rio de Janeiro, Petrobrás, CENPES, SUPEP, DIVEX, SEBIPE.

Taylor, T.R., Giles, M.R., Hathon, L.A., Diggs, T.N., Braunsdorf, N.R., Birbiglia, G. v., Kittridge, M.G., MacAulay, C.I., Espejo, I.S., 2010. Sandstone diagenesis and reservoir quality prediction: Models, myths, and reality. *American Association of Petroleum Geologists Bulletin* 94, 1093–1132. <https://doi.org/10.1306/04211009123>

Tribaldos, V. & White, N. 2018. Implications of preliminary subsidence analyses for the Parnaíba cratonic basin. In: Daly, M.C., Fuck, R.A., Julià, J., Macdonald, D.I.M. & Watts, A.B. (eds) *Cratonic Basin Formation: A Case Study of the Parnaíba Basin of Brazil*. Geological Society, London, Special Publications, 472. <https://doi.org/10.1144/SP472.3>

Tucker, M.E., 2001. *Sedimentary Petrology: An introduction to the origin of Sedimentary Rock*. Blackwell Science, Oxford.

Vaz, P.T., Resende, N.G.A.M., Wanderley Filho, J.R., Travassos, W.A., 2007. Bacia do Parnaíba. *Bol. Geociencias Petrobras* 15, 253–263.

Wang, Z., Luo, X., Lei, Y., Zhang, L., Shi, H., Lu, J., Cheng, M., Liu, N., Wang, X., He, Y., Jiang, T., 2020. Impact of detrital composition and diagenesis on the heterogeneity and quality of low-permeability to tight sandstone reservoirs: An example of the Upper Triassic Yanchang Formation in Southeastern Ordos Basin. *Journal of Petroleum Science and Engineering* 195. <https://doi.org/10.1016/j.petrol.2020.107596>.

Worden, R. H. & Morad, S. 2003. Clay minerals in sandstones: controls on formation distribution and evolution. In: Worden, R. H. & Morad, S. (Eds.). *Clay minerals cements in Sandstones*, International Association of Sedimentologists Special Publication 34 (Ed. by R.H. Worden and S. Morad), Blackwell Publishing, Oxford, pp. 109–128.

Worden, R.H., Burley, S.D., 2009. Sandstone Diagenesis: The Evolution of Sand to Stone, in: *Sandstone Diagenesis*. Blackwell Publishing Ltd., pp. 1–44. <https://doi.org/10.1002/9781444304459.ch>

Worden, R.H., Armitage, P.J., Butcher, A.R., Churchill, J.M., Csoma, A.E., Hollis, C., Lander, R.H., Omma, J.E., 2018. Petroleum reservoir quality prediction: Overview and contrasting approaches from sandstone and carbonate communities, in: *Geological Society Special Publication*. Geological Society of London, pp. 1–31. <https://doi.org/10.1144/SP435.21>

Wu, H., Zhao, J., Wu, W., Li, J., Huang, Y., Chen, M., 2021. Formation and diagenetic characteristics of tight sandstones in closed to semi-closed systems: Typical example from the Permian Sulige gas field. *Journal of Petroleum Science and Engineering* 199. <https://doi.org/10.1016/j.petrol.2020.108248>.

Xu, L., Yang, K., Wei, H., Liu, L., Jiang, Z., Li, X., Chen, L., Xu, T., Wang, X., 2021. Pore evolution model and diagenetic evolution sequence of the Mesoproterozoic Xiamaling shale in Zhangjiakou, Hebei. *Journal of Petroleum Science and Engineering* 207. <https://doi.org/10.1016/j.petrol.2021.109115>.

Yuan, G., Cao, Y., Schulz, H., Hao, F., Gluyas, J., Liu, K., Yang, T., Wang, Y., Xi, K., Li, F., 2019. A review of feldspar alteration and its geological significance in sedimentary basins: from shallow aquifers to deep hydrocarbon reservoirs. *Earth Sci. Rev.* 191, 114–140. <https://doi.org/10.1016/j.earscirev.2019.02.004>.

6 CONSIDERAÇÕES FINAIS

A análise e associação de fácies da formação Poti indica que os sedimentos foram depositados no *shoreface* superior (AF1) e *shoreface* inferior/*offshore* (AF2) em ambientes de plataforma rasa dominada por ondas de tempestade e sob variações climáticas que mudavam constantemente a linha base de ação das ondas (Fair Weather Base). Ambas as associações são texturalmente homogêneas e diferem na granulometria, sistema deposicional e intensidade dos eventos diagenéticos, os quais afetaram o sistema permo-poroso dessas rochas.

Os arenitos da Formação Poti foram classificados em quartzoarenitos e arenitos subarcósios com granulometria variando de areia fina a grossa e silte; os grãos são moderadamente a mal selecionados, subangulosos e subarredondados com esfericidade baixa. Texturalmente são imaturos com menos de 5% de matriz argilosa na composição, porém, são maturos composicionalmente, já que possuem mais de 90% de quartzo em seu arcabouço.

Foram identificadas porosidades do tipo intergranular, com valor médio de 11%, intragranular, com média de 0,25 % e porosidade móldica, por fraturamento de grãos e agigantada com valores menores que 1%. A porosidade intergranular se concentra nas camadas superiores da sucessão e alcança valor máximo de 28%. A porosidade intragranular relaciona-se principalmente à dissolução parcial de grãos de feldspatos e influência de fluidos ácidos provindos de hidrotermalismo da Formação Sardinha, a qual apresentou maior influência na formação de poros agigantados, que apresentaram valor máximo de 4,0 % nos arenitos próximo à essa intrusão.

Com a integração de dados faciológicos, petrografia, padrão de paleocorrente e análises químicas qualitativas, e processos diagenéticos foi possível determinar as características e qualidade do reservatório da Formação Poti, para o ambiente de plataforma dominado por ondas de tempestade. Os processos diagenéticos identificados foram: infiltração mecânica de argila, compactação mecânica e química, sobrecrecimento/cimentação de quartzo, dissolução, alteração, substituição de grãos e cimentação de hematita e óxido de titânio. A cimentação de argila e hematita não tiveram um impacto negativo na associação de fácies de *Shoreface* Superior e nas camadas superiores, não afetando tanto a qualidade do reservatório, que tiveram sua porosidade preservada. Por outro lado, os arenitos da associação de fácies de *Shoreface* Inferior/*Offshore* foram bastante afetados por esses processos, resultando em uma diminuição significativa da porosidade.

Através do padrão de paleocorrente, análise petrográfica de minerais pesados e imagens de catodoluminescência, foi possível determinar que as rochas fonte de sedimentos da Formação Poti é o Complexo Granjeiro, o qual pertence ao Domínio Rio Grande do Norte na

Província Borborema, sendo caracterizado por rochas metamórficas peraluminosas de alto grau, rochas metassedimentares, associações de TTG e granitos ricos em feldspato potássico, que tem origem relacionada ao final do Ciclo Brasiliano.

Portanto, os diferentes ambientes deposicionais, tectonismo, rochas fonte de sedimentos e diagênese modificaram ou mantiveram a porosidade, permeabilidade e aspectos texturais das rochas da Formação Poti. Mais pesquisas suplementares em outras regiões da Bacia do Parnaíba são necessárias e recomendadas para definir com maior precisão a evolução diagenética de outros ambientes deposicionais, influência do hidrotermalismo nas características petrofísicas da rocha. A utilização e análise de dados de testemunhos de sondagem, também, é altamente recomendável.

REFERÊNCIAS

- ALMEIDA, F.F.M., CARNEIRO, C.D.R. Inundações marinhas fanerozóicas no Brasil e recursos minerais associados. In: Mantesso-Neto, V., Bartorelli, A., Carneiro, C.D.R., Brito-Neves, b.b (org (Eds.), **Geologia do Continente Sul-Americano: evolução da obra de Fernando Flávio de Almeida.** 2004, pp. 43-58.
- AUGUSTSSON, Carita; BAHLBURG, Heinrich. Cathodoluminescence spectra of detrital quartz as provenance indicators for Paleozoic metasediments in southern Andean Patagonia. **Journal Of South American Earth Sciences**, [S.L.], 2003. v. 16, n. 1, p. 15-26.
- BACCOCOLI, G. **Situação da sísmica terrestre no Brasil.** Organização Nacional da indústria do Petróleo. Brasil. Rio de Janeiro. 2004. pp 90.
- BOGGS, S., JR.. **Petrology of Sedimentary Rocks.** New York: Cambridge University Press, 2009, pp. 612.
- BOGGS, S., KRINSLEY, D. Application to Cathodoluminescence Imaging to the Study of Sedimentary Rocks. Cambridge University Press, Cambridge, 2006, pp 177.
- BERNET, M., BASSET, K. Provenance analyses by single-quartz-grain SEM-CL/optical microscopy. **Journal of Sedimentary Research**, 2005. V 75, n. 3, p. 492-500.
- CAPUTO, M.V. **Stratigraphy, tectonics, paleoclimatology and paleogeography of northrn basin of Brazil.** Tese de doutorado. University of California, Santa Barbara, USA, 1984. pp.603 .
- CAPUTO, M.V., LIMA, E.C. Estratigrafia, idade e correlação do Grupo Serra Grande – Bacia do Parnaíba. Congresso Brasileiro de Geologia, XXXIII. 1984, Rio de Janeiro. **Anais do Congresso Brasileiro de Geologia**, Rio de Janeiro. S.E., 1984. PP. 740-753.
- CAPUTO, M.V. Glaciações neodevonianas e eocarboníferas na América do Sul. In: Congresso Brasileiro de Geologia, XLIII. 2006, Aracajú. **Anais de congresso Brasileiro de Geologia**, Salvador: Franca-Rocha (org), 2008.pp. 640-645.
- CARDOSO, A.R. et al. Mesozoic lacustrine system in the Parnaíba Basin northeastern Brazil: Paleogeographic implications for West Gondwana. **Journal of South American Earth Sciences**, 2017. [S.L], V. 74, pp. 41-33.
- CESERO, P. *et al.* Técnicas de preparação de lâminas petrográficas e de moldes de poros na Petrobrás. **Boletim de Geociências da Petrobrás**, 1989. v.3, p.105-116.
- COELHO, D.L.O. et al. Deep crustal architecture of the Parnaíba Basin of NE Brazil from receiver function analyses: Implications for basin subsidence. **Geological society Special Publication.** (S.I.): Geological Society of London, 2018, v 472, p. 83-99.
- CHOQUETTE, P. W. & L. C. PRAY. Geologic nomenclature and classification of porosity in sedimentary carbonates. **American Association of Petroleum Geologists Bulletin**, v. 54, 1970. p.207-250.

CULLITY, B.D., STOCK, S.R. **Elements of X-Ray Diffraction.** Prentice Hall, Upper Saddle River.2001, pp. 696.

CUNHA, F.M.B. **Evolução paleozóica da Bacia do Parnaíba e seu arcabouço tectônico.** Dissertação de Mestrado, Universidade Federal do Rio de Janeiro, Rio de Janeiro, 1986. 6-46p.

DALRYMPLE, R.W. Tidal Depositional systems. In: JAMES, N.P., DALRYMPLE, R.W. (Eds.), **Facies Model**, 4th Ed. St. Jhon's Newfoundation. Geological Association of Canada, 2010. Pp. 201-231.

DALY, M.C. et al. Cratonic basin formation: A case study of the Parnaíba Basin of Brazil, **Geological Society Special Publication.** (S.I.): Geological Society of London, 2018, V. 472, p. 1-15.

DE ROS, L. F. Heterogeneous generation and evolution of diagenetic quartzarenites in the Siluro-Devonian Furnas Formation of the Paraná Basin, Southeer Brazil. **Sedimentary Geology**, 116. 1998. p.99-128.

DICKINSON W. R. Interpreting provenance relations from detrital modes of sandstones. In.: Zuffa, G. G. (ed.), Provenance of Arenites. Reidel, Dordrecht. 1985. p.333-361.

EL-KHATRI, F. et al. Diagenetic Alterations and Reservoir Quality Evolution of Lower Cretaceous Fluvial Sandstones: nubian formation, sirt basin, north-central libya. **Journal Of Petroleum Geology**, [S.L.], 2015. v. 38, n. 2, p. 217-239, 20.

FOLK, R.L. **Petrology of sedimentary rocks.** Hemphil's Public, Texas. 1968, pp. 101.

GALEHOUSE, J.S. Sedimentation analyses. In: Carver, R.E. (Ed.), **Procedures in Sedimentar Petrology.** John Wiley and Sons, New York, NY, 1971. pp. 653.

GÓES, A.M. et al. Estágio exploratório e perspectivas Petrolíferas da Bacia do Parnaíba. **Boletim de Geociências da Petrobrás**, Rio de Janeiro, 1990. V. 4, n.(1), pp. 55-64.

GÓES, A.M., FEIJÓ, F.J. Bacia do Parnaíba. **Boletim de Geociências da Petrobrás**, Rio de Janeiro, 1994. V. 8, n. (1), pp. 57-67.

GÓES, A.M. **A Formação Poti (Carbonífero Inferior) da Bacia do Parnaíba.** Tese de Doutorado, Universidade de São Paulo, Instituto de Geociências, São Paulo, 204 p. 1995.

HASUI, Y. et al. A Geologia do Brasil, São Paulo. Ed. Beca, 2012, p. 900.

KAHN, J.S. The analyses and distribution of the properties of packing in sand size sediments. **Journal of Geology**, 1956. V. 64, n. (4), p. 385-395.

LIMA, E.A.M., LEITE, J.F. Projeto estudo Global dos Recursos Minerais da Bacia do Parnaíba: Integração geológico-metalogenética. **Relatório Final da etapa III.** DNPM – Departamento Nacional de Produção Mineral, CPRM – Companhia de Pesquisa de Recursos Minerais. Recife, pp. 212.

- MAGOON, L.B., DOW, W.G. The petroleum system: From source to trap''. **The American Association of Petroleum Geologists**, Oklahoma. AAPG Memoir, 1994. n (60), p. 3-24.
- MENDONÇA, P.M.M. et al. Exploração na Petrobrás: 50 anos de sucesso''. **Boletim de Geociências da Petrobrás**, 2004. V. 12, n. (1), p. 9-58.
- MESNER, C.J., WOOLDRIDGE, C.P. Maranhão Paleozoic basin and Cretaceous coastal basin, north Brazil. **Bull. Am. Association. Petroleum Geology**, 1964. V. 48, n. (9), p. 1475-1512.
- MORAD, S. **Diagenesis of Clastic Sedimentary Rocks**. Department of Mineralogy and Petrology, Institute of Geology, Uppsala University, 1991. p. 287.
- MORAD, S. et al. Spatial and temporal distribution of diagenetic alterations in siliciclastic rocks: implications for mass transfer in sedimentary basins. **Sedimentology**, 2000. V. 47. P. 1-27.
- MORAD, S., RAMADAN, K.A., KETZER, J.M., DE ROS, L.F. The impact of diagenesis on the heterogeneity of sandstone reservoirs: A review of the role of Depositional facies and sequence stratigraphy. **AAPG Bulletin**, 2010. V 94. Pp. 1267-1309.
- OLIVEIRA, C.E.S. et al. Integrated methodology for determining provenance of detrital quartz optical petrographic microscopy and cathodoluminescence (CL) properties. **Marine and Petroleum Geology**, 2017. V. 88. p. 41-53.
- OLIVEIRA, D.C., MOHRIAK, W.U. Jaibaras trough: An importante elemento in the early tectonic evolution of the Parnaíba interior sag Basin, Northen Brazil. **Marine and Petroleum Geology**, 2003. V. 20, p. 352-383.
- QUASIM, M.A., KHAN, S., SRIVASTAVA, V.K., CHAZNAVI, A.A., AHMAD, A.H.M. Role of cementation and compaction in controlling the reservoir quality of the middle to Late Jurassic sandstones, Jara dome, Kachh Basin, Western India. **Geological Journal**, 2021. V. 56, p. 976-994.
- ROSSETTI, D.F., GÓES, A.M. Caracterização paleoambiental de depósitos Albianos na borda sul da Bacia de São-Luís Grajaú: Modelo de delta fluvial influenciado por tempestade. **Revista Brasileira de Geociências**. 2003. V. 33, n. (3). p. 299-312.
- READING, H.G. **Sedimentary Environment and facies**, third Ed. Blackwell Scientific Publication, Oxford, 1996. pp. 704.
- SANTOS, M.E.C.M, CARVALHO, M.S. Paleontologia das Bacias do Parnaíba, Grajaú e São Luís – Reconstituições Paleobiológicas. CPRM – Companhia de Pesquisa de Recursos Minerais, Rio de Janeiro, 2009. p. 212.
- SILVA, C.R. **Paleoambiente e aspectos petrofísicos do sistema petrolífero da Bacia do Parnaíba – região de Elesbão Veloso (PI)**. Trabalho de conclusão de curso, UFPA, Belém, 2003, pp 60.

SOARES, G.L. **Estratigrafia de alta reolução no intervalo do limite formacional Longá/Poti (Neoevoniano/Eocarbonífero) em testemunhos de sondagem da Bacia do Parnaíba.** Trabalho de Conclusão de Curso – Universidade Federal do Rio de Janeiro, 2007. p. 112.

SOARES, G.L., BORGHI, L. Sequence stratigraphy of the Longá/Poti Formation boundary (Lower Carboniferous) using subsurface data from the Parnaíba Basin. **Boletim de Geociências da Petrobrás**, Rio de Janeiro, 2014. V. 22, n (2), p. 213-235.

SILVA, A.D. *et al.* Bacias sedimentares paleozóicas e meso-cenozóicas interiores. In: BIZZI, L.A., SCHOBENHAUS, C. GONÇALVES, J.H., BAARS, F.J., DELGADO, IM., ABRAM, M.B., LEÃO NETO, R., MUNIZ DE MATOS, G.M., SCHNEIDER SANTOS, J.O. **Geologia, tectônica e recursos minerais do Brasil:** Sistemas de Informações Geográficas – SIG e mapas na escala 1:2. 500.000, 2003. pp. 55-85.

TIAB, D., DONALDSON, E.C. **Petrophysics: Theory and practice of measuring reservoir rock and fluid transport properties.** 3rd Ed. Oxford. Elsevier, 2012. p. 976.

TUCKER, M.E. **Sedimentary petrology: An introduction to the origin of sedimentary rocks.** 3rd Ed. Oxford, Blackwell, 2001. p. 291.

VAZ, P.T. *et al.* Bacia do Parnaíba. **Boletim de Geociências da Petrobrás**, Rio de Janeiro, 2007. V. 15, pp. 253-263.

WALKER, R.G. Facies, **Facies model and modern stratigraphic concepts.** In: WALKER, R.G., JAMES, N.P. (4th Ed.), Facies models: Response to sea level change, Canadá, **Geological Association of Canada**, 1992, pp. 1-14